CANADA
DEPARTMENT OF MINES AND TECHNICAL SURVEYS
DOMINION OBSERVATORIES

PUBLICATIONS

OF THE

Dominion Observatory

OTTAWA

VOLUME XIX No. 2

A THREE-COMPONENT AIRBORNE MAGNETOMETER

BY

P. H. SERSON, S. Z. MACK

AND

K. WHITHAM

EDMOND CLOUTIER, C.M.G., O.A., D.S.P.
QUEEN'S PRINTER AND CONTROLLER OF STATIONERY
OTTAWA, 1957

1,000-1956

86463—1

CONTENTS

CONTENTS—Concluded

A Three-Component Airborne Magnetometer

BY

P. H. SERSON[1], S. Z. MACK[2] AND K. WHITHAM[1]

ABSTRACT

A three-component airborne magnetometer has been designed and built at the Dominion Observatory. The magnetometer is mechanically linked to a gyro-stabilized platform which is maintained horizontal, independent of the motions of the aircraft. The gyroscopes are precessed at a rate proportional to the time integrals of signals from accelerometers mounted on the platform. The system acts basically as a pendulum with a six-minute period. Damping is provided by phase-advance networks in the control loops. Forced oscillations of the platform are reduced by the addition of automatically computed signals proportional to the aircraft accelerations. The accuracy of the platform is 2 or 3 minutes of arc under normal survey conditions. The azimuth reference for the instrument is provided by a directional gyroscope mounted on the platform, whose drift is determined to an accuracy of 0.2° by astronomical measurements with a periscopic sextant stabilized in azimuth.

The magnetometer head contains three orthogonal magnetic detectors of the saturated transformer type, which give direct currents proportional to the fore-and-aft and transverse horizontal components and the vertical component. These and the heading of the aircraft are fed into an analog computer which displays continuously the declination in degrees, and the horizontal and vertical field components in gauss. An alternative display presents automatically the average values of these quantities over successive five-minute intervals. The accuracy of measurement of field components referred to the reference axes established by the stabilization system is estimated to be 0.1° in declination, and 20 gammas in the other components.

Sources of error in survey operations are discussed and the reduction of survey results and the determination of the corrections for the magnetic field of the aircraft described. It is concluded that the probable error of a survey observation as plotted on a chart is about 100 gammas in any component, and is principally due to errors in navigation and plotting.

INTRODUCTION

Magnetic charts showing the direction and intensity of the geomagnetic field have been prepared for over a century from observations made at points scattered over the earth's surface. The distribution of the magnetic stations on land, while it is generally adequate in well-developed areas, is often quite inadequate in others, such as the Arctic and Antarctic. Over the seas, which cover two thirds of the earth's surface, no important magnetic surveys have been made since the loss of the specially constructed ship *Carnegie* in 1929. The absence of recent observations at sea is especially serious, since the rate of change of the geomagnetic field is not constant, and extrapolation of earlier results over 25 years has undoubtedly resulted in large errors in the present world charts (1,2).

The success of the airborne total-intensity magnetometer in geophysical prospecting suggested that an airborne instrument capable of measuring the direction of the geomagnetic vector in addition to its intensity would improve greatly the reliability of magnetic charts for most parts of the world, and would be particularly useful in northern Canada. Airborne magnetic observations have the following advantages over measurements made by standard methods:

(*a*) observations can be made with one instrument and one technique over land, sea, or ice;

(*b*) large scale surveys of the accuracy required for the usual charts can be made more quickly and at less expense;

[1] Dominion Observatory, Ottawa.

[2] Defence Research Board, Ottawa.

(*c*) airborne measurements are virtually unaffected by local anomalies which can make observations at an isolated ground station useless for mapping purposes;

(*d*) an airborne magnetometer can produce continuous profiles of the magnetic components, which help the map-maker to decide which anomalies should be indicated on a particular map, and may reveal interesting geological features;

(*e*) aircraft are by nature less magnetic than other practical vehicles.

The main difficulties in making airborne magnetic measurements are:

(*a*) the establishment in a moving aircraft of an accurate direction reference system with respect to which the direction of the magnetic vector is measured;

(*b*) the problem of establishing the geographical location of the observations;

(*c*) the necessity of either compensating the magnetometer or correcting the observations for the magnetic field of the aircraft.

Two basic considerations governed the over-all design of the magnetometer. First, the instrument was to present magnetic results in a form as close as possible to that required for the preparation of magnetic charts, in order to avoid the necessity of a large staff for the processing of data. It was decided that the instrument should indicate the declination, the horizontal component and the vertical component, and that the indicators should show the three quantities directly in the usual units—degrees and oersteds. The second aim was that the accuracy of measurement should be 0.1 degree in declination, 10 gammas (10^{-4} oersted) in the horizontal component and 10 gammas in the vertical component.

From the first requirement, it was apparent that the direction reference system should be that defined by the vertical and geographical north (rather than one defined by the direction of two stars, for instance). The second aim required that the direction reference system be accurate to one minute of arc in the determination of the vertical and 0.1 degrees in azimuth. When the project was begun, the accuracy to be expected from available gyro-vertical systems was of the order of one degree. The success of this project, therefore, depended on the development of an improved system for the determination of the vertical in an aircraft.

In its broadest outline, the three-component airborne magnetometer consists of a field-measuring device mounted on a horizontal gyro-stabilized platform inside the aircraft. The role in the over-all design of the instrument of the first requirement stated above may be seen by comparing the Caandian instrument with the airborne magnetometers developed by American and British groups to measure the intensity anddirection of the earth's field.

The instrument developed in the United States—The Vector Airborne Magnetometer —has been described by Schonstedt and Irons (3). The total intensity is measured with a detector aligned in the total field, and the angles between the axis of the detector and a reference system, defined by a damped pendulum and the astronomically determined heading of the aircraft, are continuously recorded. After these angles have been averaged over a suitably long period of time, they are used to compute the components of the magnetic field with the aid of I.B.M. machines. The apparatus is relatively simple, but operation is limited to high altitudes (20,000 feet) where flying conditions are smooth, and the accuracy of measuring the magnetic field in the aircraft is probably an order of magnitude less than that considered above.

The British development (4) proposes to measure the total field and the component in the direction of the sun. A second flight, when the sun has changed position, supplies a third component. The apparatus should be nearly an order of magnitude more accurate than the Canadian instrument, but it can be used only when the sun is visible and Decca navigation is available. An electronic computer is used to convert the information to a useful form.

Although the accuracy of the present three-component magnetometer approaches the design accuracy (0.1° in declination, 10 gammas in the horizontal and vertical components) in measuring the magnetic field at the magnetometer head, its accuracy in measuring the geomagnetic field is considerably lower because of uncertainties in the corrections applied to the readings for the magnetic field of the aircraft. It is shown in Part 3 of this report that these uncertainties amount to 60 gammas in the horizontal vector and 30 gammas in the vertical component. In making geomagnetic observations on the ground, it has been customary to try for an accuracy of one gamma in three orthogonal components, which has made possible the investigation of diurnal variation and secular change. A sensitivity of 10 gammas is usually adequate in magnetic prospecting. It is thus necessary to consider the usefulness of geomagnetic measurements with a lower order of accuracy, such as are obtained with this instrument.

The amount of detail that can be shown on a magnetic chart depends on the scale—charts covering Canada at a scale of 100 miles to the inch usually show contours of the components at 1000-gamma intervals. The magnetic components at a point can be read to within 100 gammas. In drawing the contours the magnetic data must be smoothed, the degree of smoothing depending on the geographical density of observations and the geology of the area. In the case of the 100-mile-to-the-inch charts, an analysis of the differences between values read from the completed charts and the original ground observations used in their preparation showed that the smoothing produced probable deviations of two or three hundred gammas.

It is concluded that the accuracy of the three-component airborne magnetometer is sufficient for the production of charts on a scale of 100 miles to the inch, and is probably satisfactory for charts covering smaller areas, at 20 miles to the inch.

In computing and plotting airborne observations, considerable time is saved by accepting an accuracy of 50 gammas. It is usually unnecessary to correct the observed values for diurnal variation and magnetic disturbances; such corrections, in any case, can be made only in areas well supplied with magnetic observatories.

In order to facilitate the plotting of results, an automatic averaging system has been included in the present magnetometer. This device computes automatically, during flights, the average values over successive 5-minute periods of time, of the declination and the horizontal and vertical components. When observations are plotted to 50 gammas, it is usually sufficient to plot only the average values (corresponding to averages over 20-mile segments of the magnetic profiles) and a great saving in office work is achieved.

This report on the three-component airborne magnetometer is divided into three parts. The method of establishing the directional reference system and the method of making magnetic measurements with respect to that system are treated separately in Parts 1 and 2. Part 3 discusses the accuracy of the instrument as a whole, with emphasis

on the correction of observations for the magnetic field of the aircraft, and presents experimental results obtained in 1953 and an analysis of a survey of western Canada made in 1955.

The instrument described in the present paper was designed and built between 1951 and 1955 at the Dominion Observatory. One of the authors (S.Z.M.), who worked on the project until the end of 1952, was on the staff of the Defence Research Board. This paper is substantially a revision of an earlier report by the three authors written in 1954; this earlier report, D.R.B. D-45-31-30-02, 1955, was classified SECRET until November 1956. It is not intended as an account of the whole project, which dates from 1946, but as a description of the instrument in its present state of development together with results from recent surveys. Since many organizations have taken an active part in the project, particularly in its early stages, it is felt that a short history of the project should be given here.

The Universal Airborne Magnetometer Project was first placed on the program of the Subcommittee on Navigation of the Associate Committee on Aeronautical Research of the National Research Council of Canada at its third meeting on January 15, 1946. This Subcommittee was later succeeded by the Navigation Research Panel of the Defence Research Board of Canada, and the project was taken over by the new panel. These organizations have supported the project by annual grants from 1948 to the present. In the early years of its history there was considerable doubt as to the wisdom of carrying out this development in Canada, and it required pressure by the Subcommittee to keep the project active.

In 1947 W/C D. A. MacLulich, R.C.A.F., submitted to the Subcommittee a plan for a universal airborne magnetometer. This plan included an important feature which distinguishes this development from those in other countries—a gyro-stabilized horizontal platform on which is mounted the field-sensitive head of the magnetometer. The detailed design and construction of such an instrument began in 1948. W/C MacLulich, at the Central Experimental and Proving Establishment, R.C.A.F., (C.E.P.E.), undertook the construction of a gimbal-mounted platform maintained horizontal by two servomotors controlled by a vertical gyroscope. An automatic sun-compass, employing photo-electric cells to follow the sun, which was to supply the azimuth reference to the system, was developed under the direction of W/C MacLulich by the Photographic Survey Corporation in Toronto. A group working in the Department of Physics, University of Toronto, was to develop the equipment for measuring the components of the magnetic field.

A preliminary model of the stabilized platform, controlled by a war-surplus vertical gyroscope, was built by C.E.P.E., but was never tested in the air. A theoretical investigation soon showed that no commercially available vertical gyroscope would be nearly accurate enough, and the University of Toronto group designed a completely new gyroscope control system. A model of the system was built at the Dominion Observatory. C.E.P.E. constructed the servo-controlled platform to be operated from signals supplied by this system.

The first model of the airborne magnetometer, which was completed in 1950, is described in references 6 and 7. The complete instrument was flown only once, but the vertical gyroscope system was flown several times, furnishing valuable records of the

long-period accelerations of the aircraft. These experiments showed that elaborate gyro-control systems were practical for survey work, and also that the theoretical accuracy of such a system would be approached only by a platform of careful mechanical design, using the best gyroscopes available. The automatic sun-compass was found to require almost perfect weather for successful operation, and it was abandoned in favour of the more flexible combination of a manually operated sextant and a directional gyroscope. Although the instrument which is the subject of this paper bears little resemblance to the 1950 model, its design is based on information obtained and lessons learned in the operation of the earlier equipment. The authors are thus greatly indebted to the organizations which took an active part in the early developments, and particularly to W/C D. A. MacLulich.

PART 1

THE GYRO-STABILIZED PLATFORM

1.1 INTRODUCTION

The three-component magnetometer consists of two main groups of components. The first group consists of a stabilization system which is described in Part 1 of this paper and which keeps a platform horizontal and furnishes a reference direction of known true azimuth. The other group of components is described in Part 2 of this paper and comprises the magnetometer, which measures the magnetic declination and the vertical and horizontal components of the magnetic field.

The platform is maintained horizontal, independent of the rolling and pitching of the aircraft, by two servo-motors controlled by error signals from a roll and pitch gyroscope mounted on the platform. The natural frequency of these servo systems is of the order of 30 cycles per second. The gyroscopes used are the Minneapolis-Honeywell HIG units.

Also mounted on the platform are two Minneapolis-Honeywell accelerometers, one for transverse accelerations and one for fore-and-aft accelerations. Signals from these accelerometers are integrated and modified by suitable error-rate stabilization networks before being applied to the precessing torque motors on the roll and pitch gyroscopes. In this way the direction of the normal to the platform is made to coincide with the average position of the apparent vertical in the moving aircraft, the time of averaging being longer than the periods of the accelerations found in a moving plane.

Basically the platform acts as a damped pendulum with a period of six minutes (equivalent length of a simple pendulum is about 20 miles). The natural period of the system must be long for good filtering characteristics, but cannot be made too long because of the time taken for transient recovery of the platform. A period of about six minutes seems a good compromise between good filtering with poor transient response and poorer filtering with better transient recovery. Using a six-minute period, accelerations of the aircraft with an amplitude of one degree deflection of the apparent vertical (0.02g) and a period of one minute will force an oscillation of the platform with an amplitude of about two minutes of arc and the same period. It should be pointed out that the method of damping does not introduce effects due to the rolling or pitching of the aircraft.

In order to reduce the amplitude of forced oscillations of the platform due to long-period accelerations of the aircraft, an attempt is made to reduce the periodic part of the input to the integrators by subtracting from the accelerometer signals, automatically computed signals proportional to the aircraft accelerations. The computed fore-and-aft signal is the derivative of the output of a true airspeed meter, and the computed transverse acceleration signal is the product of airspeed and the rate of change of heading of the aircraft. The heading of the aircraft is obtained from a third HIG unit mounted on the stabilized platform and used as a directional gyroscope.

In order to reduce transients following large changes in heading of the aircraft, torques proportional to earth's rate are applied to the roll and pitch gyroscopes. A small Coriolis correction is applied to the roll accelerometer output.

This part of the report contains a description of the gyro-stabilized platform, the gyroscopes used, and an outline of the mechanical design of the platform. The theory of the high frequency platform servoamplifiers is briefly discussed, and the theory of the long period gyroscope erection systems fully described. The circuits required to operate and control the platform are described, and the initial alignment procedures mentioned. The synchronous periscopic sextant, used to determine the corrections to be applied to the directional gyroscope, is briefly described. Finally, the performance of the platform in flight is illustrated from field records.

1.2 GENERAL DESCRIPTION OF THE GYRO-STABILIZED PLATFORM

1.2.1 *The Platform*

Plate I shows the stabilized platform and magnetometer head. A wooden box bolted to the floor of the aircraft carries four shock-mounts Q. The shock-mounts support a rectangular wooden frame F, to which is bolted the outer gimbal ring E. The inner gimbal C can rotate about the longitudinal axis of the aircraft (the roll axis) in bearings set in gimbal E. The gyroscope platform A is supported by bearings in gimbal C which allow it to rotate about the pitch axis—an axis perpendicular to the roll axis.

The magnetometer yoke N is rigidly connected to the inner gimbal C by an aluminum pipe H. The yoke supports a small platform on two bearings which define an axis parallel to the pitch axis of the gyroscope platform. The magnetometer head G is mounted on the small platform. The magnetometer platform is mechanically connected to the gyroscope platform by a linkage parallelogram whose lower arm can be seen at J. In this way the planes of the two platforms are parallel independent of the attitude of the aircraft.

The gyroscope platform A is maintained steady in space, when the aircraft rolls or pitches, by the roll servomotor D and pitch servomotor B, which apply torques to platform A about the roll and pitch axes respectively. The signals controlling the servomotors originate in two gyroscopes, the roll and pitch gyros, fixed to platform A.

A third gyroscope K is mounted to a turntable L, which can rotate about a vertical axis in bearings carried by the platform A. A third servomotor is controlled by gyroscope K so as to maintain constant the azimuth of the turntable when the aircraft yaws or changes heading. Thus K functions as a directional gyroscope, and an angle measuring system measures the aircraft heading relative to this directional gyroscope.

The operation of the servo loops can be understood as follows. When, for instance, the aircraft rolls, friction in the gimbal bearings causes the platform to roll. Immediately, the roll gyroscope gives an electrical signal proportional to the angle through which the platform has rotated, and the roll servomotor applies a torque to the platform in the sense opposite to the torque disturbing it. For the platform to be steady to one minute of arc, the motor must develop a large torque for a small angular displacement of the platform, and the loop gain of the servo system must therefore be very large. The result is a servo system with a high natural frequency and a stability problem of considerable difficulty. The following conditions must be fulfilled:

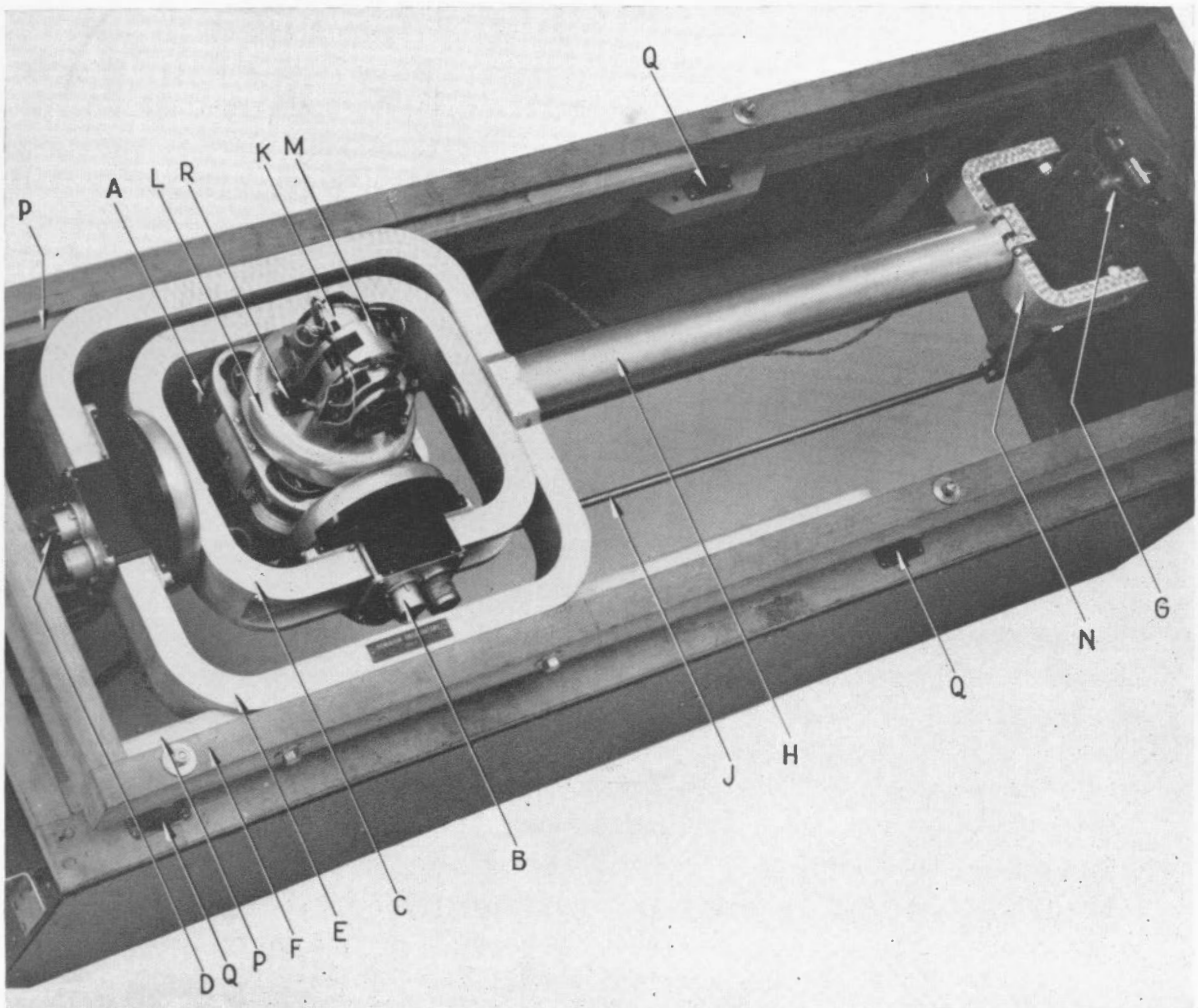

PLATE I—The gyro-stabilized platform and magnetometer head

(*a*) the gyroscopes must have a low threshold, i.e. they must give a useful signal for an angular displacement of a fraction of a minute of arc;

(*b*) the gimbal system and gear trains must be rigid, with natural frequencies much higher than the natural frequency of the servo loops;

(*c*) backlash in the gimbal bearings and gear trains must be negligible;

(*d*) damping of the servo loops must be of the error-rate type in order to avoid velocity errors of the platform when the aircraft undergoes rapid angular motions.

While the system as described will maintain the platform steady in space for a short period of time, it will not hold the platform horizontal over a long period because of the unpredictable wander rates of the gyroscopes, the rotation of the earth and the velocity of the aircraft over the earth. For the long-term stability the gyroscopes must be controlled by applying precessing torques, which are determined automatically by a computer whose inputs are navigational information and signals from two accelerometers mounted on the gyroscope platform.

The design of the long-period control system is described later in section 1.5.

1.2.2 *The Gyroscopes*

The three gyroscopes are Minneapolis-Honeywell HIG-5 units, Type GG1A-2. The electrically driven rotor is sealed in a gimbal can, which rotates about its axis of symmetry or output axis, in jewelled bearings. The spin axis of the rotor is perpendicular to the output axis. A third axis perpendicular to both the spin axis and the output axis is known as the *input axis*. The gimbal can floats in a viscous fluid, which fills the gyroscope case and provides damping, and is thermostatted at 167°F.

When the gyroscope case is rotated about the input axis, the gimbal can rotates with respect to the case about the output axis. The viscosity of the fluid is chosen to make the output angle approximately equal to the input angle. The output angle is measured by a microsyn pick-off at one end of the gimbal can. At the other end of the can is a microsyn torque generator, which is used to control the equilibrium position of the gyroscope by applying torques about the output axis.

Using rigid heat-insulating clamps, the roll and pitch gyroscopes are clamped to the gyroscope platform with their output axes vertical and their input axes parallel to the roll and pitch axes respectively. The directional gyroscope is mounted on the turntable with its output axis horizontal and its input axis parallel to the axis of rotation of the turntable.

The chief reasons for the choice of HIG-5 units, in addition to availability and compactness, are the low friction levels and low thresholds obtained in these gyroscopes.

Extremely low friction levels are attained by the technique of floating the gimbal can which permits the use of small jewelled bearings on the output axis. Low friction results in an apparently random wander-rate which is low and consistent, considering the small size of the gyroscope. As will be shown in section 1.5, in this application a constant wander-rate in the platform gyroscopes is not important, but a steadily changing wander-rate causes a constant error in the determination of the vertical, and abrupt changes in wander-rate produce transient errors which persist for a long time. The changes in

wander-rate recorded in bench-tests of the two platform gyroscopes in April 1952 were in the range 0.12 to 0.03 degrees/hour/minute and these changes were acceptably small. No sudden changes of rate were observed at this time. However, later tests on six units showed serious deterioration in performance after a few week's operation (section 3.6).

The microsyn pick-off on the output axis has a low noise level, and produces useful signals for angular displacements as small as 0.1 minutes of arc, without resorting to special circuit techniques. This low threshold is necessary for the short-term stability of the platform, as was mentioned in section 1.2.1.

1.3 THE MECHANICAL DESIGN OF THE STABILIZED PLATFORM

The aluminum castings used in the construction of the platform were supplied by the Mines Branch, Department of Mines and Technical Surveys, Ottawa, and the machining and assembly of the platform carried out in the machine shop of the Dominion Observatory.

The design of the component parts of the assembly is discussed below.

1.3.1. *The Design of the Platform Gear Trains*

The gear boxes of the roll, pitch and azimuth servo systems are identical in design. A ratio of 720 to 1 between the motor and the output shaft was chosen, allowing the platform to remain stationary for angular velocities of the aircraft up to 44°/second. In order to obtain zero backlash, each gear box includes two parallel gear trains, one of which is preloaded against the other by a single spring, as shown in Figure 1.1. Without spring-loading, the total backlash of the two gear trains amounted to about 10° at the motor shaft. The spring was wound up to produce a constant torque greater than the maximum torque of the motor reflected at the shaft in question (12 oz. in. in this design).

The gears and shafts are made from S.A.E. 62 bronze. The form of the gear teeth is American Standard Stub Tooth, 48 pitch and 20° pitch angle. The gears were cut by Precision Gear (Canada) Ltd. The large internal gears were made from a centrifugally cast bronze bushing (similar to A.S.T.M. B-139-44, Grade D) supplied by Montreal Bronze Company Ltd.

A basic aim in the design of the platform servo systems was that the loop gain should be of the order of 2×10^{11} dyne cm./radian, measured at the platform. The corresponding torque for a displacement of the platform of one minute of arc is 4 ft. lb. The moment of inertia J of the system, measured at the platform is 4×10^6 gm. cm^2. Very roughly, the natural frequency of the system is then

$$f_n = \frac{1}{2\pi}\sqrt{\frac{2 \times 10^{11}}{4 \times 10^6}} = 35 \text{ cycles/second.}$$

The angular compliance X of the gear train introduces another mode of vibration into the system with a natural frequency of the order of $f_g = \frac{1}{2\pi}\sqrt{\frac{1}{XJ}}$. In order that the servomechanism can be made stable, it is necessary that $f_g \gg f_n$, that is $X \ll 5 \times 10^{-12}$ radians/dyne cm.

In designing the gear trains, an attempt was made to estimate X using the methods shown in Appendix I.

$X = X_t + X_d + X_g + X_b$, where

X_t is the compliance due to torsion in the shafts,

X_d is the compliance due to bending in the shafts,

X_g is the compliance due to deflection of the gear teeth, and

X_b is the compliance due to radial deflection of bearings.

The following estimates were made:

$X_t = 2 \times 10^{-13}$ radians/dyne cm.

$X_d = 2 \times 10^{-13}$ radians/dyne cm.

$X_g = 1 \times 10^{-13}$ radians/dyne cm.

$X_b = 1 \times 10^{-13}$ radians/dyne cm.

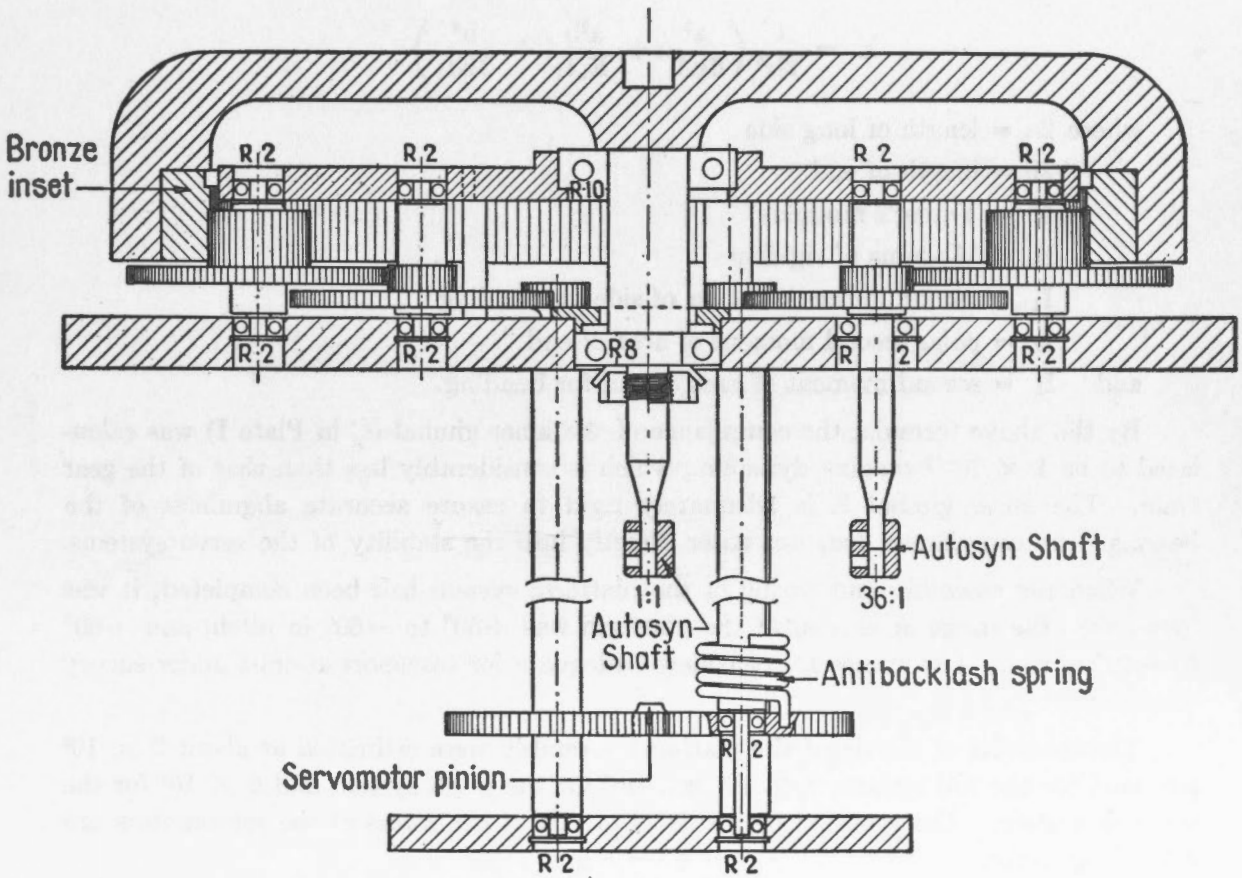

GEAR REQUIREMENTS PER UNIT

Gears:	Pinions:	
1" - 6¾" p.d. (internal)	2 - ¾" p.d.	All gears are A.S. Stub Tooth, Involute,
2" - 2" p.d (spur)	2 - ½" p.d	diametral pitch 48 and
2 - 2" p.d (")	2 - ½" p.d	pitch angle 20°.
2 - 1⅔" p.d (")	1 - ⅓" p.d	All gears cut from bronze, S.A.E. 62.
		All bearings tight tolerance bearings.

FIGURE 1.1.—High frequency gear train.

and the total compliance $X = 6 \times 10^{-13}$ radians/dyne cm., giving $f_g = 100$ cycles/second. Thus it would be expected that compliance in the gear trains would not contribute appreciably to instability of the servo system. The performance obtained in practice is discussed in section 1.4.

1.3.2 *The Design of the Platform Gimbals*

Resilience in the platform and gimbals can contribute to servo instability, and it is necessary to consider bending in the platform, the gimbals and the associated shafts and bearings. The best design aims at a reasonable compromise between rigidity and inertia.

The gimbals were machined from aluminum castings, with the long sides channeled and the ends left full for greater rigidity. The compliance of a gimbal about its axis of symmetry parallel to the long side is the sum of the compliance due to bending of the long sides, that due to bending of the ends, and that due to torsion in the ends; or

$$X = \frac{1}{2b^2}\left(\frac{a^3}{6EI_1} + \frac{a^2b}{E_nI_2} + \frac{b^3}{3EI_3}\right)$$

where $2a$ = length of long side
$2b$ = length of end
E = Young's modulus
E_n = Modulus of rigidity
I_1 = second moment of area of side for bending
I_2 = polar second moment of area of end
and I_3 = second moment of area of end for bending.

By the above formula, the compliance of the inner gimbal (C in Plate I) was calculated to be 1×10^{-13} radians/dyne cm., which is considerably less than that of the gear train. The outer gimbal E is adequately rigid to ensure accurate alignment of the bearings—its compliance does not enter directly into the stability of the servo systems.

When the assembly and wiring of the platform system had been completed, it was found that the range of motion of the platform was $+50°$ to $-60°$ in pitch, and $+60°$ to $-70°$ in roll. The ranges are considered adequate for transport aircraft under survey conditions.

The moments of inertia of the platform assembly were estimated at about 2×10^6 gm. cm^2. for the roll system, 1×10^6 gm. cm^2 for the pitch system and 6×10^5 for the azimuth system. The reflected moments of inertia of the rotors of the servomotors are 2×10^6 gm. cm^2.

1.3.3 *Gyroscope and Accelerometer Mounting*

The mounts fixing the gyroscopes to the platform must be rigid to avoid servo instability, but must also have a low thermal conductivity to reduce thermal distortion of the platform system and reduce warming-up time. The mounting rings of the platform gyroscopes and accelerometers are clamped down on bakelite insulating rings, $\frac{3}{16}$" thick, by means of annular aluminum clamps. The bakelite rings are countersunk into the platform. The natural frequency of the mount is designed to be 10^4 cycles/second.

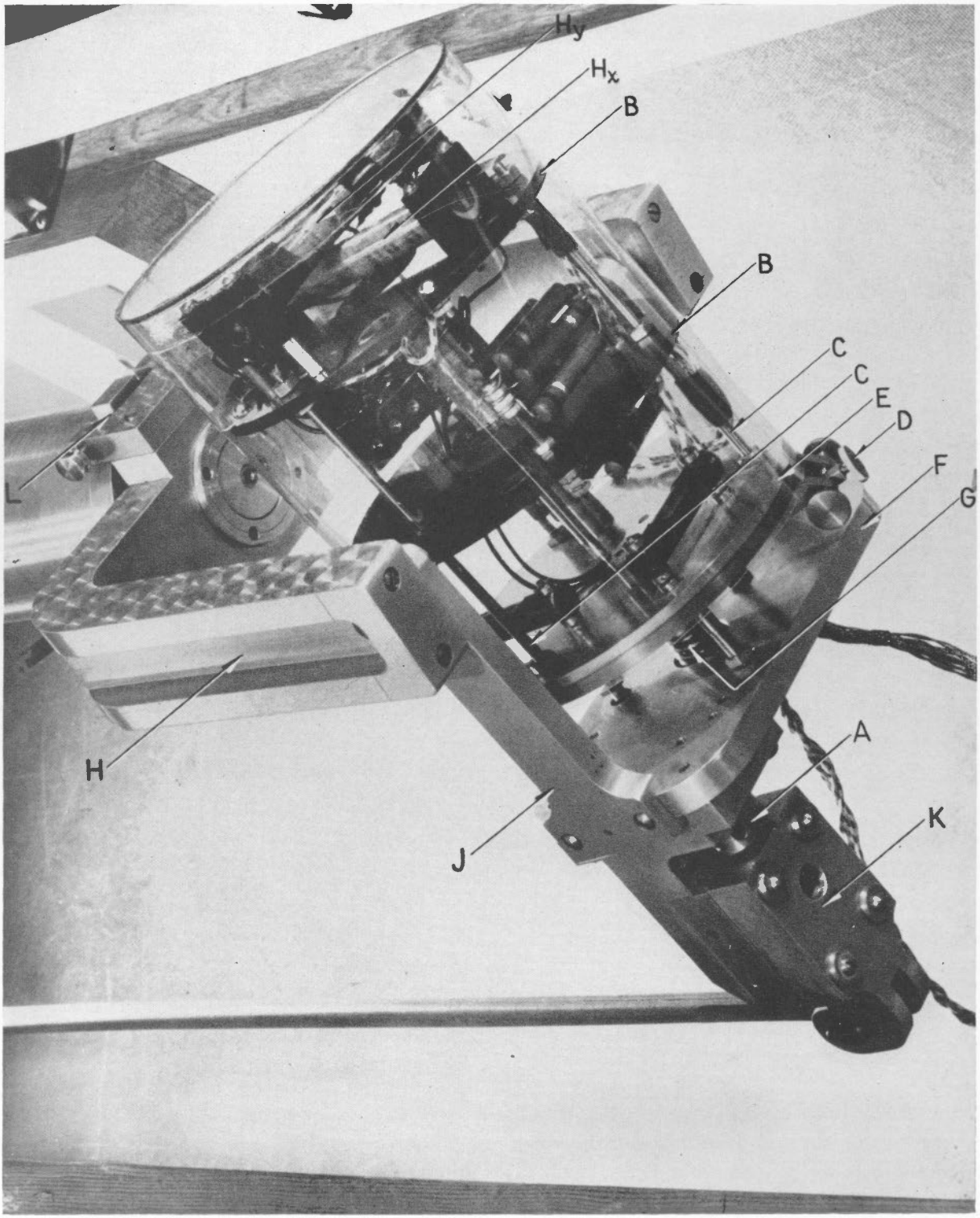

PLATE II—The magnetometer head.

1.3.4 *The Roll Transmission System*

The magnetometer yoke N (Plate I) is stabilized in roll by the pipe H connecting it rigidly to the inner gimbal C. The pipe is machined from a section of aluminum conduit, with inside diameter 3.07 inches, outside diameter 3.49 inches, and length 2.5 feet. Laboratory tests showed that at this distance the effect of magnetic components, such as ball bearings and servomotors, at the magnetometer head would be less than 10 gammas. The natural frequency of bending of the pipe with a 10-lb. load on the free end is nearly 60 cycles/second.

Cast aluminum plugs are welded into both ends of the pipe. The plug at the platform end carries an oilite collar which rotates in an oilite bearing in the outer gimbal E. The plug extends through the outer gimbal to the inner gimbal, to which it is clamped by a nut. The plug is 2.0 inches in diameter where it passes through the outer gimbal, and is strong enough to support a load of 100 lb. at a distance of 3 feet.

1.3.5 *The Pitch Transmission System*

As the aircraft pitches, the magnetometer platform is maintained parallel to the gyroscope platform by a mechanical linkage in the form of a parallelogram. The upper side of the parallelogram is 48 inches long and consists of the pipe H (Plate I), part of the inner gimbal C and the yoke N; the lower side is the $\frac{1}{2}$-inch-diameter aluminum link J. The ends of the parallelogram are 10 inches long and are formed by two platforms with their extensions projecting vertically downward (*see* K in Plate II).

In order that pitch angles with a range of $\pm 30°$ be transmitted with a maximum error of 1 minute, it is necessary that the horizontal sides of the parallelogram be equal to within .002 inches and the vertical sides be equal to .005 inches. The lengths of the link J (Plate I) and the vertical arm K (Plate II) can be adjusted by means of two turnbuckles. Each turnbuckle has threads of 12 to the inch and 13 to the inch operating differentially. A rotation of 60° changes the length by .001 inches.

The adjustment of the parallelogram is made on the ground by the following procedure. The gyroscope platform is rotated manually until the axis of the turntable is vertical within 0.2 minutes, as indicated by the level bubble on the turntable. The pitch level bubble in the magnetometer head is then brought to centre by means of the levelling screws under the head. One end of the platform assembly is raised by 2 feet, the gyroscope platform re-levelled and the transmission error read at the bubble at the magnetometer head. The error is read again with the other end of the platform assembly raised. The length of the horizontal link is adjusted to make the errors equal and of opposite sign. Then the vertical arm is adjusted to reduce the errors to less than 0.5 minutes, and the turnbuckles are firmly clamped.

It was calculated that, in operation, bending and compression in the parallelogram would produce errors of less than 0.1 minutes. No thermal distortion of the parallelogram could be observed as the gyroscopes heated or cooled.

The horizontal link is supported at each end by a $\frac{1}{4}$-inch bronze pin which turns in two R2 ball bearings set in the forked end of the vertical arm. Ball bearings are used to reduce backlash in the linkage. Their magnetic field is negligible at the magnetometer head.

86463—2½

1.3.6 *The Magnetometer Head*

The complete magnetometer head is shown in Plate II. The three orthogonal detecting elements and the thermostat heaters are mounted on the two bakelite plates, B. One of the two horizontal coils can be adjusted in azimuth relative to the other in slots in plate B. The axes of the detecting elements can be levelled by adjusting the nuts on the three threaded brass rods, C, which support the bakelite plates.

The non-magnetic base, E, of the magnetometer head contains a vertical axis with clamping screw D and two level bubbles similar to a theodolite base. The base is fixed to the magnetometer platform, F, by three threaded brass legs, which permit levelling the head assembly in pitch and roll independantly. A heavy brass spring, G, made of four turns of $\frac{1}{8}$-inch-diameter spring wire wound on a $\frac{3}{4}$-inch-diameter form, facilitates the levelling adjustment.

The platform F is made of 0.5-inch-thick aluminum and is supported from the magnetometer yoke H by substantial shaped aluminum arms, J. The two arms J carry at their upper ends 0.5 inch brass pins which turn in oilite bearings. One of the oilite bearings is a thrust bearing with a $\frac{1}{8}$-inch bakelite spacer between the arm and yoke.

The yoke was machined from an aluminum casting with a 2-by-1-inch section, except at the centre where it was thickened to three inches. The yoke has 1-inch channelled sides parallel to the roll axis. Tangent screws at L allow the yoke to be adjusted about the roll axis before it is clamped to the plug by a nut of $1\frac{1}{2}$-inch internal diameter.

The magnetometer platform assembly was designed to allow rotation of $\pm 70°$ in pitch. Great care was taken to avoid the use of any magnetic material in its construction.

1.3.7 *The Platform Mount*

This is seen in Plate I. The frame consists of wooden two by threes, with 1-inch runners, $1\frac{1}{2}$ inches deep and 42 inches long (P in Plate I), which fit into the channels of the outer gimbal, E. The outer gimbal is securely bolted by four heavy brass bolts to the frame, which is shockmounted to a sturdy wooden box, using four Lord multiplane shockmounts, Q. The box is tied to the floor of the aircraft using aluminum angle brackets and bolts, and is supplied with a cover fitted in three parts. This cover is not shown in Plate I.

The outside dimensions of the box, with cover on, are 81 inches long, 27 inches wide and $32\frac{1}{2}$ inches deep. The construction used is strong enough to avoid accidental damage to the platform under field conditions.

1.3.8. *The Shockmounting of the Units*

The centre of gravity of the mechanical system and its wooden frame is 28 inches from the outside edge of the frame and the total weight of the platform and frame is 127 pounds. The four dural multiplane vibration isolators, which shockmount the assembly, are placed symmetrically about the centre of gravity and separated along a line parallel to the roll axis by four feet. These shockmounts, designed so that their radial and axial spring rates are equal, can be seen at Q in Plate I. Shockmounts rated at 45 pounds load are used. From the data supplied by the manufacturer, it was estimated that

these should provide good vibration isolation at frequencies above about 12 c.p.s. Duraluminum assembling washers are used to form a mechanically interlocked system and to prevent excessive frame movement.

The estimated moment of inertia about a line through the centre of gravity parallel to the axis of pitch is 3.5×10^4 lb. in^2. From the deflection characteristics of the mounts it was calculated that the natural frequency of the system is 13 c.p.s. The corresponding force constant is 5.5×10^5 lb. in./radian. This natural frequency is somewhat low, but the low force constant did not produce instabilities in the platform servo systems at the natural frequencies achieved in practice. Similar considerations hold for vibrations about the roll axis.

It is convenient to note here that a number of 45-lb. vertical snubbing shockmounts are used to support the two chassis racks containing the electronic control equipment. Eight mounts are used for each rack and proved so successful in operation that no failures attributed to vibration have occurred in flight operation to date.

1.3.9 *The Azimuth Slip Ring System*

The directional gyro, K, of Plate I, and its turntable have complete freedom of rotation about a vertical axis, and therefore it is necessary to transmit signals and power to and from the units through slip rings and brushes. The slip rings are concentric silver rings cemented into a grooved plastic bed, which fits into the top plate of the azimuth gear train in the position shown in Figure 1.1. The brushes rotate with the gyro turntable, L. This design allowed uniformity of manufacture of the three platform gear trains, and avoided large increases in size, and hence in inertia, about the pitch axis.

The twelve rings were cut from a single silver plate, $\frac{1}{8}$ inch thick. They are $\frac{1}{10}$ inch wide and the spacing between successive rings is $\frac{1}{20}$ inch. The twelve screws making connection to the rings are brought out through a slot in the perspex plate. The brushes are of a commercial silver-graphite construction containing 85 per cent silver. Each brush is fitted with a flexible and a spiral spring. The brushes are divided into two groups of six, and mounted in two plastic blocks seated in the turntable L along a diameter, one on each side of the directional gyro mount, M. One of these blocks can be seen at R in Plate I. The brushes are held vertically in sleeves in the plastic blocks, and the spring compression is such that they operate at a pressure of about six lb./sq. inch. The frictional torque is then less than 0.2 lb. inch, or about one six-hundredth of the azimuth servomotor maximum output torque.

Eight of the twelve brushes have a cross-section 4mm $\times$ 3mm and four have a cross-section 10mm $\times$ 3mm. Two of the larger-section brushes are used to carry the directional gyroscope heater current. A switch at the gyroscope allows the selection of either the 5 or the 10-ohm heating coils. The lower resistance corresponds to a current of 5 amperes, or a current density of approximately 100 amp./sq. inch, and a potential drop across each brush of 0.2 volts. No trouble is caused by the relatively high figure of 1 watt brush dissipation while the gyroscope is warming up with the 5-ohm coil being used. After the gyroscope has reached operating temperature the brush dissipation is no longer continuous, and in any case is much reduced with the use of the 10-ohm heater.

The other two large brushes carry the much smaller single phase current to the gyroscope motor, and the eight smaller section brushes are distributed among the remaining circuits. In no case does the current through any of the smaller-section brushes exceed 100 m.a., which corresponds to a maximum contact drop of 3mV with these brushes and silver slip rings.

1.4 THEORY OF THE PLATFORM SERVOMECHANISMS

An outline of the theory of the pitch and roll servo systems is given below. The azimuth system is simpler theoretically but its performance is much the same.

In the design of the platform servomechanisms, two considerations are obvious. In order that the gyroscopes will not be disturbed, the servomotors should respond quickly to the angular motions of the aircraft, and should produce a large torque for small gyro errors, so that torques due to mechanical unbalance of the platform and flexure of the wiring will have a negligible effect. Preliminary measurements showed that, in rough air, angular velocities of the aircraft of 20°/sec. are not unusual. The ratio chosen for the platform gear trains (720 to 1) allows the servomotors to cancel angular velocities of the aircraft up to 44°/sec. The damping of the servo systems should be mainly of the error-rate type rather than viscous to avoid velocity-lag errors. Integral control was rejected because of the transient errors which it can introduce.

To obtain a value of the torque gain G on which the preliminary design can be based it is specified that the velocity-lag error at the platform should be less than 1 minute of arc for an angular velocity of the aircraft of 20°/sec. Then

$$G > \frac{\text{Angular velocity} \times \text{viscous damping}}{\text{velocity-lag error}}.$$

For the Kollsman Type R111-2A two-phase servomotors used on all three platform axes, we obtain $G > 2 \times 10^{11}$ dyne cm/rad., measured at the platform, corresponding to a torque of 4 ft. lb. for a displacement of the platform of 1 minute of arc.

The equations of motion of one of the servo systems are now described using the notation of Table 1.1. The gyroscope pick-off gives an electrical signal proportional to the error of the system, the angle ϕ. This signal is applied through an amplifier to a servomotor, producing a torque G(s) in a sense tending to reduce ϕ. The general case when the gyroscope output axis is at an angle θ to the true vertical is examined, and the equations of motion are obtained when the reference line in the aircraft is at an angle α to the true vertical. The relationships between the reference axis and the axes of the gyroscope are illustrated in Figure 1.2.

Consider torque about the axis Oz; then

$$T_1 = Hr - H\dot{\theta} - J_1(\ddot{\psi} - \ddot{\phi}) + K_1\dot{\phi} \qquad \text{Eqn. (1)}$$

Consider torque about the axis Oy; then

$$-G\phi = -N(J_2\ddot{\theta}_1 + K_2\dot{\theta}_1) - \frac{1}{X}\left[(\theta - \alpha) + \frac{\theta_1}{N}\right] + J_2\ddot{\alpha} \qquad \text{Eqn. (2)}$$

and $$-\frac{1}{X}\left[(\theta - \alpha) + \frac{\theta_1}{N}\right] = -H(\dot{\psi} - \dot{\phi}) + J_3\ddot{\theta} + K_3(\dot{\theta} - \dot{\alpha}) \qquad \text{Eqn. (3)}$$

TABLE 1.1—LIST OF SYMBOLS

Symbol	Meaning
J_1	Moment of inertia of gyroscope gimbal about output axis of gyroscope
J_2	Moment of inertia of servomotor driving platform
J_3	Moment of inertia about axis of rotation under discussion
K_1	Viscous damping constant between gyroscope gimbal and case
K_2	Viscous damping constant of servomotor
K_3	Viscous damping in gear train
N	Step down gear ratio between servomotor and platform
H	Angular momentum of gyroscope rotor
X	Angular compliance of gear train (angular deflection at output per unit torque)
G(s)	Frequency dependent torque gain of servo loop
r	Wander rate of gyroscope, including component of earth's rate
T_1	Torque applied about output axis to gyroscope gimbal by torque generator.
θ	Angle between true vertical and case of gyroscope
ϕ	Angle between Ox axis and axis of gyroscope rotor
ψ	Angle between true North and Ox axis
α	Angle of pitch or roll of aircraft frame
θ_1	Angle through which servomotor turns with respect to the aircraft frame

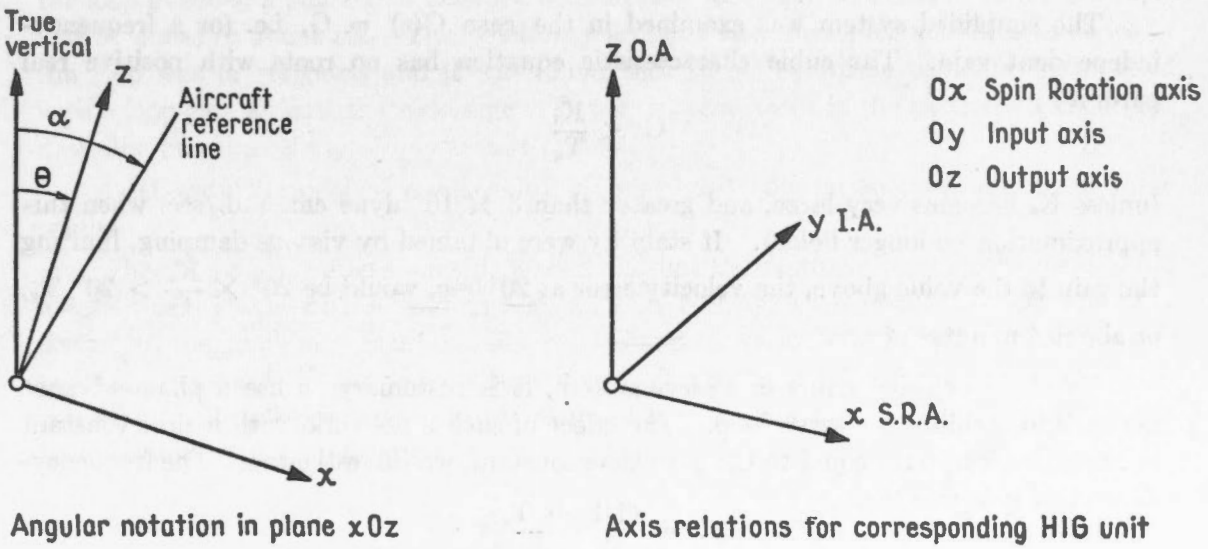

FIGURE 1.2.—Notation used in discussion of platform servomechanisms.

In equation (2) the term $J_2\ddot{\alpha}$ can be neglected since it represents the acceleration of the servomotor rotor through space, and is much smaller than $N J_{2\ 1}$.

Define $(\theta + \alpha) + \frac{\theta_1}{N} = \epsilon$ Equations (1) to (3) can be written in Laplacian notation

$$Hs\theta - (J_1s^2 + K_1s)\ \phi = -T_1 + Hr - J_1s^2\ \psi$$

$$N^2(J_2s^2 + K_2s)\ \theta + G(s)\ \phi - \left[N^2(J_2s^2 + K_2s) + \frac{1}{X}\right]\epsilon = N^2(J_2s^2 + K_2s)\ \alpha$$

$$(J_3s^2 + K_3s)\ \theta + Hs\phi + \frac{1}{X}\epsilon = Hs\psi + K_3s\alpha$$

The characteristic equation is then

$$\begin{vmatrix} Hs & -(J_1s^2 + K_1s) & 0 \\ N^2(J_2s^2 + K_2s) & G(s) & -\left[N^2(J_2s^2 + K_2s) + \frac{1}{X}\right] \\ J_3s^2 + K_3s & Hs & \frac{1}{X} \end{vmatrix} = 0 \qquad \text{Eqn. (4)}$$

The conditions for stability were investigated in two ways: in each case a preliminary study was made of a mechanically perfect gear box with $X = 0$, and hence $\epsilon = 0$. Then the characteristic equation reduces to

$$\begin{vmatrix} 1 & -(1 + T_gs) \\ (J_4s^2 + K_4s) & Hs + G(s) \end{vmatrix} = 0 \qquad \text{Eqn. (5)}$$

where $N^2J_2 + J_3 = J_4$, and $N^2K_2 + K_3 = K_4$ by definition, since $K_1 = H$ and $\frac{J_1}{K_1} = T_g$, the gyro time constant.

First Method: The system is known to be stable and non-oscillatory if there exist no roots of the characteristic equation with positive real parts.

The simplified system was examined in the case $G(s) = G$, i.e. for a frequency-independent gain. The cubic characteristic equation has no roots with positive real parts if

$$G < \frac{K_4}{T_g}$$

(unless K_4 becomes very large, and greater than 3×10^9 dyne cm./rad./sec. when this approximation no longer holds). If stability were obtained by viscous damping, limiting the gain to the value above, the velocity error at 20°/sec. would be $20° \times \frac{K_4}{G} > 20° \; T_g$, or about 4 minutes of arc.

To avoid velocity errors in a servo system, it is customary to use a phase-advance network to stabilize the servo loop. The effect of such a network, with a time constant in the phase lead term equal to the gyro time constant, was investigated. The frequency-dependent gain was then

$$G(s) = \frac{G(1 + T_gs)}{1 + \frac{T_gs}{M}}$$

where M is >1. The characteristic equation was a quartic and the condition for stability for reasonable values of K_4 became $G < \frac{MK_4}{T_g}$.

The determinantal method becomes very cumbersome if the non-rigid system with springiness is considered. If the effect of a frequency-dependent gain of the form

$$G(s) = G\,\frac{1 + T_1s}{1 + T_2s}$$

is investigated with a non-rigid system, the characteristic equation becomes sixth order.

However, an approximate trial determination with an error-rate network introducing a phase lead $T_1 = T_g$ showed that for stability in the compliant case

$$G < 8 \times 10^{11} \frac{1 + 2 \times 10^{-9} K_4 + 3 \times 10^{-21} \frac{K_4}{X}}{1 + 2 \times 10^{-9} K_4}$$

where G is in dyne cm./radian, and K_4 and X in c.g.s. units.

For a heavily damped gear box and a high-frequency gear train this reduces to the simpler condition $G < \frac{1}{X}$. Thus, for $G = 2 \times 10^{11}$ dyne cm./ rad, $X < 5 \times 10^{-12}$ rad./ dyne cm. This result was deduced earlier in the discussion of the design of the high-frequency gear trains. The degree of stability of the system is not determined by this algebraic method.

Second Method: The stability of the servo system was investigated by the Philbrick analog computer in the Division of Electrical Engineering in the National Research Council, Ottawa.

Because of the limited number of computer sub-units available, it was necessary to neglect the resilience of the gear trains. With this approximation the computer showed that the servo system should be stable with a torque gain of 2×10^{11} dyne cm./radian, if the loop included a phase lead network with a phase lead time constant of 10 milliseconds, and M equal to about six. The possibility of using two error-rate networks in series in the loop was investigated and it was found that stable operation could be maintained with a loop gain at least twice as large. Equal time constants in the two networks seemed desirable but the relationship was not critical.

A laboratory model of one servo loop was built and tested, and confirmed these results.

When the platform was built, it was found that the platform servomechanisms could not be made stable with a gain as high as 2×10^{11} dyne cm./rad. Consequently the design of the amplifiers was actually carried out empirically, trying different circuits and time constants in the phase-advance and filter circuits. The characteristics of the amplifier finally adopted as the most reliable over a reasonable range of adjustment can be expressed approximately by

$$G(s) = \frac{1 + .040\ s}{1 + .004\ s} \times 3.0 \times 10^{10} \text{ dyne cm./rad.}$$

Inserting this value of G(s) in equation (5), and neglecting some high-order terms and gear train damping, a characteristic equation of the third order is obtained:

$$s^3 + 1.7 \times 10^2\ s^2 + 4.7 \times 10^4\ s + 1.0 \times 10^6 = 0.$$

By well-known methods of solution (8), it can be shown that the transient error is then of the form $\theta = Ae^{-25t} + Be^{-74t} \cos 2\pi\ (32t)$. Thus transient errors decay to 10 per cent of their initial value in less than 0.1 seconds.

Although the loop gain achieved in practice is 7 times less than that aimed at in the design of the gear trains, the frequency of the oscillatory part of the preceding transient solution (32 cycles/sec.) approaches the natural frequency roughly calculated in section 1.3.1 (35 cycles/sec.). This may account for the lack of success in obtaining stability

at the higher gain. The velocity-lag error with the lower gain is of course 7 minutes of arc for aircraft velocities of 20°/second. It should be noted that the velocity-lag error of the gyroscope is equal to that of the platform since at operating temperature the gimbal transfer function of the gyroscope $H/K_1 = 1$.

1.5 THEORY OF THE VERTICAL STABILIZATION SYSTEM

Airborne vertical reference systems including various combinations of gyroscopes and accelerometers have been systematically compared by Mack (5) on the basis of their theoretical performances using gyroscopes now available. Mack's discussion of the system used in the three-component airborne magnetometer is reproduced here, with slightly modified notation.

The following notation will be used throughout this section:

In the horizontal plane

V = ground speed of the aircraft
D = angle between the ground speed vector and the roll axis of the aircraft
ψ = true heading of the roll axis of the platform
λ = west longitude
ϕ = north latitude
ω = angular velocity of the earth
g = acceleration of gravity
a = horizontal component of the acceleration of the aircraft with respect to the earth
a_v = vertical component of the acceleration of the aircraft with respect to the earth.

Two vertical planes are considered, one containing the roll axis and the other normal to it. The vertical stabilization system establishes reference directions, given by the directions of the spin axes of two HIG gyroscopes, from which angles can be measured. Angles measured in the plane containing the roll axis will be indicated by the subscript p for pitch, and those measured in the other vertical plane will be indicated by the subscript r for roll.

The true vertical is defined as the direction of gravity. This is not a fixed direction in space because the earth is rotating. The coordinate system chosen by the planes defined above is a non-inertial system because the aircraft to which it is attached may be subject to accelerations a, which are functions of time. According to D'Alembert's principle, we may treat it as an inertial system provided a fictitious force $-ma$ is supplied to each mass, m. The equilibrium position of a pendulum in this system is called the apparent vertical, and is in the direction of the vector sum of $-a$ and g. In normal flight a is much less than g.

An accelerometer is a device which measures the component of acceleration along its sensitive axis. Two Minneapolis-Honeywell HAU accelerometers are mounted on the stabilized platform. One accelerometer has its sensitive axis parallel to the roll axis of the platform, and the other is perpendicular to it. The outputs of the accelerometers

a_p and a_r thus contain the components of the vector acceleration a about the pitch and roll axis respectively, together with the components of gravity along their axes produced by platform tilt.

Since the acceleration vector can be resolved into two components, one $\frac{dV}{dt}$ parallel to the velocity vector, and the other $V\left[\frac{d\psi}{dt} + \left(\frac{d\lambda}{dt} - 2\omega\right) \sin \phi\right]$ normal to it, resolution along the roll and pitch axes of the platform gives

$$a_p = (g + a_v)\,\theta_p + \frac{d}{dt}(V \cos D) - V \sin D\left[\frac{d\psi}{dt} + \left(\frac{d\lambda}{dt} - 2\omega\right) \sin \phi\right] \qquad \text{Eqn. (6)}$$

$$a_r = (g + a_v)\,\theta_r + \frac{d}{dt}(V \sin D) + V \cos D\left[\frac{d\psi}{dt} + \left(\frac{d\lambda}{dt} - 2\omega\right) \sin \phi\right] \qquad \text{Eqn. (7)}$$

where θ_p, θ_r are the angles between the true horizontal plane and the roll and pitch axes of the platform respectively, i.e. are the components of platform tilt. Neglecting wind, equations (6) and (7) can be written

$$a_p = (g + a_v)\,\theta_p + \dot{V} \qquad \text{Eqn. (8)}$$

$$a_r = (g + a_v)\,\theta_r + V[\dot{\psi} + (\dot{\lambda} - 2\omega) \sin \phi] \qquad \text{Eqn. (9)}$$

We note that $-2\omega V \sin \phi$ is the horizontal component of the well-known Coriolis acceleration and $\dot{\lambda} \sin \phi$ is the rate of converging of meridians at latitude ϕ.

Let the natural wander-rates of the two gyroscopes used be r_p, r_r measured about the appropriate reference axes. The gyroscopes precess away from the vertical because the vertical changes direction in space as the earth rotates and as the aircraft moves over the earth's surface. The components of platform tilt, θ_p and θ_r also change when the aircraft heading changes. It can be shown that because an aircraft, even when flying straight, may have fluctuations in azimuth of the order of 2°, θ_p and θ_r must be less than 0.5° to keep any error in the system due to apparent gyroscope fluctuations less than one minute of arc. This difficulty is removed when the gyroscopes are mounted on the stabilized platform. The fundamental problem of vertical stabilization is to find a system satisfying

$$\theta_p = \theta_r = 0 \qquad \text{Eqn. (10)}$$

$$\dot{\theta}_p = \dot{\theta}_r = 0 \qquad \text{Eqn. (11)}$$

Equation (10) shows that some form of closed loop control must be used, and equation (11) can only be satisfied if corrections are applied at appropriate points in the loop to compensate for the effects described above. The closed loop control must also compensate for the natural wander rate of the gyroscope.

The linear erection system with integral control used for the airborne magnetometer is now described. In his discussion, Mack (5) has shown that this system makes fewer demands upon gyroscope performance than do the other schemes he described. The system is self-checking in that a change in wander-rate becomes apparent from a change in the output of the integrators. The platform can be erected at any time during flight, and oscillations of the system can be damped without introducing errors into the determination of the vertical.

Figure 1.3 shows the projections of the directions considered above as they appear on either of the planes of reference. A generalized symbol is used for both the roll and pitch cases, which are theoretically equivalent. Since in normal flight, horizontal accelerations are much less than g, $\delta = -a/g$.

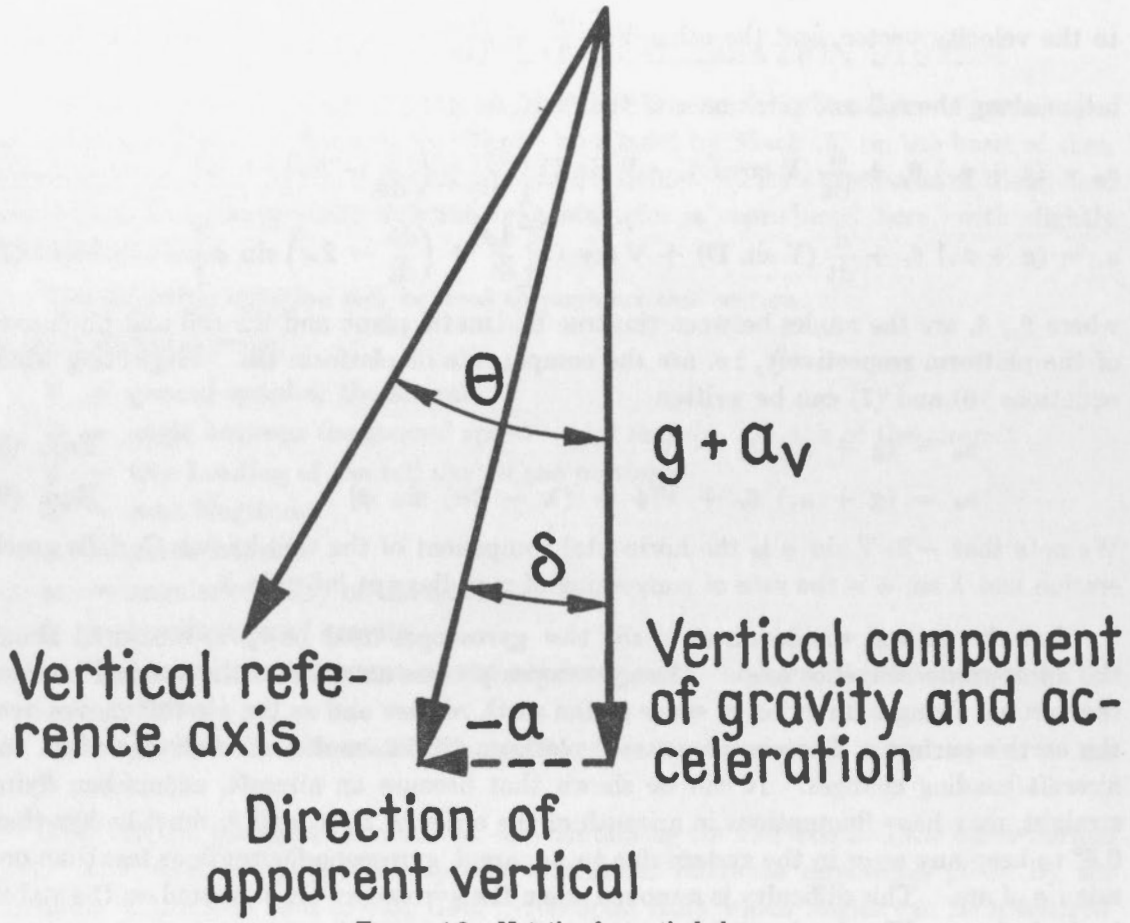

FIGURE 1.3.—Notation for vertical planes.

The control system produces a torque $F(t) \times (\theta - \delta)$ which erects the gyroscope according to the equation

$$\frac{d\theta}{dt} = r - \omega_c F(t) \times (\theta - \delta) \qquad \text{Eqn. (12)}$$

where r is the gyroscope wander rate, and ω_c is a reciprocal time constant.

Taking the Laplace transform of equation (12), we have

$$s\theta(s) = r - sY(s)\,[\theta(s) - \delta(s)] \qquad \text{Eqn. (13)}$$

where $s\,Y(s) = \omega_c\,L\,\{\,F(t)\,\}$

Assuming Y(s) is the transform of a linear differential operator,

then $$\theta = \frac{Y\delta}{1+Y} + \frac{\frac{r}{s}}{1+Y} \qquad \text{Eqn. (14)}$$

In equation (14), r represents the uncorrected and random wander rate of the gyroscope, the rate associated with the earth's rotation being compensated for.

The requirement that the system behaves as a sharp-cut-off filter to periodic accelerations δ, places a condition on the form of Y(s). A reasonably sharp cut-off is obtained if

$$\lim_{s \to \infty} \frac{Y(s)}{1 + Y(s)} \approx \left(\frac{\omega_n}{s}\right)^2 \to 0$$

where ω_n is a reciprocal time constant. The requirement for zero steady state error due to gyro wander is

$$\lim_{s \to 0} \frac{\frac{r}{s}}{1 + Y(s)} \approx k_1 s \to 0, \text{ i.e. } \lim_{s \to 0} s\, Y(s) \approx \frac{k_2}{s} \to \infty$$

From the consideration of these limits, it is deduced that a control Y(s) of the form

$$Y(s) = \left(\frac{\omega_n}{s}\right)^2 \frac{s^n + b_{n-1} s^{n-1} + \ldots + b_0}{s^n + a_{n-1} s^{n-1} + \ldots + a_0} \qquad \text{Eqn. (15)}$$

is required.

A mechanical filter has been described by Serson (6) and Mack (7) with a transfer function

$$Y(s) = \left(\frac{\omega_n}{s}\right)^2 \frac{s^2 + 2g_1 \omega_1 s + \omega_1^2}{s^2 + 2g_2 \omega_2 s + \omega_2^2} \qquad \text{Eqn. (16)}$$

In the present arrangement, a simpler function is used of the form

$$Y(s) = \left(\frac{\omega_n}{s}\right)^2 \frac{s + a\,\omega_n}{s + b\,\omega_n} \qquad \text{Eqn. (17)}$$

An electrical circuit with this transfer function consists of two integrators in series with a phase-lead network of the type used in error-rate damping. While the mechanical filter described by equation (16) has a slightly better transient response than the electrical filter described by equation (17), the flexibility of the electrical system permits a more accurate realization of the transfer function and in practice better transient response is achieved electrically. Figure 1.4 is a schematic diagram of the gyroscope control system with the transfer function of equation (17) obtained by using an electrical filter.

In the following development the effects of wind and the velocity of the aircraft with respect to the earth are neglected, and the platform is assumed to be nearly horizontal.

Equation (14) now becomes

$$\theta = \frac{\omega_n^2 (s + a\,\omega_n)\,\delta + s^2 (s + b\,\omega_n)\frac{r}{s}}{s^3 + b\,\omega_n s^2 + \omega_n^2 s + a\,\omega_n^3} \qquad \text{Eqn. (18)}$$

The characteristic equation is a cubic, and the relation between parameters for the optimum transient response is well known (8). The optimum values of a and b are $a = \frac{1}{4}$, $b = \frac{3}{2}$ and substituting these, equation (18) becomes

$$\theta = \frac{\omega_n^2 (s + \frac{1}{4}\omega_n)\,\delta + (s + \frac{3}{2}\omega_n)\,rs}{(s + \frac{1}{2}\omega_n)(s^2 + s\omega_n + \frac{1}{2}\omega_n^2)}$$

Solving for a unit step in wander rate, $r = \frac{1}{s}$, we obtain

$$\theta = \frac{s + \frac{3}{2}\omega_n}{(s + \frac{1}{2}\omega_n)(s^2 + s\omega_n + \frac{1}{2}\omega_n^2)}$$

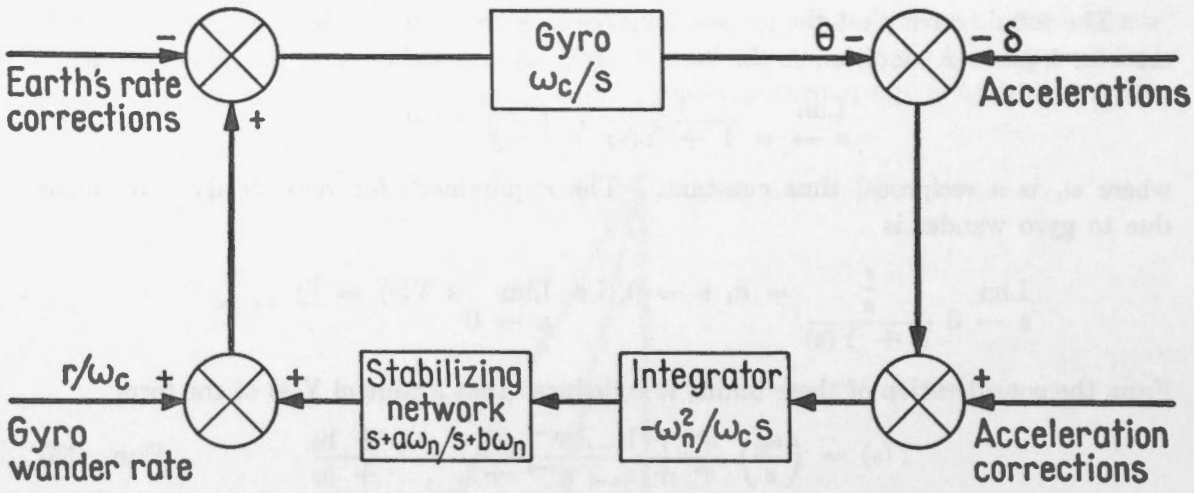

	Earth's Rate Corrections	Acceleration Corrections
Pitch plane	$\omega \cos\phi \sin\psi$	dV/dt
Roll plane	$\omega \cos\phi \cos\psi$	$V[d\psi/dt+(d\lambda/dt-2\omega)\sin\phi]$

FIGURE 1.4.—Schematic of gyro erection system.

The inverse Laplace transform of this yields the following transient response

$$h_c(t) = 4e^{-\frac{1}{2}\omega_n t} - e^{-\frac{1}{2}\omega_n t}\left[4\cos\tfrac{1}{2}\omega_n t - 2\sin\tfrac{1}{2}\omega_n t\right].$$

The response to a unit impulse in r is defined as

$$h_b(t) = L^{-1}\left[\frac{\frac{1}{s}}{1+Y}\right] = \frac{d}{dt}\left\{L^{-1}\left[\frac{\frac{1}{s^2}}{1+Y}\right]\right\} = \dot{h}_c(t)$$

and can thus be found by differentiation. The response to a unit impulse in δ is defined as $h_a(t) = -\dot{h}_b(t)$, since

$$h_a(t) = L^{-1}\left[\frac{Y}{1+Y}\right] = \frac{d}{dt}\left\{L^{-1}\left[\frac{Y}{s(1+Y)}\right]\right\}, \text{ and}$$

$$h_b(t) = L^{-1}\left[\frac{\frac{1}{s}}{1+Y}\right] = L^{-1}\left[\frac{1}{s} - \frac{Y}{s(1+Y)}\right]. \text{ Therefore}$$

$$h_a(t) = \frac{d}{dt}\left[L^{-1}\left(\frac{1}{s}\right) - h_b(t)\right] = -\dot{h}_b(t).$$

In Figure 1.5, $h_a(t)$, $h_b(t)$ and $h_c(t)$ are shown plotted as functions of time. Measurements in transport aircraft show that under good flying conditions, accelerations of the aircraft with periods of 1 or 2 minutes can be expected with amplitudes corresponding to a deflection of the vertical of 1 or 2 degrees. If the filtering action of the system is to attenuate these deflections to 1 minute of arc, the period of the system would have to be of the order of 15 minutes, and transients in the system would require a very long time to decay. As a compromise between good filtering and rapid decay of the transients,

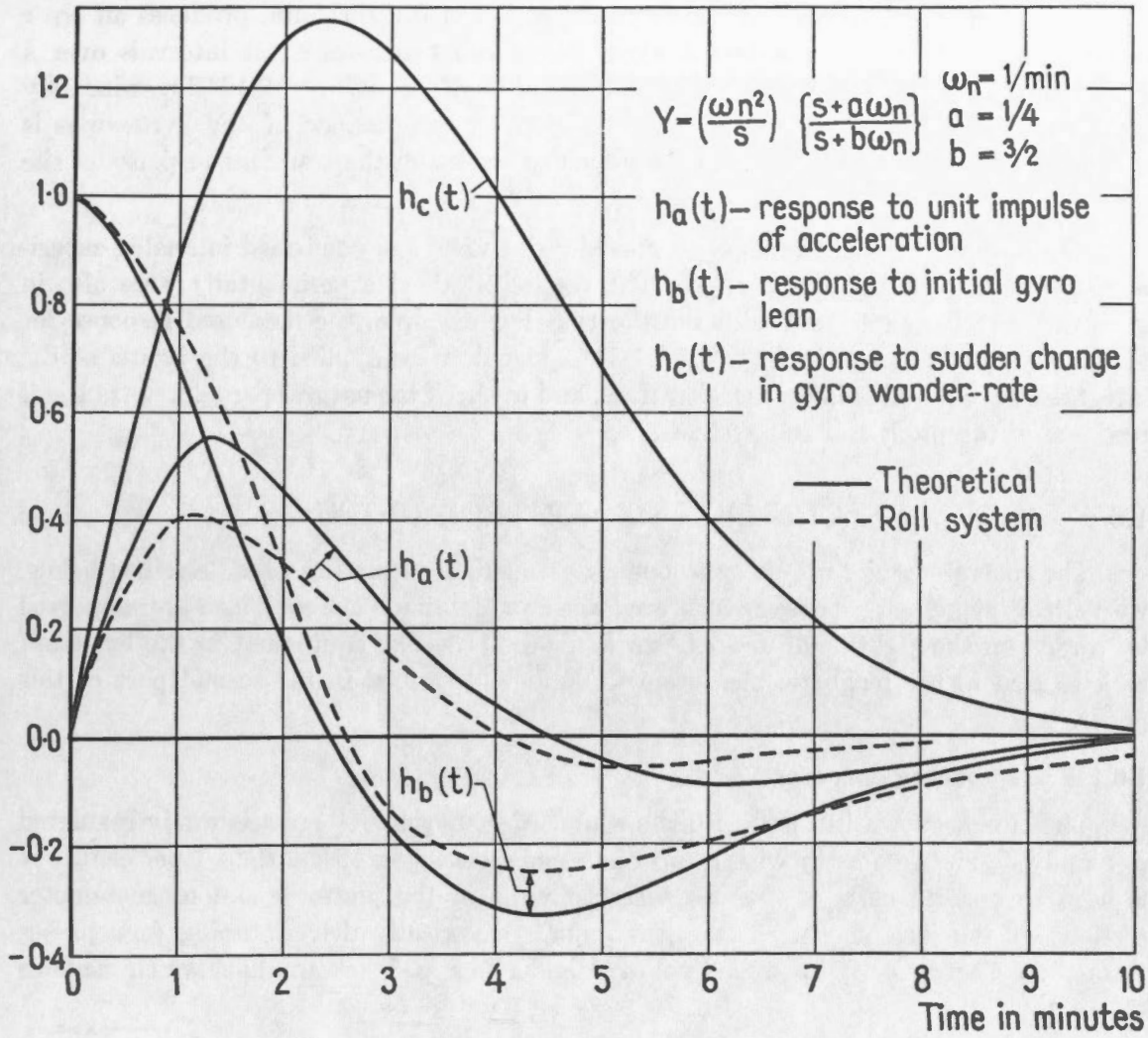

FIGURE 1.5.—Transient response of gyro erection system.

a period of 2 π minutes was chosen for the filter, making $\omega_n = 1.0$ per minute. All three types of transients then fall to at least a tenth of their maximum value within 8 minutes.

The curves may be interpreted by considering the following fictitious, though typical, information: (a) suppose that the system is given an acceleration of 1° lasting for 1 minute. The curve $h_a(t)$ shows that a peak error of 0.55° or 33 minutes will build up. Nine minutes after the impulse was applied the error is reduced to 1 minute of arc. (b) suppose the platform has an initial lean of 0.5°. The curve $h_b(t)$ shows that 9 minutes after, the lean is reduced to 1 minute of arc. (c) suppose the wander rate r of either of the two platform gyroscopes suddenly changes by 10°/hr. The curve $h_c(t)$ shows that an error of 13 minutes of arc is built up and after 9 minutes this error is reduced to less than a minute of arc.

If the wander rate of one of the two platform gyroscopes has a constant rate of change, an error

$$\epsilon = L^{-1}\left[\frac{bsr}{a\omega_n^2}\right] = \frac{b\dot{r}}{a\omega_n^2}$$

is produced in the platform. A wander acceleration of 0.1°/hr./min. produces an error of 0.6 minute of arc. A number of gyros have been bench-tested at intervals over a period of four years, and wander accelerations of 0.03°/hr./min. to 0.12°/hr./min. only were obtained initially. The later deterioration in performance of the gyroscopes is discussed fully in section 3.6, where the influence of this on the transient response of the platform is outlined.

The optimum transient response considered above was confirmed in analog experiments with the Philbrick computer. The results obtained experimentally were also in good quantitative agreement with the theory. For example, the measured response for the roll system is shown in Figure 1.5. D.C. signals were applied to the inputs of the integrators to simulate aircraft accelerations, and to check the natural period and transient response of the pitch and roll systems.

1.6 DESCRIPTION OF CONTROL CIRCUITS

The control circuits necessary to operate the stabilized platform are described below, with circuit diagrams. These circuits are built into aluminum chassis which are supported by a rack on the right-hand desk shown in Plate III. The equipment in the left-hand rack is used in the magnetic measurements and is described in the second part of this paper.

1.6.1 *The Frequency Standard*

The circuit shown in Figure 1.6 is a source of 400-cycle voltage accurately regulated in amplitude and frequency with a total harmonic distortion of less than 1 per cent. It is used to operate most of the computing circuits in the platform and magnetometer sections of the instrument. The output of an electrically driven tuning fork passes through an electronically controlled voltage divider to a feedback amplifier which includes

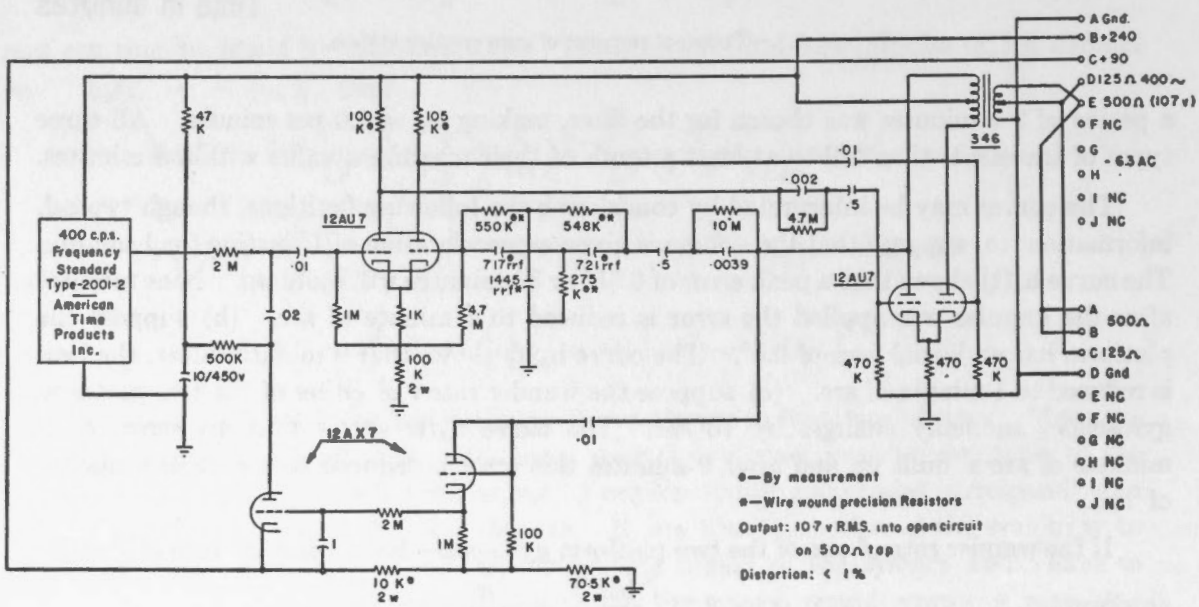

FIGURE 1.6.—Frequency standard.

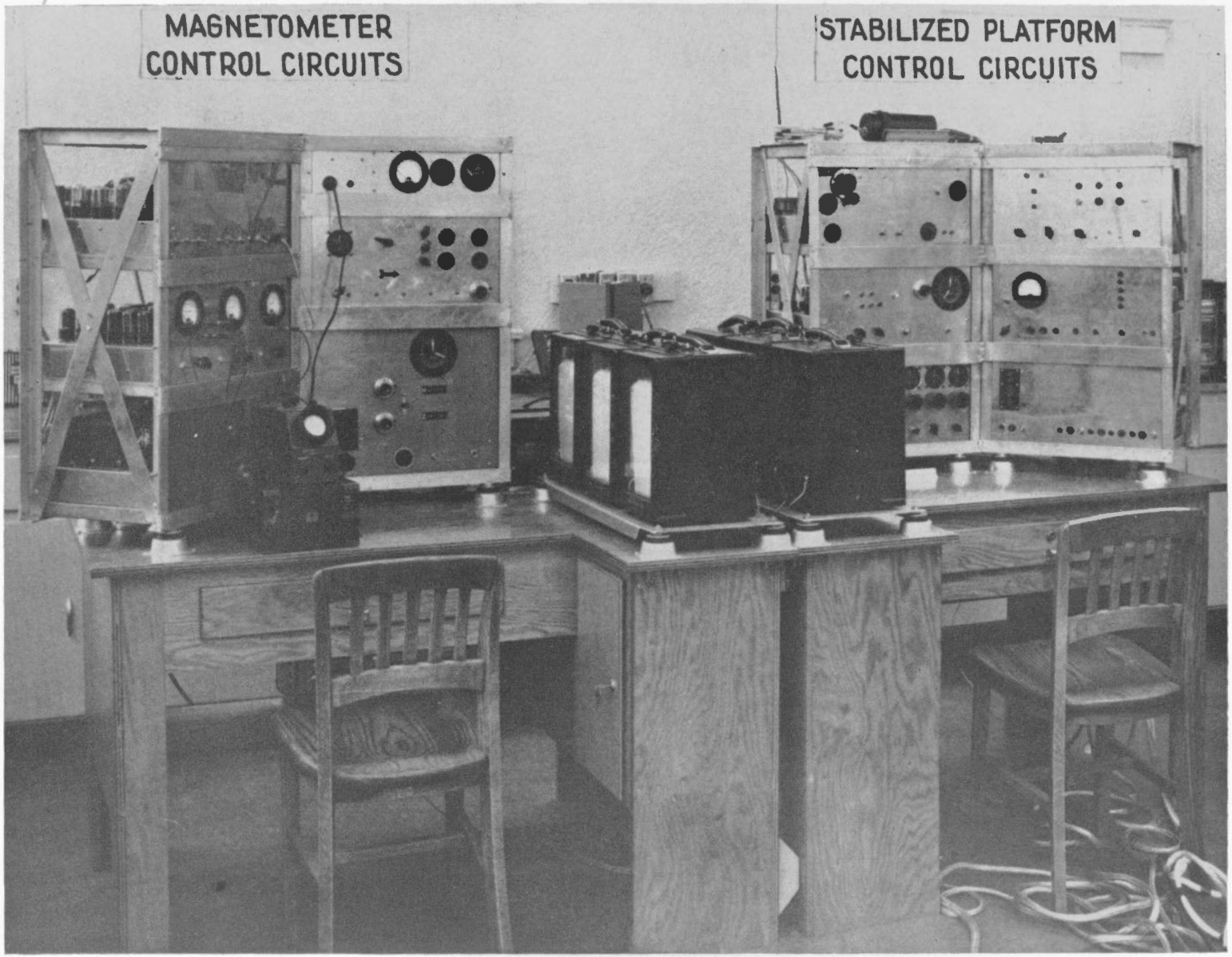

PLATE III—The control console.

a twin-T circuit to reduce harmonics. The output voltage of the amplifier is rectified and compared with a regulated D.C. reference voltage, and the difference controls the voltage divider.

When the magnetometer was first built, a 440-cycle tuning fork was used to avoid low-frequency beats with the 400-cycle aircraft inverters. Flight experience showed, however, that most aircraft inverters tend to operate nearer to 440 cycles than 400 cycles, and so the tuning fork was changed to a 400-cycle unit.

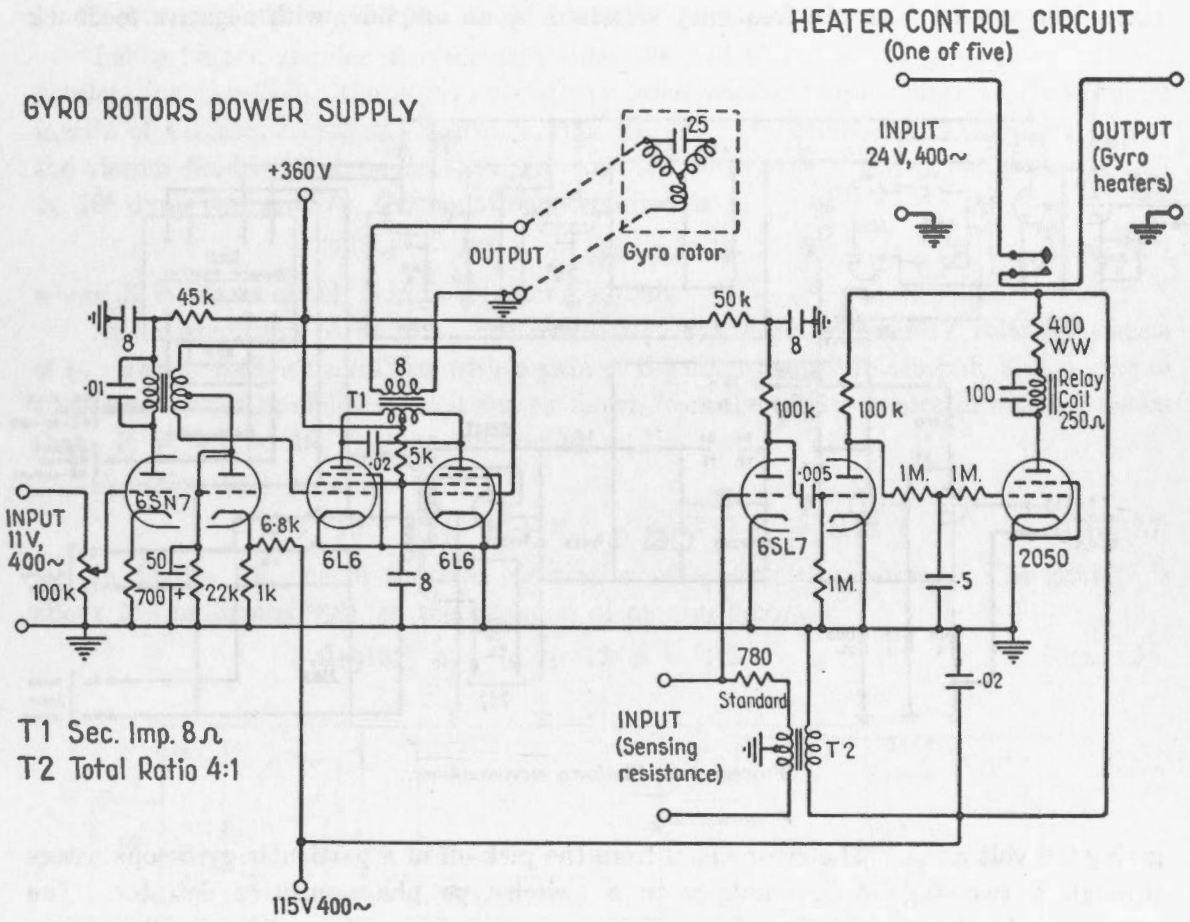

FIGURE 1.7.—Gyro rotor power supply and heater control circuit.

1.6.2 *Heater Control Circuits and Gyro Rotor Supply*

The temperatures of the gyroscopes and accelerometers are individually maintained at 165°F. by the heater control circuits shown in Figure 1.7. A temperature-sensing element in the unit is connected in a bridge circuit with a 780-ohm manganin resistor and a balanced transformer winding. The transformer is excited at 400 cycles, and the error signal of the bridge is amplified, rectified and applied to the control grid of a thyratron. The thyratron controls a relay which applies 400 cycle A.C. to a heater winding in the unit. When the temperature of the unit reaches 165°F., the resistor of the sensor is 780 ohms, the bridge balances cutting off the thyratron and the relay opens the heater circuit. The sensitivity of the circuit is limited by noise induced in the sensor winding to about 0.7°F. Warning lights supply a visual check on the operation of the heater units.

Power to operate the rotors of the three gyroscopes is supplied by a common class AB_2 push-pull power amplifier excited from the frequency standard. Each gyroscope has its own phase-splitting capacitor to give three phases from the single phase supply.

1.6.3 *The Platform Servoamplifiers*

Figure 1.8 shows the circuit of one of the three platform servoamplifiers with their common power supply and pick-off excitation amplifier. The gyroscope pick-offs are excited in parallel from the frequency standard by an amplifier with negative feedback

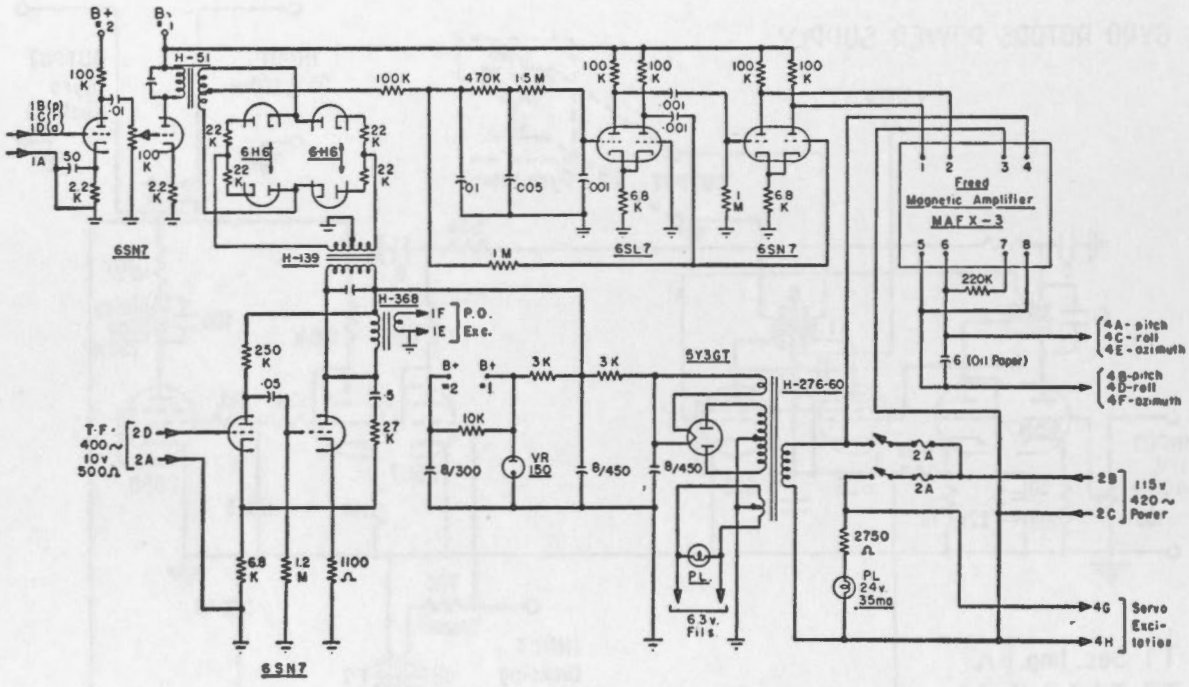

FIGURE 1.8—Platform servoamplifier.

giving 0.5 volt r.m.s. The error signal from the pick-off of a particular gyroscope passes through a two-stage A.C. amplifier to a switch-type phase-sensitive detector. The output of the detector is filtered and applied to two balanced amplifiers. The output of the first of these amplifiers is added, through an A.C. coupling network with a time constant of 1 millisec. to the output of the phase-sensitive detector at the grids of the second amplifier. The first amplifier thus introduces a phase advance of about 40 millisec. accompanied by a lag of 1 millisec.—corresponding to a phase-advance network with M = 40 (section 1.4). The filter following the phase-sensitive detector adds another lag of about 3 millisec. The plates of the second amplifier are connected to the control winding of a fast-response magnetic amplifier. A small amount of negative feedback is introduced around the magnetic amplifier (by the 220 K resistor) to increase its linearity and stability. The servoamplifier gives its full output of 10 watts into one winding of the servomotor for a steady input signal of 40 millivolts when the gain is adjusted for 3×10^{10} dyne cm./rad. The other winding of the servomotor is connected across the 115-volt 400-cycle line.

1.6.4 *The Accelerometer Control Circuits*

The accelerometers (Minneapolis-Honeywell HAU) are similar to the HIG gyroscopes except that, instead of a gyroscope rotor, the floated can contains a mass displaced from the axis of rotation of the can. The output signal of the pick-off is amplified and applied to the torque generator to produce a torque which tends to maintain the pick-off in its null position. When the accelerometer is subjected to an acceleration parallel to its axis of sensitivity, the torque necessary to accelerate the off-centre mass is supplied by the torque generator, and the torque generator current is a measure of the acceleration.

Let ϕ be the angular displacement from the null of the signal generator when the acceleration parallel to the input axis of the accelerometer is $g\delta$. Since the moment of inertia of the accelerometer element is 300 gm. cm.^{2}, the coefficient of damping due to the viscous fluid is 10^5 dyne cm./rad./sec. and the sensitivity of the accelerometer is 1.18×10^5 dyne cm./gravity, the equation of motion is

$$300\ \ddot{\phi} + 10^5\ \dot{\phi} + K\phi = 1.18 \times 10^5\ \delta \qquad \text{Eqn. (22)}$$

where K is the feedback gain in dyne cm./radian.

At an excitation of 55 m.a., the sensitivity of the pick-off is 18.7 volts per radian of ϕ. For a feedback amplifier with a gain of G milliamps per volt input, and a torque generator excitation of 100 m.a., it can be shown from the torque generator characteristics that $K = 4.7 \times 10^3$ G dyne cm./radian.

Equation (22) becomes

$$3 \times 10^{-3}\ \ddot{\phi} + \phi + 4.7 \times 10^{-2}\ G\ \phi = 1.18\ \delta \qquad \text{Eqn. (23)}$$

In Figure 1.9, one of the two identical control circuits is shown. The gain G is about 250 milliamps/volt, so the equation of motion becomes

$$3 \times 10^{-3}\ \ddot{\phi} + \dot{\phi} + 12\ \phi = 1.2\ \delta \qquad \text{Eqn. (24)}$$

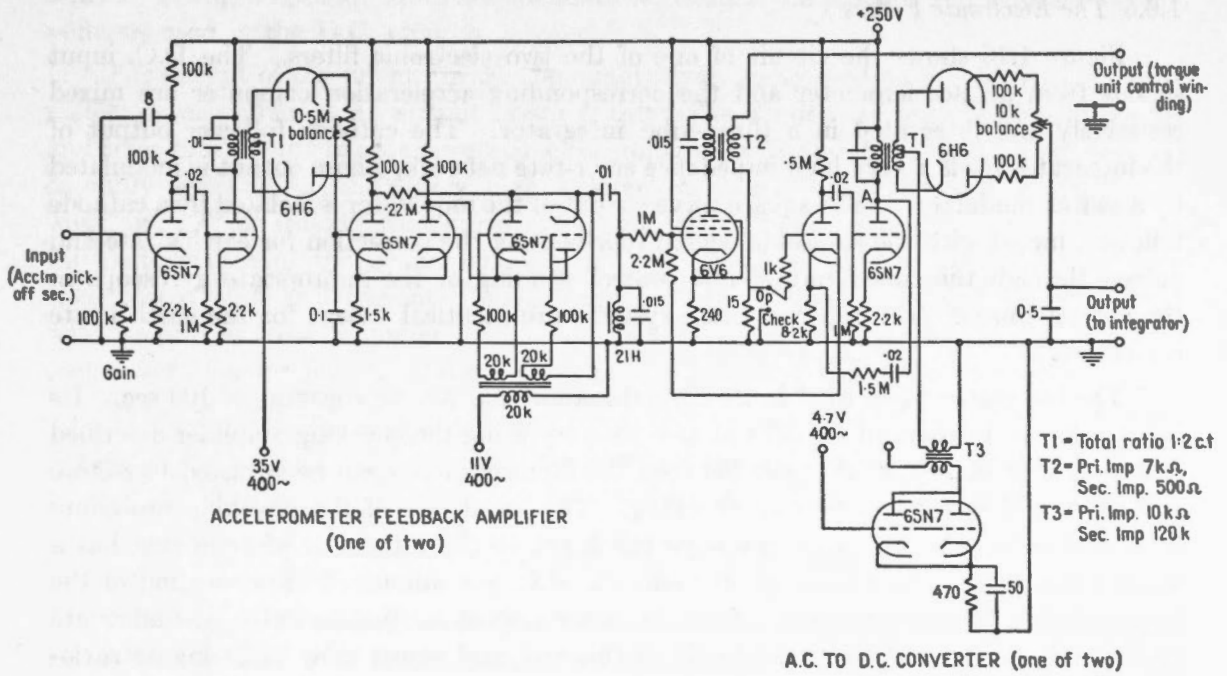

FIGURE 1.9.—Accelerometer control circuit.

The accelerometer is required to have a range corresponding to $-5° < \delta < +5°$. At the maximum accelerations, ϕ becomes 30 minutes of arc. The longer time constant of the accelerometer system is 80 milliseconds. When a higher gain was used the feedback loop became unstable because of amplifier lags.

When $\delta = 1$ minute of arc, the minimum detectable acceleration in which we are interested, $\phi = 0.1$ minute and this corresponds to an in-phase signal of 0.7 millivolt against a total noise background of 30 millivolts. It is necessary therefore to amplify, convert to D.C., amplify and modulate the output. The output current in the control winding of the torque generator passes through a 15-ohm resistance. The in-phase voltage across this resistance is proportional to the acceleration being measured.

The 6V6 output tube can deliver a maximum output of 60 milliamps corresponding to a torque of 1.5×10^4 dyne-cms. or $\pm 7.3°$ of δ. This range of acceleration was quite satisfactory in this application. The null voltage across the control winding was 0.1 volt quadrature and second harmonic. Provision was made in the circuit for a balancing adjustment. A small feedback ratio across the 6V6 helps stabilize the phase of the 400-cycle voltage across the 15-ohm resistance.

This 400-cycle voltage proportional to acceleration is amplified by an amplifier whose gain is stabilized by negative feedback, and converted to D.C. by a phase-sensitive detector supplied with a large reference voltage for linearity. One minute of δ is equivalent to an in-phase voltage of 2.06 millivolts across the 15-ohm resistance, and the gain was adjusted by feedback so that this produced 100 millivolts D.C. at the output of the phase-sensitive detector. The output was a linear function of the input to $\pm$ 30 volts ($\delta = \pm 5°$), after which the gain decreases. At the maximum output of $\pm$40V, the gain has decreased by 15 per cent. Provision was made for zeroing the acceleration output circuits.

1.6.5 *The Electronic Filters*

Figure 1.10 shows the circuit of one of the two electronic filters. The D.C. input signals from an accelerometer and the corresponding acceleration computer are mixed resistively and integrated in a three-tube integrator. The cathode follower output of the integrator feeds a very high impedance error-rate network, whose output is modulated by a switch modulator. The square wave output of the modulator is isolated by a cathode follower, mixed with the sinusoidal signal representing the correction for earth's rate and passed through the tuned torque-unit control winding of the appropriate gyroscope in the correct phase. The roll and pitch systems are identical except for the earth's rate correction.

The integrator when used in its normal manner has a time constant of 100 sec. Its input grid can be checked for drift at any time by using the checking amplifier described later. A balancing potentiometer between the input cathodes can be adjusted to restore the input grid voltage to zero on checking. The sensitivity of this checking procedure is 10 millivolts, which is sufficient since the input to the integrator after mixing has a value corresponding to a scale of 50 millivolts D.C. per minute of arc deflection of the apparent from the true vertical. In flight, after a short settling period it was adequate to check the zeros of all the D.C. circuits of this sort, and adjust their balancing potentiometers accordingly, about once each hour. Laboratory tests on this D.C. circuit showed

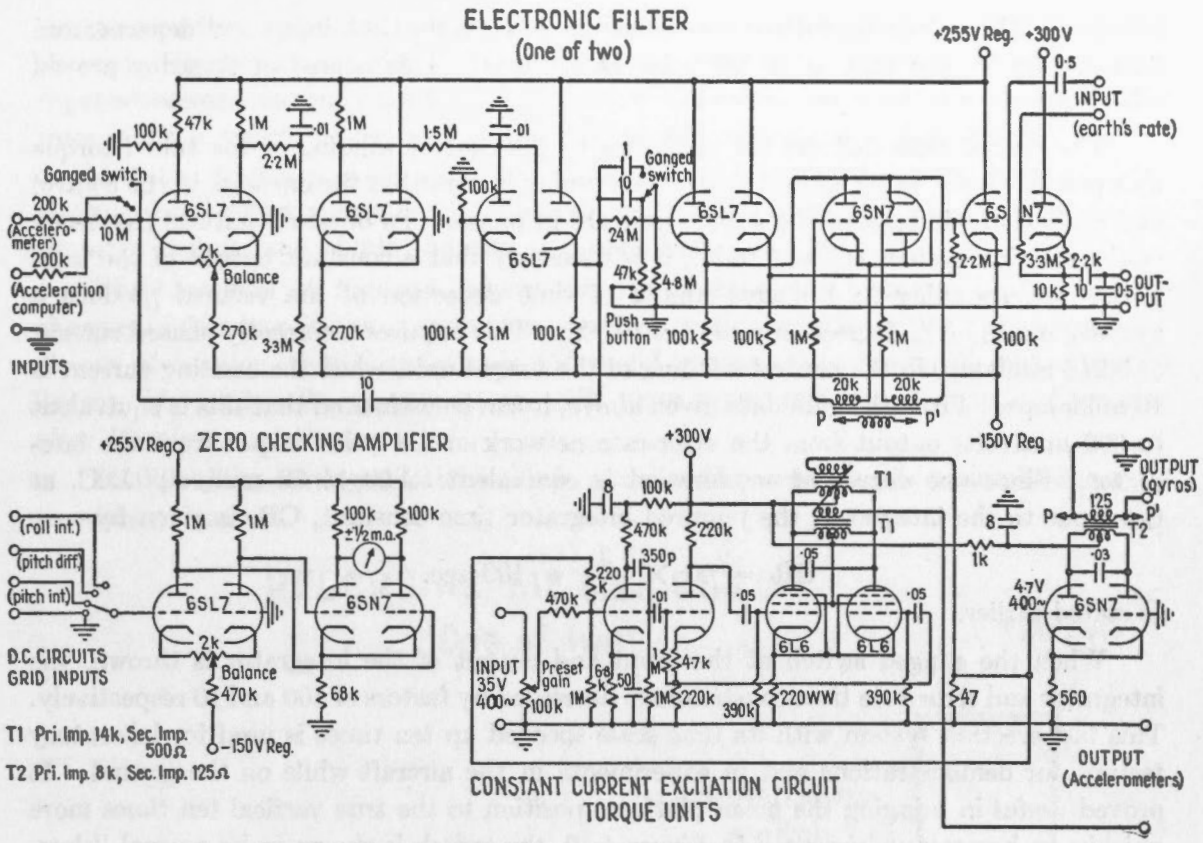

FIGURE 1.10.—Electronic filter and constant current excitation circuit.

that a 10 per cent change in heater voltage produced a cathode potential change of about 4 mV. Voltage regulator tubes are adequate to regulate the positive and negative supply voltages used in the D.C. circuits.

The output of the integrator can be qualitatively monitored on a ± 50 V panel voltmeter, or measured at an output check point. The condensers used in the integrator and error-rate circuits to obtain long time constants were 10 microfarad oil-filled condensers, carefully selected for their very high leakage resistance and freedom from condenser 'soaking'. Their leakage resistances are greater than 10^9 ohms. and no deterioration in the performance of the condensers was found over three years. No difficulties were encountered with grid currents, but leakage across the input tube pins in very humid weather proved troublesome at first. This leakage was eliminated by cleaning the tube socket very thoroughly, and taking great care in soldering the socket connections.

The maximum output of the integrator is ± 40 volts; since the time constant is 100 secs., the integrator is easily capable of handling accelerations of 2 degrees lasting for 2 minutes, which are the maximum accelerations normally found in flight. The required output is

$$120 \int_0^{120} \frac{50 \times 10^{-3}\ dt}{100} = 7.2 \text{ volts.}$$

The error-rate network is straight-forward, with its time constant of 240 secs. (corresponding to $a\omega_n = \frac{1}{4}$ per minute) and D.C. gain of $\frac{1}{6}$ (corresponding to $a/b = \frac{1}{4}/\frac{3}{2} = \frac{1}{6}$). To avoid loading the network, the switch modulator was fed from a cathode

follower. The switch modulator was linear to ± 15 volts D.C. input and departs from linearity by 12 per cent at ± 30 volts D.C. input. This degree of linearity proved adequate.

The output tube delivers 2.0 milliamps to the control winding of the tuned torque unit per volt input at its control grid. The tuning is such that the currents in the control and excitation windings of the torque unit are in phase. To obtain a natural frequency of the erection system $\omega_n = 1/\text{min.}$, it is necessary that a constant output of the integrator corresponding to 1 degree-minute of time deflection of the vertical produce a gyroscope rate of $^3/_b$ degrees/minute, i.e. 10°/hr. This requires a correctly phased current of 0.216 milliamp. in the control winding of the torque unit, when the exciting current is 10 milliamps. From the gain data given above, it can be estimated that this is equivalent to 300 millivolts output from the error-rate network or 1.8 volts output from the integrator. Since one degree of acceleration is equivalent to 60 × 50 millivolts D.C. at the input to the integrator, the required integrator time constant, CR, is given by

$$CR = 60 \times \frac{3}{1.8} = 100 \text{ sec.}$$

as stated earlier.

When the ganged switch at the input and output of the integrator is thrown, the integrator and error-rate time constants are decreased by factors of 100 and 10 respectively. This fast-erection system with its time scale speeded up ten times is used for laboratory testing, for demonstrations and in experiments in the aircraft while on the ground. It proved useful in bringing the mean platform position to the true vertical ten times more quickly on becoming airborne. In Figure 1.10, the switch is shown in its normal "slow-erection" position. The integrator time constant must be changed by 10^2 (rather than changing the gain of the torque unit amplifier for instance) so that when the system has reached equilibrium the output of the integrator will be at the proper level when the switch is thrown to "slow-erection".

In order to avoid transients in the system due to the apparent change in rate of the platform gyroscopes when the heading of the aircraft changes, torques are applied to

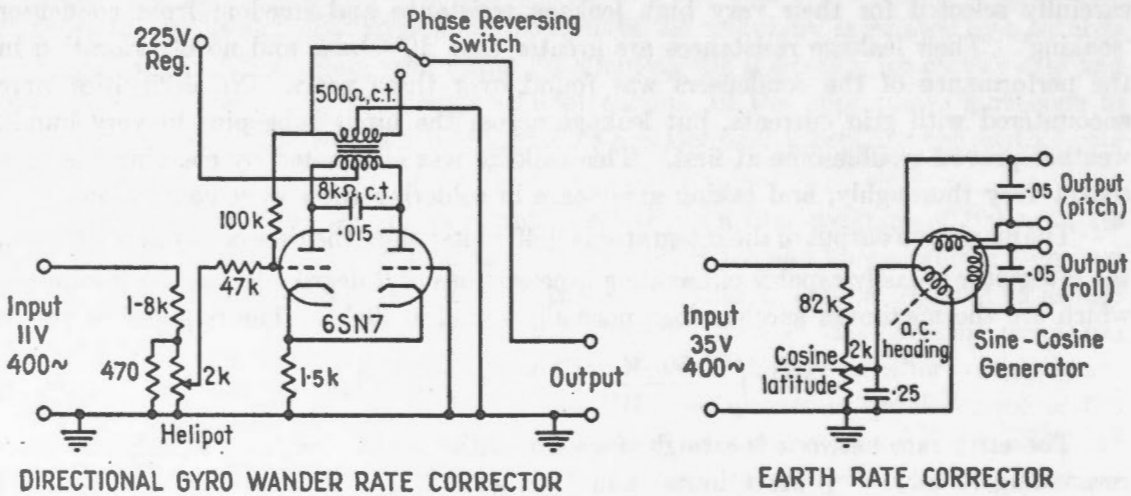

FIGURE 1.11.—Gyro rate corrector circuits.

the gyroscopes proportional to the components of the earth's rotation. The method is shown in Figure 1.11. A 400-cycle voltage proportional to the cosine of latitude ϕ, from a potentiometer manually set to the latitude, is applied to the rotor of a resolver. The rotor shaft is set manually to the heading of the aircraft, ψ. The voltages induced in the stator windings, $\omega \cos \phi \sin \psi$ and $\omega \cos \phi \cos \psi$, are added to the outputs of the pitch and roll filters respectively. The resolver windings are tuned to minimize potentiometer loading, and obtain the correct phase of the outputs.

The curve $h_e(t)$ of Figure 1.5 shows the type of transient which would occur on large changes of heading if these corrections for the earth's rotation were not applied. A change of heading of 180° at latitude 45° would produce a maximum platform error of $2\omega \cos 45° \times 1.3 = 28$ minutes of arc. The error would reduce to 1 minute of arc only after 10 minutes of time.

In flight, the settings of the latitude and heading controls are maintained correct to within 5° or so.

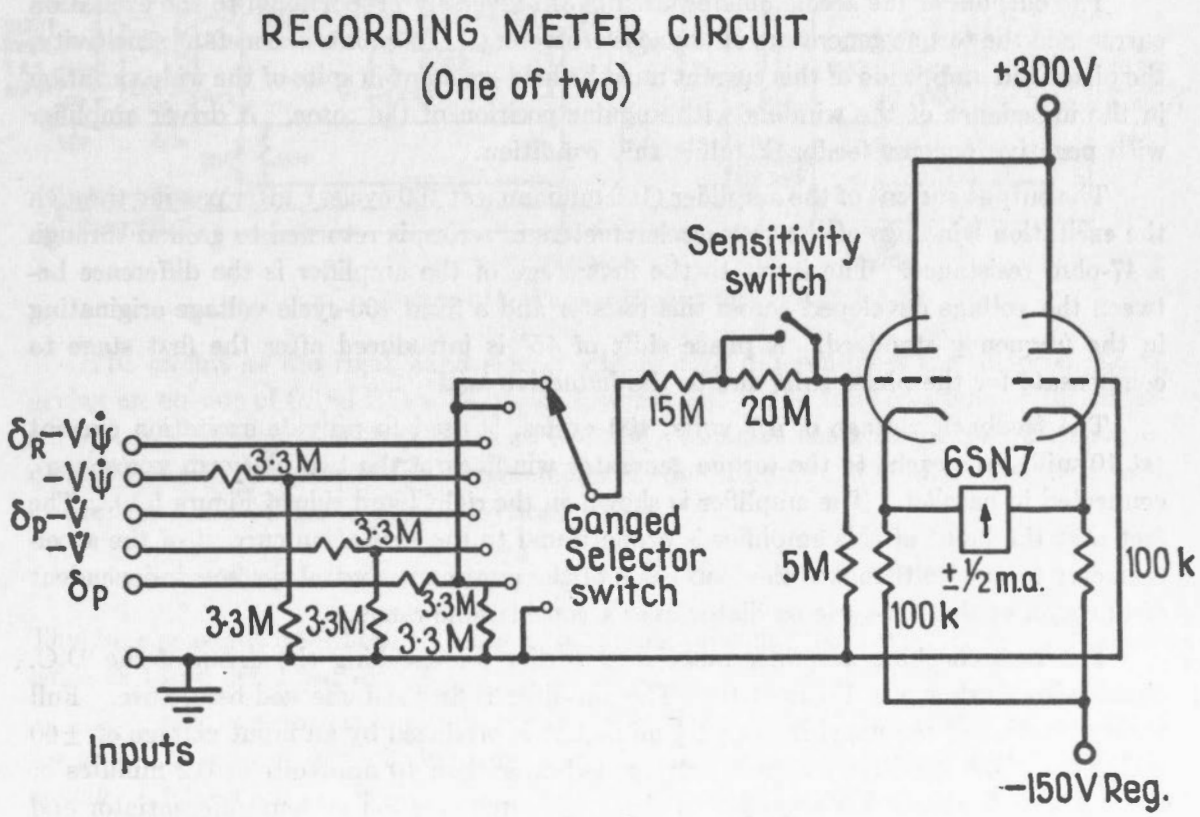

FIGURE 1.12.—Recording meter circuit.

1.6.6 *The Recording Meter Circuits*

The input signals to the electronic filters are recorded by means of two Esterline-Angus Strip Chart meters. The chart drives are mechanically coupled and operate at $\frac{3}{4}$ inch per minute. Figure 1.12 shows one of the two meter amplifiers.

A selector switch at the input of the amplifiers allows recording of 8 different combinations of signals δ_p, δ_r, $-\dot{V}$, $-V\dot{\psi}$, $\delta - \dot{V}_p$, $\delta_r - V\dot{\psi}$, using the notation of section

1.5. Two sensitivities are provided, corresponding to meter ranges of $\pm 5°$ of δ and $\pm 2\frac{1}{2}°$ of δ. Linearity, accuracy of scale adjustment ($\pm 3\%$), and zero stability are satisfactory.

These meter records are very important in the evaluation of the platform performance. It is possible to examine them to determine the performance of the acceleration computation and correction methods used, to investigate platform transient response and to estimate the accuracy of stabilization to about five minutes of arc under steady flight conditions. In the positive identification of magnetic anomalies, this is very helpful.

It should be clear that such records constitute the data upon which the design of this stabilizing system can best be modified; the choice of the natural frequency of the gyroscope erection system depended on the spectrum of long period accelerations deduced from the records obtained using an earlier model (6, 7) of the stabilized platform.

1.6.7 *The Torque Generator Excitation Circuit*

The outputs of the accelerometer circuits are inversely proportional to the excitation currents in the torque generators of the accelerometers. To maintain constant sensitivity, the phase and amplitude of this current must be held constant in spite of the wide variation in the impedance of the winding with angular position of the rotor. A driver amplifier with negative current feedback fulfils this condition.

The output current of the amplifier (100 milliamps at 400 cycles), after passing through the excitation windings of the two accelerometers in series, is returned to ground through a 47-ohm resistance. The input to the first stage of the amplifier is the difference between the voltage developed across this resistor and a fixed 400-cycle voltage originating in the frequency standard. A phase shift of 45° is introduced after the first stage to compensate for the phase shift due to the inductive load.

The feedback voltage of 4.7 volts, 400 cycles, is used to provide excitation current (at 10 milliamps each) to the torque generator windings of the two platform gyroscopes, connected in parallel. The amplifier is shown on the right hand side of Figure 1.10. The fact that the input of this amplifier is proportional to the excitation current of the accelerometer torque units makes the loop gains of the gyroscope control systems independent of the level of the 400-cycle oscillator over a considerable range.

The zero checking amplifier mentioned earlier for checking the drifts of the D.C. circuits is also shown in Figure 1.10. The amplifier is first self checked before use. Full scale deflection of the panel meter ($\pm \frac{1}{2}$ milliamp) is produced by an input voltage of ± 60 millivolts. The sensitivity of zero settings is better than 10 millivolts or 0.2 minutes of arc. A switch allows this amplifier to check the pitch erection system differentiator and integrator, and the roll system integrator. The action of checking does not disturb the operation of the circuit being checked.

1.6.8 *The Pitch Acceleration Computer*

If wind velocity is neglected, the fore-and-aft component of the acceleration of the aircraft is simply $\dot{V}$, the rate of change of airspeed. This approximate acceleration is automatically computed as a D.C. voltage, and subtracted from the pitch accelerometer output by the resistive network at the input to the pitch system integrator.

Airspeed is supplied continuously to the acceleration computer by a Kollsman True Airspeed Meter (Type 1239 B-O-4) in the form of a synchrotel output signal with a sensitivity of 36°/100 knots and a range of 0 to 650 knots. The shaft of a 10-turn precision potentiometer with a resolution of 1 part in 10,000 is driven by a servomotor and autosyn combination to follow this signal at a ratio of 10.8°/knot. Since a steady D.C. potential of 105 volts is applied across the potentiometer, a D.C. signal proportional to the airspeed, at 0.186 volt/ft./sec. is obtained at the slider of the potentiometer.

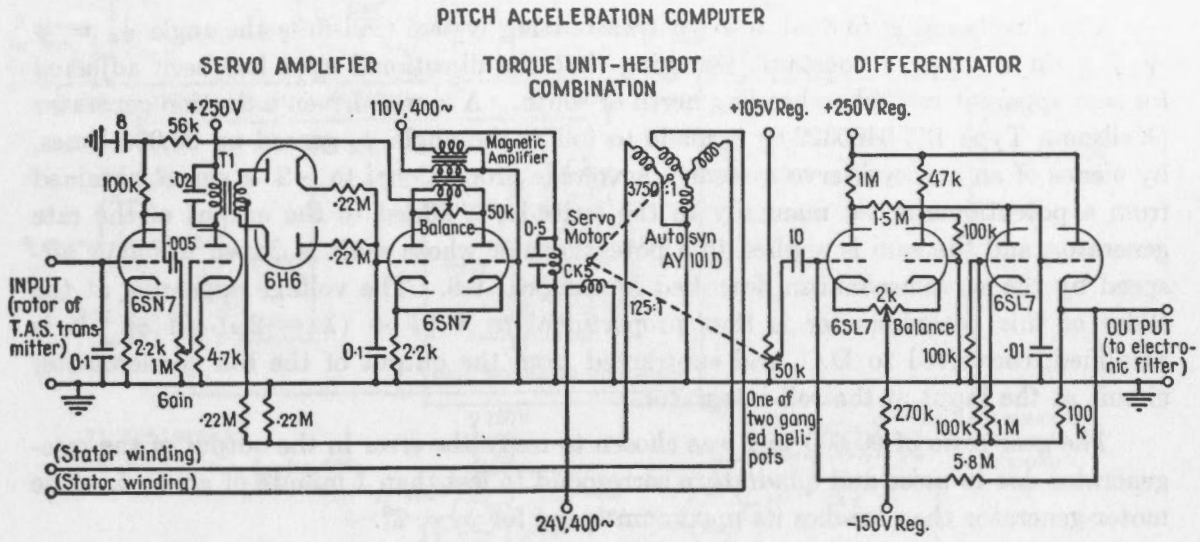

FIGURE 1.13.—Pitch acceleration computer.

The circuit at the right hand side of Figure 1.13 differentiates the airspeed signal, giving an output of 0.186 RC volts/ft/sec.^{2}, where RC is the time constant of the differentiator in seconds. The time constant is chosen to make the scale of the differentiator output equal to the scale of the accelerometer circuit output, i.e. 100 millivolts per minute of arc deflection of the apparent vertical. Thus

$$0.186 \text{ RC} \times 32 \times \frac{2\pi}{360 \times 60} = 0.100, \text{ or RC} = 58 \text{ sec.}$$

This time constant was obtained using a 10-microfarad condenser with the same characteristics as those described earlier.

The servo system has a natural frequency of about 1 c.p.s., and is critically damped for a voltage gain of 300, or about one half of maximum. The helipot resolution corresponds to 0.03 knot and is adequate. The 0.1-microfarad condenser across the rotor of the synchrotel transmitter ensures zero reaction in all positions of the rotor shaft.

It will be noticed that instead of applying differentiated airspeed to the input of the integrator a signal proportional to airspeed could have been subtracted directly from the output of the integrator. Although the present system makes a smaller demand on the operating range of the integrator, the advantage is in fact unimportant, since the integrator can easily handle the accelerations of normal flight. However, the method adopted has the advantage that it allows the recording of the estimated and measured pitch accelerations under different flight conditions. A great deal was learned about

the usefulness of this type of correction from a comparison of these records, as is discussed later. Furthermore, difficulties about the D.C. level of operation of the pitch control system were avoided by using a differentiator.

1.6.9 *The Roll Acceleration Computer*

The component of acceleration about the roll axis of the aircraft, if wind is neglected, has been proved equal to $V[\dot{\psi} + (\dot{\lambda} - 2\omega) \sin \phi]$ in the notation established earlier in the theoretical discussion (section 1.5).

The directional gyro dual autosyn transmitting system transmits the angle $\psi_s = \psi + \int \dot{\lambda} \sin \phi \, dt +$ a constant, assuming that the directional gyro has been adjusted for zero apparent rate when heading north or south. A motor-driven induction generator (Kollsman Type 133-0460322-0) is made to follow the angle ψ_s geared up 90,000 times, by means of an autosyn servo system. A voltage proportional to $-2 \omega \sin \phi$, obtained from a potentiometer set manually to the latitude, is added to the output of the rate generator, and the sum is applied to a potentiometer whose shaft is driven to follow airspeed by the servomechanism described in section 1.6.8. The voltage appearing at the slider of this potentiometer is thus proportional to $V[\dot{\psi} + (\dot{\lambda} - 2\omega) \sin \phi]$. It is amplified, converted to D.C. and subtracted from the output of the roll accelerometer circuit at the input of the roll integrator.

The gear ratio of 90,000 to 1 was chosen to make the error in the output of the rate-generator due to noise and quadrature correspond to less than 1 minute of arc in δ. The motor-generator then reaches its maximum speed for $\delta = 7°$.

Figure 1.14 shows the complete roll acceleration computer circuit. Considerable care was required in damping the rate-generator servo system to make it follow smoothly the wide range of angular velocities it must handle. Damping was obtained by adding to the autosyn error signal a rate signal from the generator. Since the autosyn system operates at line frequency and the generator is excited from the frequency standard, the two signals are demodulated before mixing at the grids of the tube controlling the magnetic amplifier which drives the motor-generator. The correction $- 2\omega \sin \phi$ is introduced by the potentiometer labelled "Coriolis Correction", which is graduated in latitude from 30° to 90°.

The temperature coefficient of the rate-generator is between -0.2 and -0.3 per cent per C° in the range 10°C to 70°C. Since the greater part of the computer output is periodic, the steady component amounting to only a few minutes of arc in δ, temperature changes have a negligible effect on the accuracy of the platform.

Figure 1.14 also shows the automatic cut-out circuit. Both the roll accelerometer circuit and the roll acceleration computer saturate with accelerations of $\pm$ 7° in δ. The input to the integrators is grounded automatically by the cut-out circuit whenever the roll acceleration exceeds this value to avoid developing large transients in the stabilization system during major changes of heading. The A.C. output signal of the roll accelerometer is applied to a negatively biassed detector. When the output of the detector is positive, the thyratron closes the relay, cutting off the input to both the roll and pitch integrators. A release time constant of 8 seconds is provided to allow the aircraft to settle on its new heading after the turn is completed. This cut-out is very important

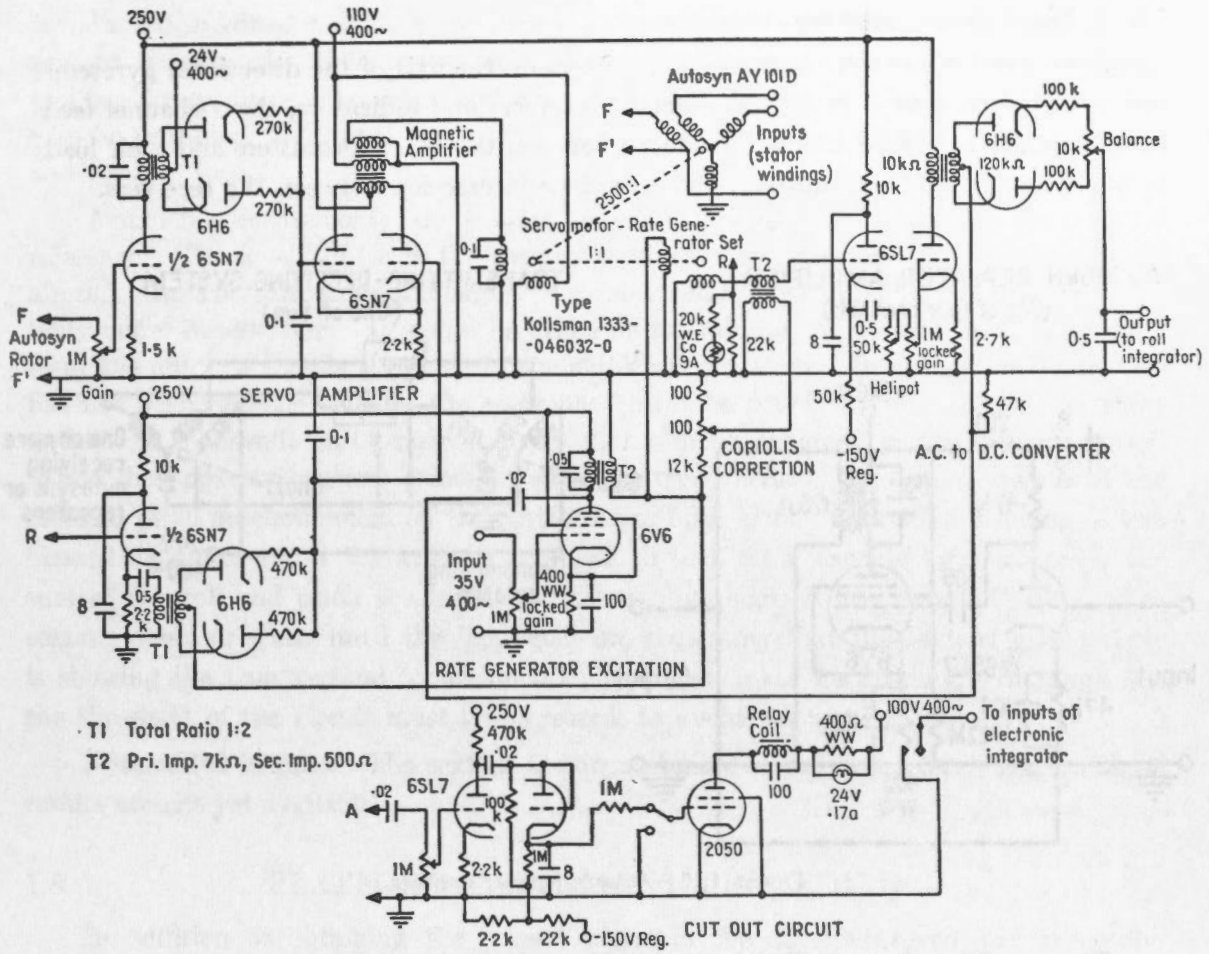

FIGURE 1.14.—Roll acceleration computer and cut-out circuit.

since without it, a turn of 180° in one minute would produce a transient reaching a maximum error value of about 4°, and 9 minutes later the platform could still be 7 minutes in error.

1.6.10 *The Directional Gyroscope Rate Corrector*

The directional gyro, unlike the roll and pitch gyros, is not provided with automatic control of its rate. It is allowed to wander, and the corrections to be applied to its readings are determined at 10 or 15 minute intervals. However, its rate must be kept at less than 5° per hour to avoid introducing errors of 1 minute of arc into the platform through the roll acceleration computer. A low rate also makes reduction of the magnetic declination results easier.

A calibrated control is provided to apply a torque to the directional gyro and change its rate by a known amount up to a maximum of ± 140° per hour. The circuit shown on the left-hand side of Figure 1.11 applies the calibrated voltage to one winding of the directional gyro torque generator. The other winding is excited at 10 m.a. by the constant current source described in section 1.6.7.

1.6.11 *The Autosyn Repeater Amplifiers*

Since the 1:1 and 36:1 autosyn transmitters on the axis of the directional gyroscope turntable are connected to several different receivers and indicators, the 4-channel feedback amplifier of Figure 1.15 is introduced between the two transmitters and their loads to avoid loading the transmitters, and to reduce interaction between the receivers.

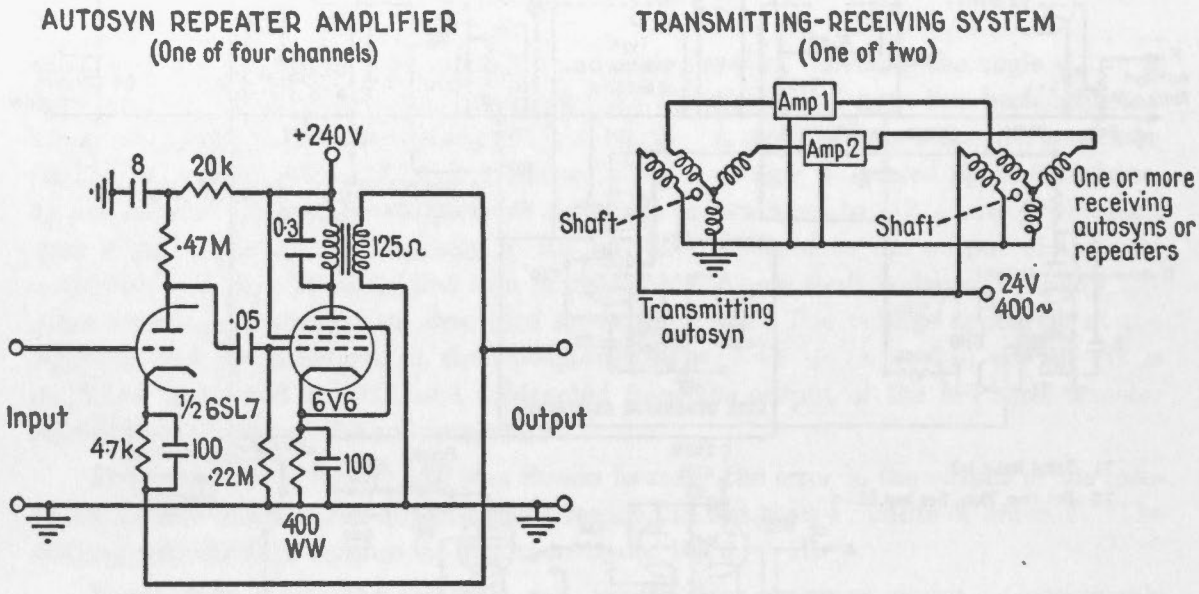

FIGURE 1.15.—Autosyn repeater amplifier.

The amplifier shown will drive two self-synchronizing indicators and two receivers with maximum errors of 1°, corresponding to less than 2 minutes of arc when the 36:1 gear ratio is considered.

The condensers across the primary windings of the output transformers are required to prevent high frequency oscillation.

1.7 THE SYNCHRONOUS PERISCOPIC SEXTANT

The corrections to be applied for drift of the directional gyroscope are determined in flight by measuring, every 10 or 15 minutes, the angle in azimuth between the axis of the directional gyro and the sun or a star. This is done with a periscopic sextant (Kollsman Type 1471C-01), whose mount (Kollsman Type 1708-01) has been modified by the addition of a servomotor, a gear train, and an autosyn. The servo system keeps the index of the graduated circle in the mount parallel to the axis of the directional gyro, using the 36 to 1 autosyn, independent of yawing of the aircraft. When the observer looks into the eyepiece of the sextant, he sees an image of the sun, the sextant level bubble and cross-hairs, and a segment of the graduated circle. The angle read on the graduated circle is the angle between the gyroscope axis and the sun.

In the modified mount, a mechanical connection is also provided to stabilize the sextant in azimuth. This stabilization helps greatly in obtaining accurate readings, and enables readings to be taken under broken cloud when observations would not otherwise be possible. A tangent screw for adjusting the sextant in azimuth helps in setting and reading to 0.2°.

Azimuth measurements are subject to errors arising from errors in the vertical reference. The level bubble in the sextant is affected by horizontal accelerations of the aircraft, and azimuth errors of a degree or so may result, depending on the altitude of the body under observation. It would be desirable to stabilize the sextant in roll and pitch from the autosyn signals available in the stabilized platform. In the present case, this has not been possible because the equipment must be fitted into any aircraft on short notice. A makeshift stabilization, in effect, has been achieved in the following way. When the apparent vertical coincides with the true vertical, the output signals of the roll and pitch accelerometers on the platform are both zero. A circuit consisting of two biassed detectors and a thyratron is arranged to turn on a warning light whenever the sum of the roll and pitch accelerations (disregarding sign) is less than 0.1° of δ. The sextant operator waits until the light goes on, indicating that the sextant level-bubble is showing the true vertical to within 0.1°, and then takes his reading. In rough air, the threshold of the circuit must be increased, to avoid waiting indefinitely.

Note added in proof: The sextant is now stabilized in roll and pitch. Experimental results are not yet available.

1.8 PLATFORM ALIGNMENT PROCEDURES

In addition to obtaining the correct phase in the different servo and gyroscope control loops, and the correct voltage relationships throughout the gyroscope erection systems, a number of other preliminary adjustments were required. These included:

(i) The alignment of the two autosyns on the directional gyroscope turntable shafts;

(ii) the adjustment of the parallelogram linkage system in the way described earlier;

(iii) the adjustment of the roll tangent screw at the magnetometer yoke. This was made by pitching the system and looking for errors about the roll axis between the level bubble in the direction gyroscope turntable and the one on the magnetometer head. An accuracy of adjustment about the roll axis of 0.5° is easily adequate.

The platform gyroscopes were rotated in their mounting clamps so that their sensitive axes were parallel to the axes of roll and pitch of the platform to within 15 minutes of arc. The lean of each accelerometer is defined as the angle between the jewelled axis of the accelerometer and the turntable axis. The clamps were adjusted so that these angles were less than 1 minute of arc for both accelerometers.

Great care was taken that the signals introduced for the Coriolis and earth's rate corrections were in the correct phase.

1.9 POST-FLIGHT ANALYSIS OF THE PLATFORM RECORDS

A number of conclusions were reached from an examination of the fifty hours of records obtained during the 1953 field season;

(i) in very bumpy air, the $\dot{V}$ correction should not be introduced because of overshooting of the airspeed transmitter and turbulance around the pitot head.

(ii) in smooth flight, the magnitude of the longer period accelerations, $(\delta_p - \dot{V})$, is about one half to one third that of δ_p. At times the correction can be almost perfect; e.g. in Figure 1.16, a tracing of δ_p and $-\dot{V}$ records taken during a flight on September 5th, 1953, is shown. The smoothed record of $-\dot{V}$ is nearly equal to the image of δ_p, and during the twenty minute interval $(\delta_p - \dot{V})$ consisted of very low amplitude, high frequency signals which are easily filtered by the pitch control system.

(iii) the improvement in platform accuracy using the roll acceleration computer is obvious. Figure 1.17 shows tracings of δ_r and $(\delta_r - V\dot{\psi})$ over a typical 20-minute interval. Corrections to the aircraft's course such as are made in flight every 20 minutes or so are seen at A and C, and at B a turn of 40° occurred. At A and C the input signals to the roll erection system $(\delta_r - V\dot{\psi})$ show that the platform must remain very close to the true horizontal with the long period (6.3 minutes) control system used. The amplitude of any forced oscillation of the system is negligible, even while the heading is changing. Without the centrifugal acceleration computer, magnetic observations in the 5-minute periods after the turns at A and C would require corrections for forced oscillations of the platform. At B, the turn of 40° was made so slowly that the relay did not cut off the signals to the roll and pitch integrators. The turn was also made without an adjustment of the earth's rate corrector. The big improvement in transient response is again seen: the next 5 minutes of magnetic records did however require critical examination, since the acceleration compensation was not perfect.

It is concluded that the additional complexity required for computing estimates of acceleration and correcting for these estimates is justified for a three-component airborne magnetometer. The estimation of centrifugal accelerations during turns is essential to the efficient operation of the instrument.

The records obtained in the 1954 field season confirm the conclusions listed above. The only difficulties are those associated with apparently false short-period signals from the airspeed transmitter, and these do not affect platform performance.

1.10 A DISCUSSION OF PLATFORM ERRORS

Errors in the system are primarily due to aircraft accelerations. If the aircraft flies along a great circle at constant speed the principal acceleration term vanishes, but a correction for the horizontal component of the Coriolis component of acceleration is still required. The Coriolis correction has been allowed for, and navigational turning accelerations or centrifugal accelerations associated with the curvature of rhumb-lines compensated in the roll acceleration computer. For a North Star aircraft, flying east

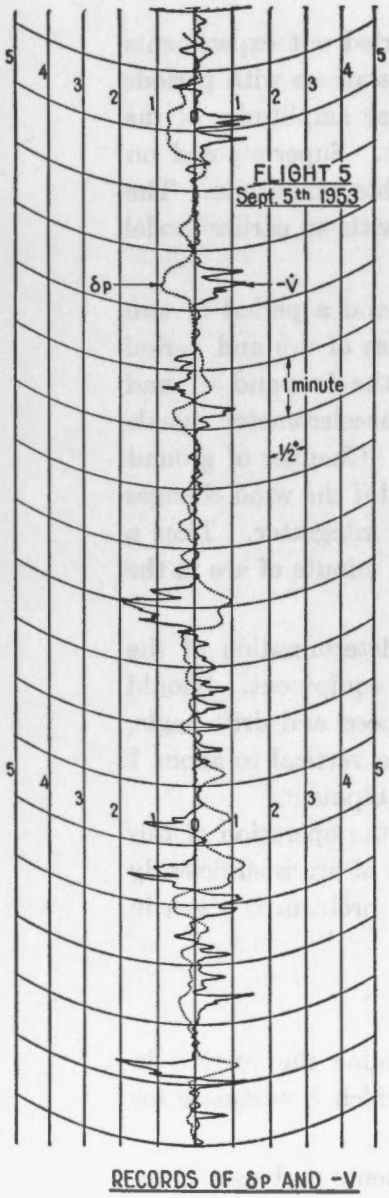

FIGURE 1.16.—Comparison of pitch accelerometer output and computed acceleration.

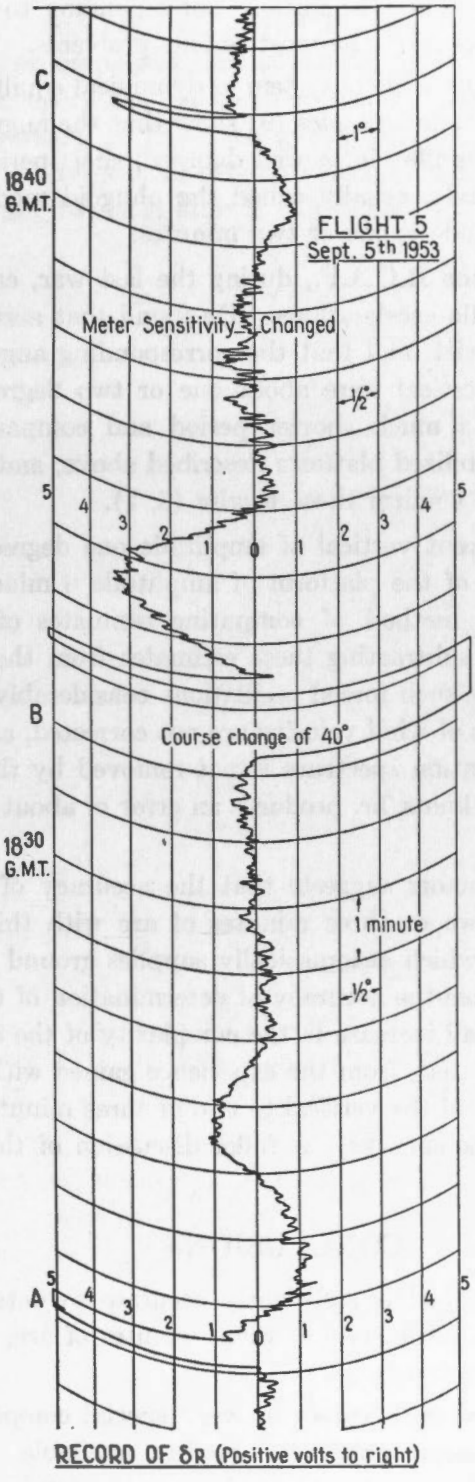

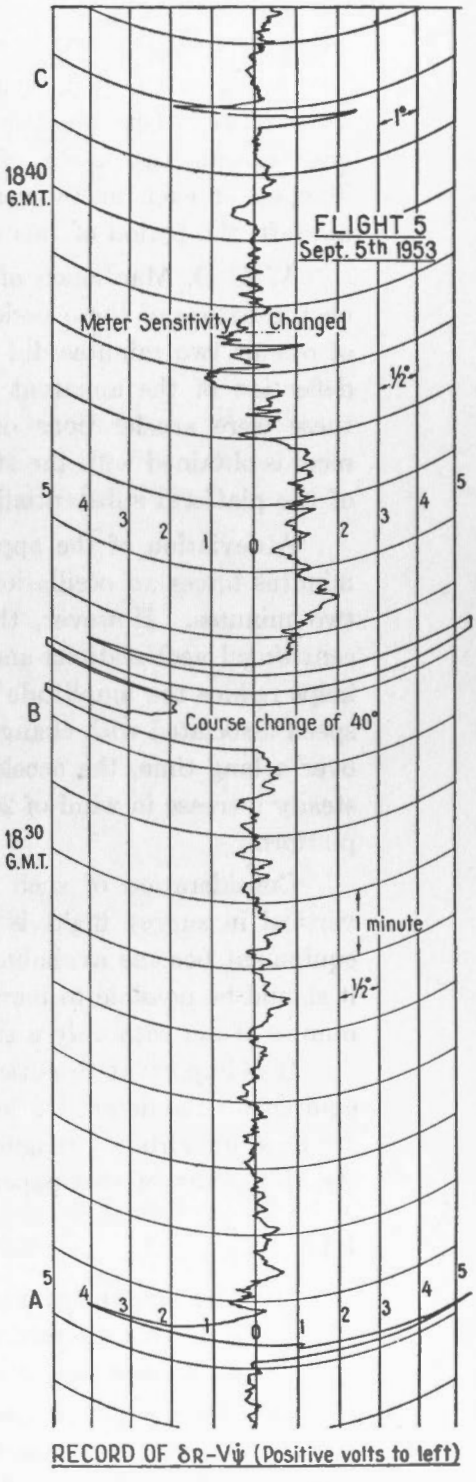

FIGURE 1.17.—Comparison of roll accelerometer output and input to roll integrator.

over Ottawa the Coriolis correction is about 3.5 minutes of arc, and the convergency term in the roll acceleration computation compensates for the rhumb-line correction of 0.5 minute of arc. Consequently accelerations corresponding to random alterations of course and fluctuations in speed are the most serious problems.

An aircraft in flight is a mechanical system in dynamical equilibrium with the earth's atmosphere. Text books on aerodynamics (9) show that the angular motions of an aircraft contain two modes of oscillation, a well damped, short-period mode and a poorly damped or even unstable mode, usually called the phugoid mode. For a North Star aircraft, the period of this mode is one or two minutes.

W/C D. MacLulich of the R.C.A.F., during the last war, carried out experiments on the nature of these periodic accelerations. He found that accelerations with periods of one or two minutes did exist, and that the corresponding angular amplitudes of the deflection of the apparent vertical were about one or two degrees. Superimposed on these were accelerations of a much shorter period and comparable amplitude. The records obtained with the stabilized platform described above, and with an earlier model of the platform substantially confirm these results (6, 7).

A deviation of the apparent vertical of amplitude one degree and a period of two minutes forces an oscillation of the platform of amplitude 6 minutes of arc and period two minutes. However, the method of computing estimates of the fore-and-aft and centrifugal accelerations and subtracting these estimates from the accelerometer signals helps reduce the amplitude of such forced oscillations considerably. Changes of ground speed associated with changes of wind velocity are not corrected, and if the wind changes over a long time, the acceleration spectrum is not removed by the integrator. Thus a steady increase in wind of 20 knots/hr. produces an error of about 1 minute of arc in the platform.

Consideration of such factors suggests that the accuracy of determination of the vertical in survey flight is two or three minutes of arc with this equipment. Should equipment become available which automatically supplies ground speed and drift angle, it should be possible to increase the accuracy of determination of the vertical to about 1 minute of arc with only a small increase in the complexity of the equipment.

It is important to notice that, from the experience gained with the operation of this equipment, the determination of the vertical to two or three minutes of arc is sufficiently accurate for airborne magnetic surveys. A fuller discussion of this problem is given in the third part of this paper.

1.11 CONCLUSIONS

(i) The equipment described is sufficiently accurate to determine the vertical in a moving aircraft to within two or three minutes of arc, which is adequate for large scale magnetic surveys.

(ii) The equipment described involves no very special components and uses gyroscopes, electromechanical units, etc. readily available. Although bulky the individual parts of the system are fundamentally simple and easy to maintain and service. The airborne serviceability record in three seasons of operation proved excellent.

(iii) It was found necessary to use first-order acceleration computers in order to obtain this degree of accuracy.

(iv) The gyroscope control system used, with its less severe demands on gyroscope performance than other proposed schemes, proved adequate for this application and reliable in operation, for periods of a hundred hours flying or more. It was found necessary to have the gyroscopes overhauled at the factory after each season. The reasons for this deterioration and its effect on the performances of the system are discussed later in this paper.

APPENDIX: THE ANGULAR COMPLIANCE OF HIGH FREQUENCY GEAR TRAINS

In computing the contributions to compliance, the following were estimated:

(i) torsion in the shafts. Elementary books on mechanics show that the torque T is related to the angle of twist by the relation

$$T = \frac{\pi a^4 E_n}{2l} \theta$$

where E_n = modulus of rigidity,
a = radius of shaft of circular cross-section,
and l = length of shaft.

The contribution to compliance at the output shaft,

$$X_t = \sum_{\text{shafts}} \frac{\theta}{T} \cdot \frac{1}{N^2}$$

where N is the gear ratio to the output shaft.

$$\text{Therefore} \quad X_t = \Sigma \frac{2l}{\pi a^4} \cdot \frac{1}{E_n N^2}$$

and in this design equals 2×10^{-7} rads./lb.in. approximately.

(ii) bending of the shafts. The bending of the shaft of the cast aluminum turntable can be estimated. If its deflection is Δ, the contribution to angular compliance is $X_d = \frac{\Delta}{2FR^2}$ where the bending force is 2F, and the radius of the internal gear is R.

Elementary books on mechanics show that for a cantilever loaded at one end and supported rigidly by the other $\frac{\Delta}{2F} = \frac{l^3}{3EI}$

where E = Young's modulus,
l = length of cantilever,
and I = second moment of inertia.

Therefore $X_d = \frac{l^3}{3EI\ R^2}$ and in this design equals 2×10^{-7} rads/lb.in. approximately. The contribution of the other shafts is much smaller.

(iii) deflection of the gear teeth.

A typical example of the calculation involved in estimating the deflection of external involute gear teeth is given below.

A two-inch diameter gear engages a half-inch pinion. Both gears are 48 pitch, and consequently 4 teeth are wholly or partially in contact. A parabolic section AOA (Figure 1.18) was assumed, and consideration of the number of teeth in contact suggested that a good approximation would be to regard the total force F on one tooth at the centre along the pitch circumference.

With the notation of Figure 1.18, the geometrical moment of inertia of the shaded area is $Ak^2 = \frac{bt^3}{12} \cdot \frac{(h - x)^{3/2}}{h^{1/2}}$.

86463—4½

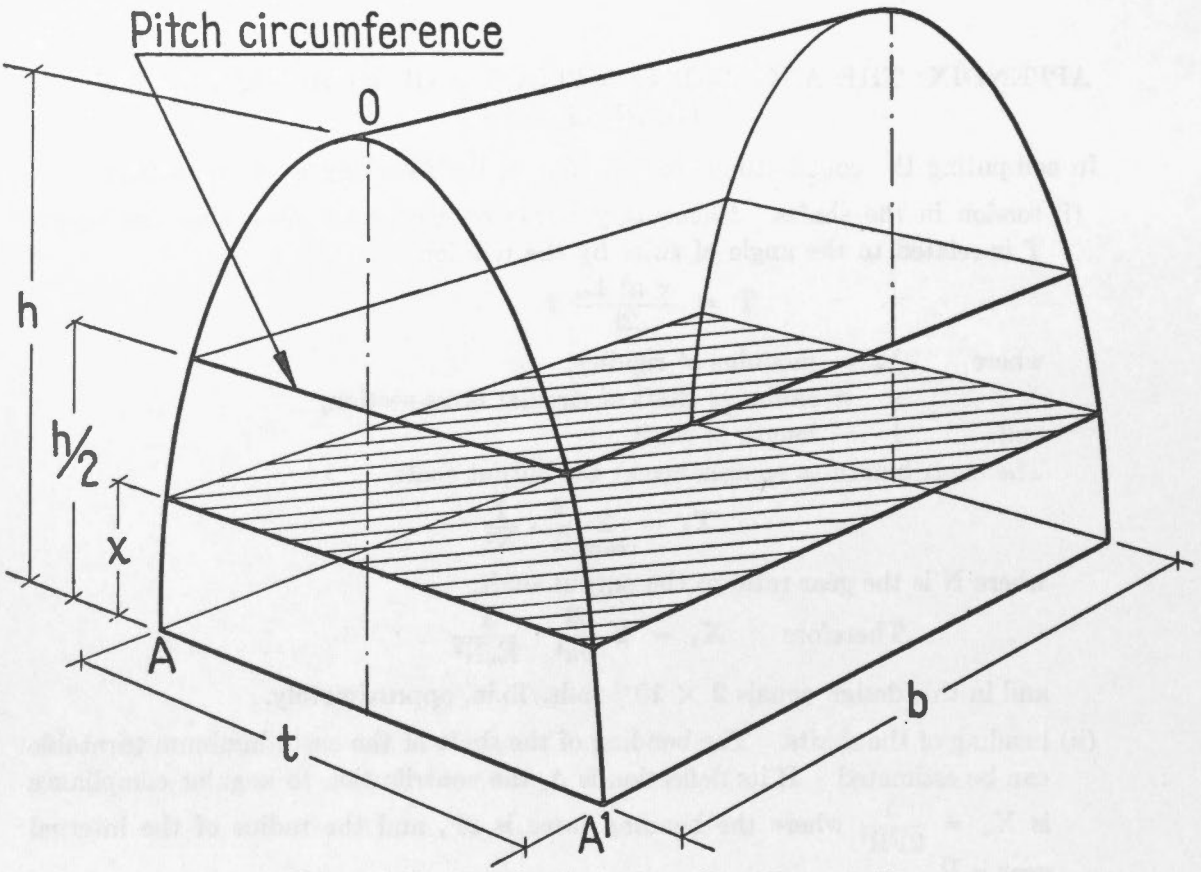

FIGURE 1.18.—Approximation to shape of involute gear teeth.

Then the external applied bending moment is $F\left(\frac{h}{2} - x\right) = EAk^2 \frac{d^2y}{dx^2}$ where E = Young's modulus, and $1/\frac{d^2y}{dx^2}$ = radius of curvature of tooth at section where deflection is y. Integrating twice and using the conditions $\frac{dy}{dx} = 0$ when $x = 0$ and $y = 0$ when $x = 0$, we have y at the point $x = \frac{h}{2}$ gived by $y_{\frac{h}{2}} = \frac{0.6F}{Eb}\left(\frac{h}{t}\right)^3$. Other approximations lead to numerical factors similar to 0.6.

But the deflection $\Delta = y_{\frac{h}{2}}$, and if R is the radius of the gear, the torque transmitted is $T = FR$, and the angular deflection is $\theta = \Delta/R$.

The contribution to the compliance at the output shaft is therefore $X_g = \sum_{\text{gears}} \frac{\theta}{T}\frac{1}{N^2} = \Sigma \frac{0.6}{Eb}\left(\frac{h}{t}\right)^3 \frac{1}{R^2N^2}$, and in this design equals 1×10^{-7} rad./lb.in. approximately.

(iv) the radial deflection of the bearings. This is difficult to estimate, but for light preloading using tight tolerance bearings it appears likely from the manufacturer's curves that $X_b = \sum_{\text{bearings}} \frac{4 \times 10^{-7}}{N^2R^2}$, or in this design about 1×10^{-7} rad./lb. in.

PART 2

THE MAGNETOMETER

2.1 INTRODUCTION

This part of the report describes the section of the airborne magnetometer which measures the intensity and direction of the magnetic field with respect to the direction reference system supplied by the gyro-stabilized platform.

The field-sensitive head of the magnetometer is mounted on the gyro-stabilized platform inside the cabin of the aircraft. It contains three mutually perpendicular magnetic detectors of the saturated transformer type, each of which is continuously maintained at the null by a direct current flowing in a solenoid surrounding it. The direct current is thus proportional to the magnetic field component along the sensitive axis of the detector. One of these units, mounted with its axis of sensitivity vertical, measures the vertical component; the others measure the fore-and-aft and the transverse horizontal components respectively.

The direct current proportional to the vertical component is measured by an automatic potentiometer. Geared to the potentiometer is a counter which indicates the vertical component in the desired units—tens of gammas.

The outputs of the two horizontal field-measuring units are combined in an electrical resolver to give the intensity of the horizontal component and the magnetic heading of the aircraft. The horizontal intensity is displayed by a counter geared to an automatic potentiometer. The magnetic heading is continuously subtracted from the gyro heading of the aircraft (supplied by the directional gyroscope), and the difference is displayed on a dial in degrees. The dial reading, when corrected for the difference between gyro-heading and the true heading, is the magnetic declination.

During normal survey flights, a switch controlling the operation of the indicators is thrown to "Average". The declination dial and the two counters, instead of following the changes in the magnetic field, now remain fixed at the last average values determined for D, H, and Z. At the end of a 5-minute period, each indicator turns automatically to a new value representing the average value of its component over the preceding 5-minute period. While the instrument is being used in this manner, three recording milliammeters record the difference between the instantaneous value of each component and the value appearing on the corresponding indicator. Thus continuous values of any component can be read from the meter records using the last determined average as a baseline.

2.2 THE MEASUREMENT OF MAGNETIC COMPONENTS

2.2.1 *The Magnetic Detectors*

The magnetic detectors are of the saturated transformer type described by V. V. Vacquier (10). The circuit in which they are used, however, is believed to represent a new technique for obtaining greater sensitivity combined with discrimination against unwanted harmonics.

The detector contains two parallel strips of Mumetal, 4.0 × 0.10 × .014 inches. Each strip is surrounded by a primary coil consisting of a single layer of No. 30 wire, close

wound. The two primary coils are connected in series opposition to a source of 1000-cycle alternating current. The two Mumetal strips with their primaries are slipped into a common secondary coil of about 3300 turns of No. 36 wire. The whole unit is mounted in a bakelite tube of 0.375-inch internal diameter. The bakelite tube is threaded on the outside, at 80 threads per inch, and the solenoid which carries the direct current is wound in the grooves in a single layer.

The two units which measure the horizontal components are fixed with bakelite clamps to a horizontal bakelite plate supported by three vertical threaded rods. The vertical component measuring unit is clamped with its axis vertical to a similar bakelite plate supported by the same rods. The rods are supported by an aluminum plate carrying level bubbles which can be rotated about a vertical axis in making alignment adjustments. A transparent plastic cover encloses the magnetometer head. The magnetometer head is shown in Plate II.

The magnetometer head is thermostatted at about 30°C., although this is probably not necessary if the aircraft heating system operates normally. The temperature sensor is a thermistor which is one arm of a bridge excited at line frequency. The bridge error signal is amplified to operate a relay which applies line voltage to six carbon resistors distributed about the head assembly.

The balanced detector described above gives an output signal composed of even harmonics of the frequency of the oscillator supplying the excitation current. The amplitude is proportional to the component of the earth's field along the axis of the coils, provided this component is small, and the waveform inverts when the sign of the component is reversed. If the signal is applied to a phase-sensitive detector whose reference is double the excitation frequency, a centre-zero indication of the magnitude and sign of the component of field is obtained. However, the second harmonic content of the signal is low—of the order of 10 microvolts per gamma—and if sufficient amplication to give the required sensitivity precedes the phase-sensitive detector, the amplifier and detector are saturated by the higher harmonics of the signal. This difficulty is usually overcome by using a band-pass filter to attenuate the undesired frequencies. Any of the simpler filters with enough discrimination introduce a phase-shift which changes rapidly with frequency and with variation in the components of the filter. When a phase-sensitive detector is used, this uncertain phase-shift presents a serious problem.

It has been found possible to avoid the use of filters by tuning the magnetic detector. If the secondary coil of the Vacquier detector is tuned to the second harmonic by a condenser connected across its terminals, a great increase in sensitivity occurs as well as a relative reduction in the other harmonics. The effect is quite different from that of a tuned inductance elsewhere in the circuit—for example, infinite sensitivity and 'more than infinite' sensitivity, or instability, are easily obtained if the resistance of the secondary winding is below a critical value. The sensitivity can be reduced to a convenient value by a rheostat connected as a shunt across the secondary.

To show that this effect can be used in a practical instrument, it is necessary to investigate the variation in the sensitivity and phase of the second harmonic output of the tuned detector for small changes in the operating conditions. The non-linearity of the Mumetal cores makes analysis difficult, but it can be shown that the cores should be

saturated for 28.5 per cent of the time to make the sensitivity independent of excitation amplitude. There is a value of tuning capacity for which the sensitivity is independent of frequency. If the shunting resistance is adjusted for infinite sensitivity with the optimum excitation and capacity, it can be calculated that for variations of ± 5 per cent in the excitation current, ± 5 per cent in the excitation frequency, ± 10 per cent in the tuning capacity, and ± 10 per cent in the shunt resistance, the sensitivity of the detector will remain above 1 millivolt per gamma. With the above changes in operating conditions, the variations in the phase of the detector output relative to the excitation phase are 1.2°, 0.5°, 0.5°, and 0.9° respectively. The theory of the tuned detector, from which these results were calculated, has been published elsewhere (11).

2.2.2 *The Magnetic Detector Circuits*

This section describes the circuits which excite the magnetic detectors, and produce three direct currents proportional to the three components of the magnetic field. The primary of each magnetic detector is supplied with 1000-cycle current at about 100 milliamps by a separate push-pull excitation circuit. The three excitation circuits are driven by a common Wien bridge oscillator, but each excitation circuit has its own output meter and output control.

The secondary coil of each of the magnetic detectors is connected to a tuning capacitor in parallel with a shunting rheostat, which is used as a loop gain control. The signal is amplified by a two-stage amplifier including a low-Q resonant circuit tuned to 2000 cycles. The amplified signal is detected by a phase-sensitive detector, supplied with a 2000-cycle reference signal of fixed phase by a frequency doubler common to the three channels. The D.C. output of the phase-sensitive detector is integrated by a two-stage Miller integrator, whose output is fed back to the nulling solenoid on the magnetic detector. The current passing through the solenoid is returned to ground by a manganin resistor.

Referring to Figure 2.1, the field due to the current in the solenoid is $-(A/R_s)e_3$, and the field acting on the detector is $H - (A/R_s)e_3$. Writing $R_1C_1 = T_1$ and $R_2C_2 = T_2$, and combining the three equations $T_1\dot{e}_2 = G_1e_1 - e_2$, $T_2\dot{e}_3 = e_2 - e_3/G_2$ (since $R_2 >> R_1$), and $e_1 = k(H - Ae_3/R_s)$, we obtain

$$\frac{T_1T_2R_s}{kAG_1}\ddot{e}_3 + \frac{R_s}{kAG_1}\left(T_2 + \frac{T_1}{G_2}\right)\dot{e}_3 + \left(1 + \frac{R_s}{kAG_1G_2}\right)e_3 = \frac{R_s}{A}H .$$

For $k = 200$ volts/oersted
$A = 40$ oersted/ampere.
$G_1 = 200$
$G_2 = 50$
$R_s = 200$ ohms,

the coefficient of e_3 in the differential equation is $1 + \frac{1}{400,000}$, and variation in the gain will not affect the output seriously.

If $T_1 = 0.01$ second and $T_2 = 50$ seconds, the differential equation becomes

$$\frac{1}{16,000}\ddot{e}_3 + \frac{1}{160}\dot{e}_3 + e_3 = \frac{R_s}{A}H.$$

The natural frequency of the system is $\frac{\sqrt{16,000}}{2\pi}$, or 20 cycles/second, and the damping ratio is $\frac{16,000}{160 \times 2\sqrt{16,000}}$, or 0.4 of critical.

In practice, a small oscilloscope is connected to a check-point in the 2000-cycle amplifier and the shunt resistance across the magnetic detector is increased until the system

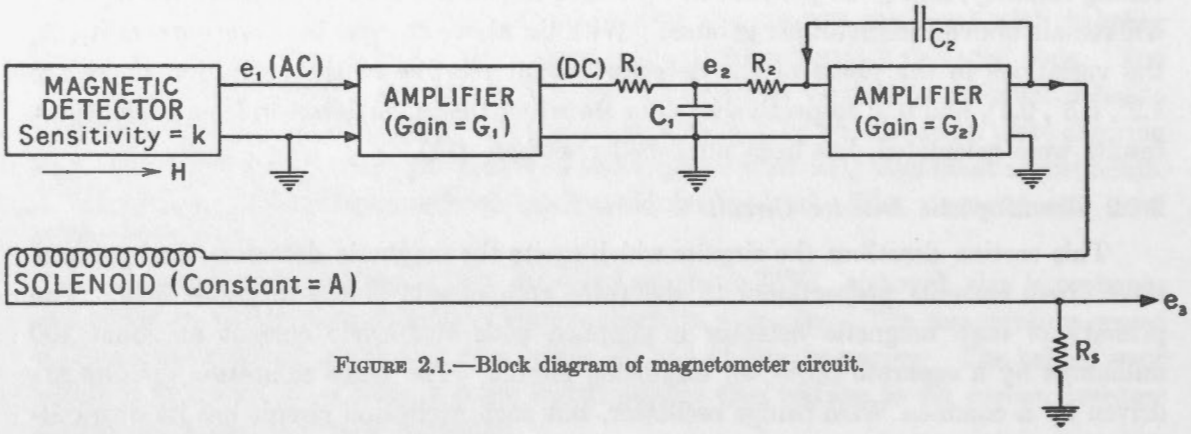

FIGURE 2.1.—Block diagram of magnetometer circuit.

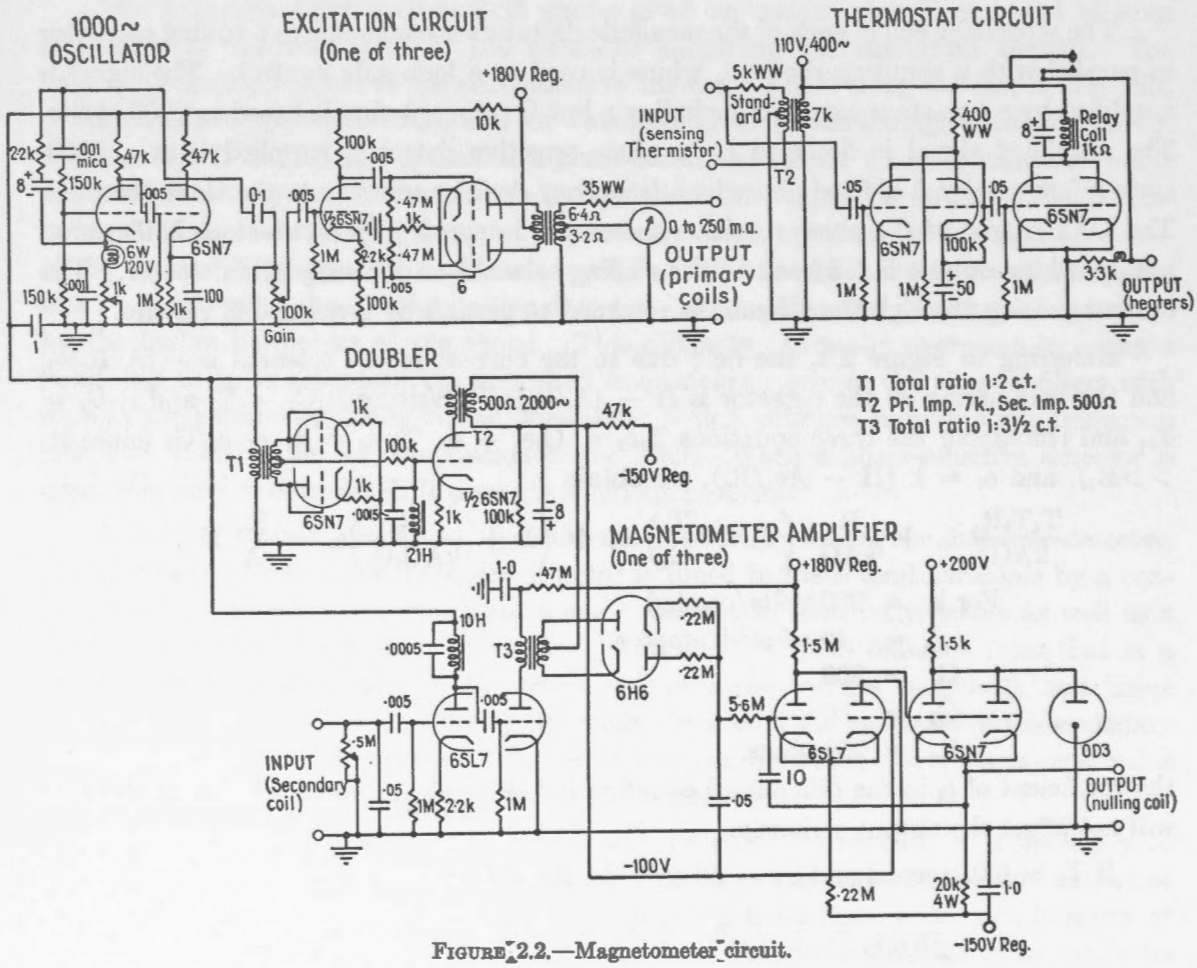

FIGURE 2.2.—Magnetometer circuit.

breaks into oscillation. The shunt is then reduced until the system is just stable. At any time during operation, the observer can check that the loop gain is high by increasing the shunt resistance slightly and observing the frequency of oscillation on the oscilloscope. A magnetic detector circuit is shown in Figure 2.2.

The two Mumetal strips in the detectors and their primary windings are never identical. If they are unbalanced by 1 per cent and the excitation current contains 1 per cent of second harmonic, a second harmonic signal will be induced in the secondary coil with an amplitude corresponding to about 30 gammas when the detector is in zero steady field. To avoid zero-errors of this type in measuring the components of the field, an adjustment (not shown in the figures), is provided to remove second harmonic distortion from the excitation current. The balance can be checked by throwing a reversing switch in the leads to the primary winding of the detector; if a zero-error due to harmonics in the excitation current is present, its sign is changed by the reversal, and the reading of the magnetometer will change. The setting of the adjustment usually is changed only when tubes are changed, but the adjustment can be checked at any time by throwing the switch and watching the loop error signal on the oscilloscope.

2.3 COMPUTATION AND DISPLAY

2.3.1. *Computation of Magnetic Heading and the Horizontal Component*

The direct currents passing through the solenoids of the fore-and-aft and transverse component measuring devices (with constants A_X and A_Y respectively) are returned to ground through manganin resistors R_X and R_Y, producing D.C. signal voltages (R_X/A_X) H_X and $(R_Y/A_Y)H_Y$, where H_X and H_Y are the components of the horizontal field. The two signals are combined to give a shaft angle equal to the magnetic heading of the aircraft and a signal proportional to the horizontal component of the geomagnetic field by means of an electromechanical resolver, which operates on A.C. signals.

Figure 2.3 shows the method of converting the D.C. signals to A.C., and the method of measuring the output of the resolver. A steady D.C. voltage E is applied to potentiometer P_H from a 6-volt storage battery. A steady 400-cycle A.C. voltage e is superimposed on the D.C. voltage by a transformer in series with the battery. Across the other potentiometers P_X and P_Y the voltages $k_X(E + e)$ and $k_Y(E + e)$ appear, where $k_X \approx k_Y$. The slider of potentiometer P_X is driven by a servomotor to maintain equal the two input voltages of the H_X servoamplifier, $(R_X/A_X)H_X$ and $k_XE\theta_X$. Thus $\theta_X = (R_X/k_XEA_X)\ H_X$. Then the A.C. voltage input of the H_X driver amplifier is $k_Xe\theta_X = \frac{R_X}{A_X} \cdot \frac{e}{E} \cdot H_X$. Similarly, the A.C. input to the H_Y driver amplifier is $\frac{R_Y}{A_Y} \cdot \frac{e}{E} \cdot H_Y$. The driver amplifiers are feedback amplifiers with gains of approximately one, and are designed to produce in the stator windings alternating magnetic fields accurately proportional to their input signals.

The signal induced in one of the rotor windings of the resolver controls, through the D servoamplifier, a motor geared to the resolver rotor shaft. This winding is thus maintained perpendicular to the resultant alternating magnetic field produced by the stator currents, and the A.C. voltage induced in the second rotor winding is then proportional to the resultant field. When the transformer constant of the resolver is K,

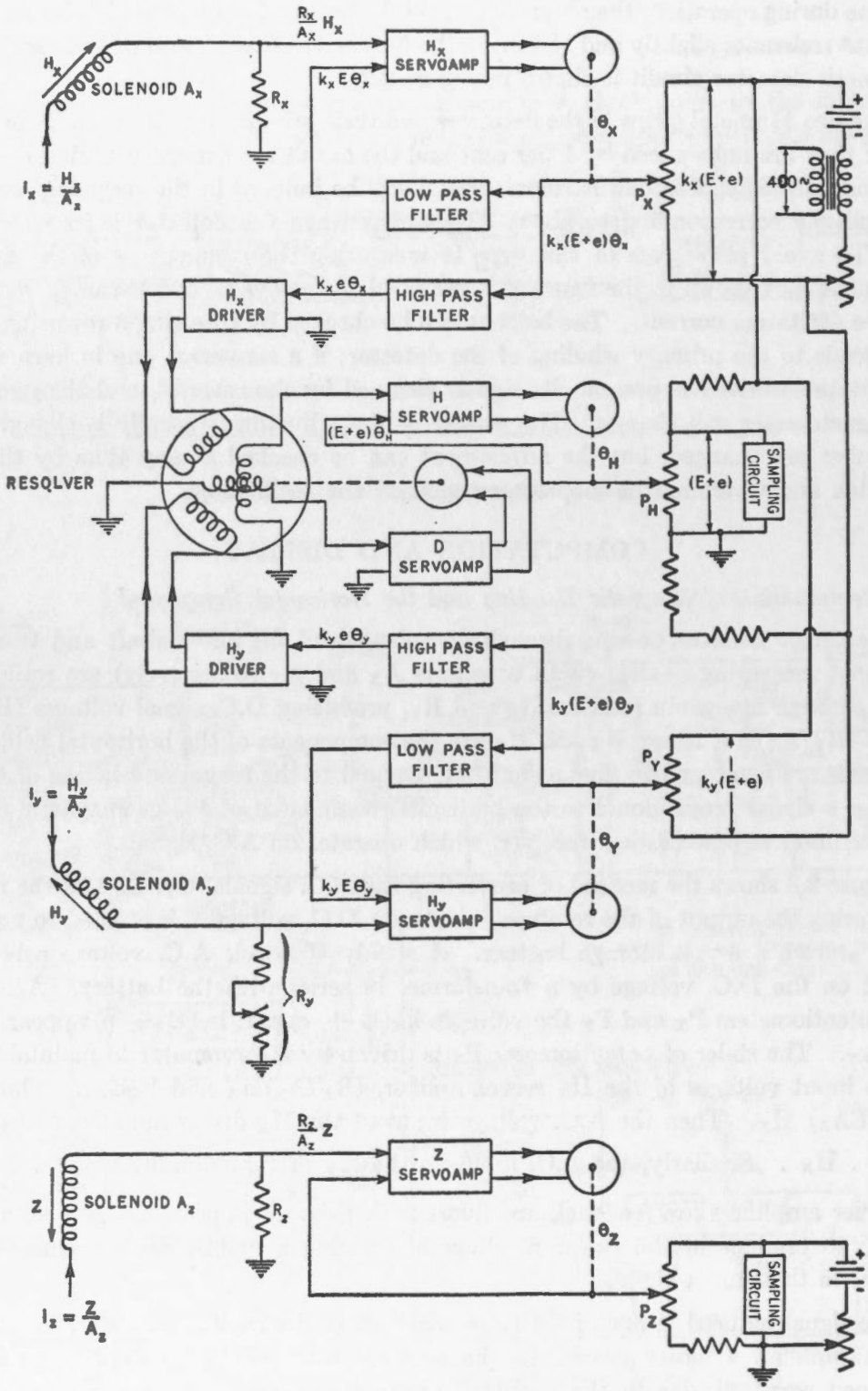

FIGURE 2.3.—D.C. measuring circuits.

the output signal is $K \frac{e}{E} \sqrt{\left(\frac{R_X}{A_X}\right)^2 H_X^2 + \left(\frac{R_Y}{A_Y}\right)^2 H_Y^2}$. If, by adjustment of R_Y, R_Y/A_Y is made equal to R_X/A_X, the output of the resolver becomes $K. \frac{e}{E} \cdot \frac{R_X}{A_X} \sqrt{H_X^2 + H_Y^2}$, or $K \frac{e}{E} \cdot \frac{R_X}{A_X} H$ and the shaft angle of the resolver is equal to the magnetic heading of the aircraft.

The slider of potentiometer P_H is geared to a servomotor controlled by the H servo-amplifier to keep the A.C. signal at the slider equal to the output of the resolver. Thus $e\theta_H = K \frac{e}{E} \cdot \frac{R_X}{A_X} . H$ where H is the horizontal component of the geomagnetic field, and $\theta_H = \frac{K}{E} \cdot \frac{R_X}{A_X} . H$. A counter geared to the shaft of P_H can be made to read the horizontal component in the desired units simply by setting the D.C. voltage E at the appropriate value.

In the construction of the instrument, it was necessary to put the potentiometers P_X and P_Y on a different chassis from potentiometer P_H. The impedance of the connecting cables introduces no error in the computation, provided it is the same for A.C. as for D.C. It will also be noticed that the potentiometers P_X and P_Y do not have to have a high degree of linearity.

The gear ratio between the shafts of the H indicator counter and the 10-turn potentiometer P_H is 48 to 1, giving a range of 0 to 48,000 gammas, where the right-hand digit on the counter represents 10 gammas. Since the linearity of the potentiometer is 0.05 per cent, the accuracy of reading is 24 gammas. Originally the range of H was limited to 0 to 20,000 gammas—sufficient for Canada—to keep the potentiometer error at 10 gammas. After the first survey it was realized that such precautions were unrealistic, and the range was increased to 0 to 48,000 gammas to cover any part of the world. The values of resistance shown in Figure 2.4 are those for the earlier range.

2.3.2. *Computation of the Vertical Component*

The circuits for the measurement and indication of the vertical component of the field are simpler than those for the horizontal component because there is no necessity for accurate conversion of signals from D.C. to A.C. The D.C. voltage produced by the current flowing through the resistor R_Z is (R_Z/A_Z) Z (Figure 2.3). It is compared with the voltage at the slider of potentiometer P_Z, and the difference is reduced to zero by the servomotor geared to the shaft of P_Z. The indicator counter, geared 80 to 1 to this shaft, is made to read in the proper units by adjusting the voltage across the potentiometer P_Z.

The range of the measuring circuit in Z is $-10{,}000$ to $+70{,}000$ gammas for the northern hemisphere, or $+10{,}000$ to $-70{,}000$ gammas for the southern hemisphere. The overlap is to avoid difficulties at the magnetic equator. The non-linearity of the potentiometer P_Z of 0.05 per cent can result in errors of 40 gammas in the reading. Originally the range was limited to the 20,000 gammas between 48,000 and 68,000.

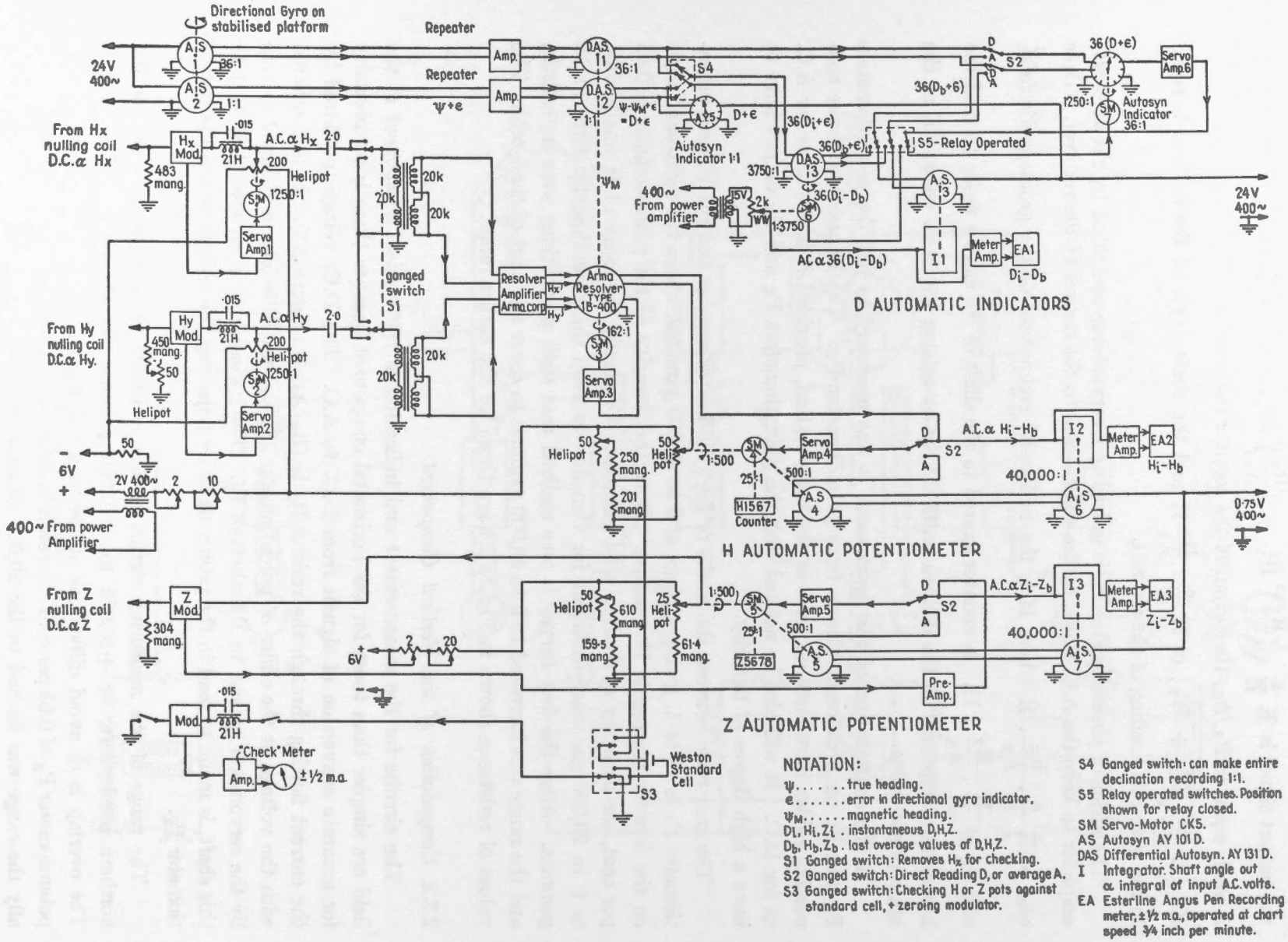

FIGURE 2.4.—Magnetometer recording system.

2.3.3 *Computation of Declination*

The vertical axis of the turntable carrying the directional gyroscope on the stabilized platform turns two autosyn transmitters, one directly and the other geared up 36 times (see Figure 1.1). The signals from these autosyns, after passing through feedback amplifiers with gains of -1 (see Figure 1.14), are applied to the stator windings of two differential autosyns geared to the shaft of the resolver, one at a 1-1 ratio, the other at 36-1. The rotor signals of the differential autosyns represent angles which are the difference between the gyro heading of the aircraft and the magnetic heading, and 36 times that angle, respectively. The 1-1 signal is applied to a self-synchronizing autosyn driving a pointer indicating from 0 to 360° on one scale of a dual indicator. The second pointer of the indicator, reading from 0 to 10°, is connected to the shaft of an autosyn receiving the 36-1 signal. The error signal induced in the rotor of this autosyn controls a servomotor geared to the autosyn shaft. (Servo operation is necessary in the case of the 36-1 pointer because of the requirements of the automatic averaging system.)

Since, generally, the directional gyroscope is not pointing north, a correction must be added to the readings of the dual indicator to obtain declination. The determination of this correction is discussed in Part 3.

Figure 2.4 shows schematically the computation of D, H, and Z. Switch S_1 is used to remove one or the other of the inputs to the resolver, to allow aligning the autosyn systems of the declination indicator.

2.3.4. *Amplifiers with D.C. Input Signals*

Three amplifiers in the magnetometer computing circuit (labelled "H_X servoamp", "H_Y servoamp" and "Z servoamp" in Figure 2.3) are required to operate servomotors on D.C. input signals of a fraction of a millivolt. The input signals are modulated at 400 cycles by vibrator-type modulators (the Brown 400-cycle converter). The resulting 400-cycle signal is amplified by an A.C. amplifier and applied to a phase-sensitive detector, whose D.C. output controls a magnetic amplifier driving the motor (Figure 2.5). Although the servomotors have heavy magnetic damping, it was found advisable to include a phase-lead network between the phase-sensitive detector and the magnetic amplifier to reduce the tendency toward instability due to the finite resolution of the potentiometers.

In order to maintain accuracy, these amplifiers must be zeroed carefully. A checking amplifier, with a vibrator modulator at the input and a centre-zero meter on the output, is included in the equipment. The checking amplifier is zeroed with its input short-circuited. It is then connected across the input of the servoamplifier to be checked while the servo is operating, and the servoamplifier is balanced to make the checking amplifier read zero. This check, which is made periodically in flight without interfering with the operation of the instrument, also insures the proper mechanical operation of the computing servomechanisms.

2.3.5. *Standardizing Circuits*

It is shown in sections 2.3.1 and 2.3.2 that the counter readings are related to the horizontal and vertical components by constants which depend on the steady D.C. voltages impressed upon the potentiometer networks. While the instrument is operating,

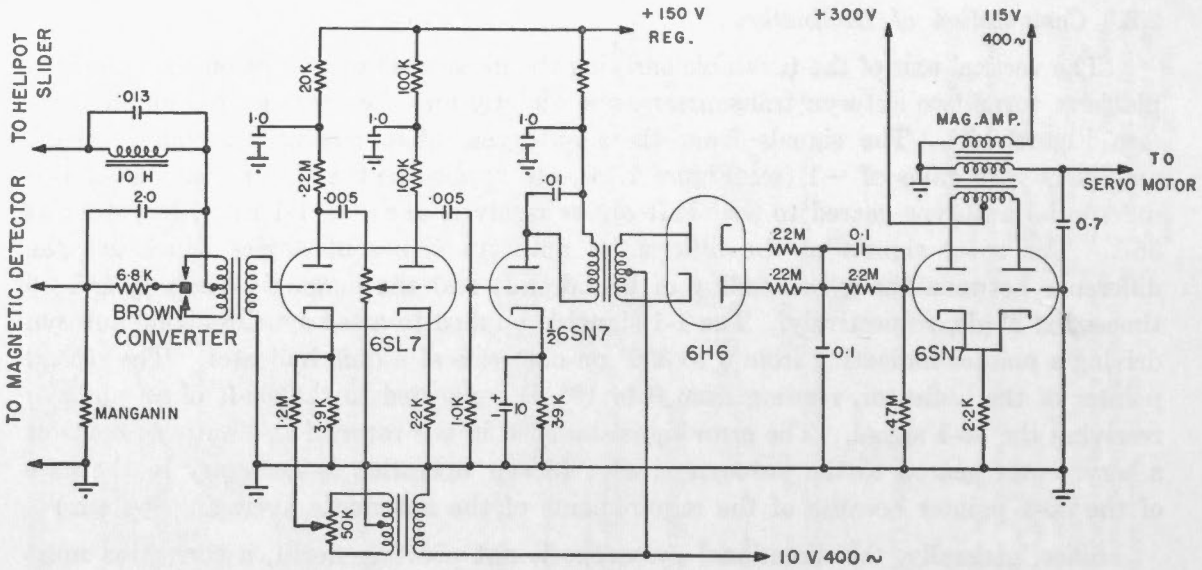

FIGURE 2.5.—Servoamplifier with D.C. input.

the two D.C. voltages must be maintained constant and at the proper value to the overall accuracy desired.

The D.C. voltages across the potentiometers P_H and P_Z (Figure 2.3) are sampled by resistive networks giving voltages of 1.018 volts when the D.C. levels are properly adjusted. The outputs of the sampling networks are compared with the e.m.f. of a standard cell, using the checking amplifier mentioned in section 2.3.4. The two sampling networks include preset helical potentiometers to allow setting the scale values in initial tests.

2.4 AUTOMATIC AVERAGING

When a switch on the magnetometer indicator panel is thrown from "Direct" to "Average", the three indicators remain fixed instead of following the changes occurring in D, H, and Z. To start the averaging process, a button is pushed, bringing into operation for 10 seconds three servo systems which align each indicator with a corresponding autosyn transmitter in the averager unit. Each of the autosyns is geared, through a 40,000 to 1 ratio, to a motor-generator unit, which is used as an integrator (Figure 2.6). The motor is controlled to make the generator output signal (which is proportional to its speed of rotation,) equal to an A.C. input signal. The input signal of each integrator is a voltage proportional to the difference between the actual value of the magnetic component in question and the value appearing on the indicator. At the end of a 5-minute period, the autosyn of an integrator will have turned through an angle proportional to the integral, with respect to time, of the input signal, and a set of relays closed by a timing circuit bring into operation the servo loop mentioned above, aligning the indicators with their integrators. A period of 10 seconds is allowed for this alignment, after which the integrating process starts again.

It will be seen that by a proper choice of integrator rate, the indicator readings can be made to represent the average of the three components of the field over the preceding

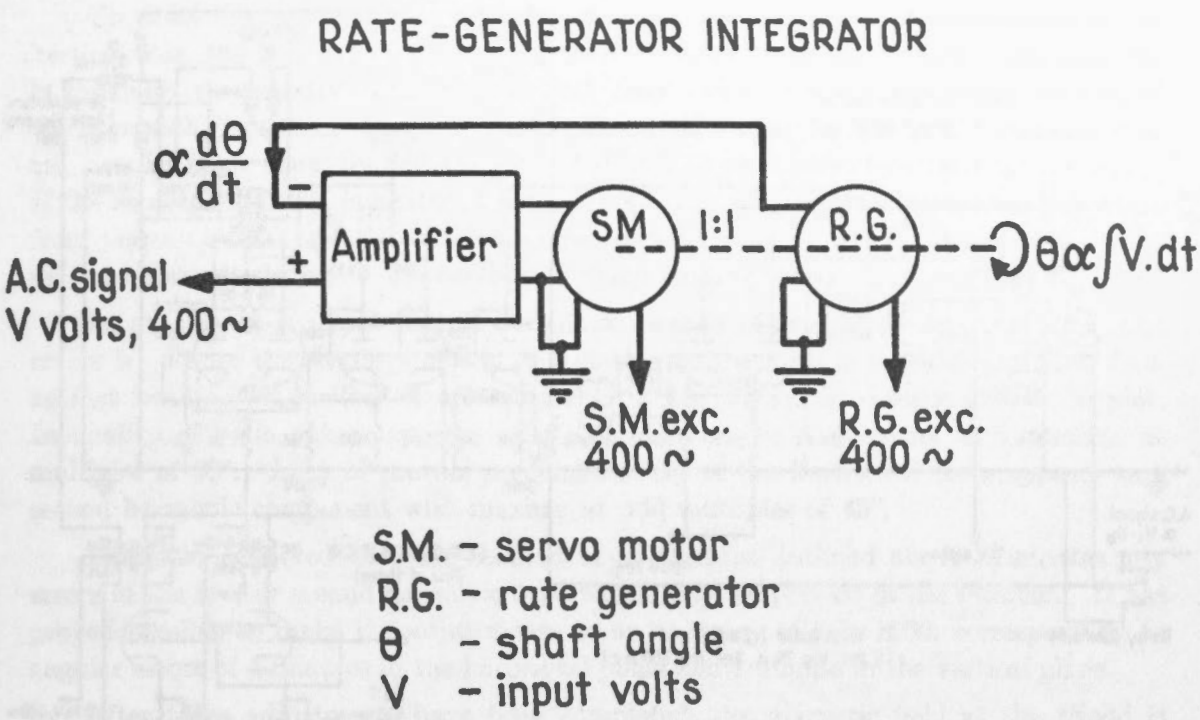

FIGURE 2.6.—Schematic of integrator in averaging circuit.

5-minute period. Since the integrators are required to accept only the range of values normally encountered during 5 minutes, the accuracy of the integration process need not be high. Errors due to incorrect integrator rate are not cumulative, and may be expected to average out over several integrating periods under normal magnetic conditions.

The gear ratios of the integrators have been chosen so that continuous gradients up to 5° in 5 minutes in D and 1600 gammas in 5 minutes in H and Z can be handled. Sharp anomalies as large as 12° in D and 4000 gammas in H and Z are handled without saturating the integrators. Close to the magnetic pole, larger gradients and anomalies may be encountered in D. Under such conditions, a switch (S_4 in Figure 2.4) is thrown to transfer the input of the averager from 36-1 system to the 1-1 system, increasing the range of the averager 36 times. The second pointer of the declination indicator is then read against the 0 to 360° scale, and the accuracy of the reading is correspondingly reduced.

In the chassis containing the automatic averager are three meter amplifiers (Figure 2.7), each consisting of a stage of A.C. amplification, a phase-sensitive detector and a cathode-follower, which are connected to three centre-zero Esterline-Angus Strip Chart Recorders. The input of each amplifier is connected in parallel with the input of the corresponding integrator. Thus the meters record continuously the difference between the instantaneous values of D, H, and Z and the values appearing on the three indicators.

The gains of the meter amplifiers are set to give full scale deflections for $\pm 2.5°$ in declination and ± 500 gammas in H and Z. Three switches are used to insert additional resistance in the meter circuits to reduce the sensitivity to one half, when large anomalies are encountered. The meters are normally operated at a chart speed of $\frac{3}{4}$ inch per minute. The chart drives are mechanically connected to maintain sychronism.

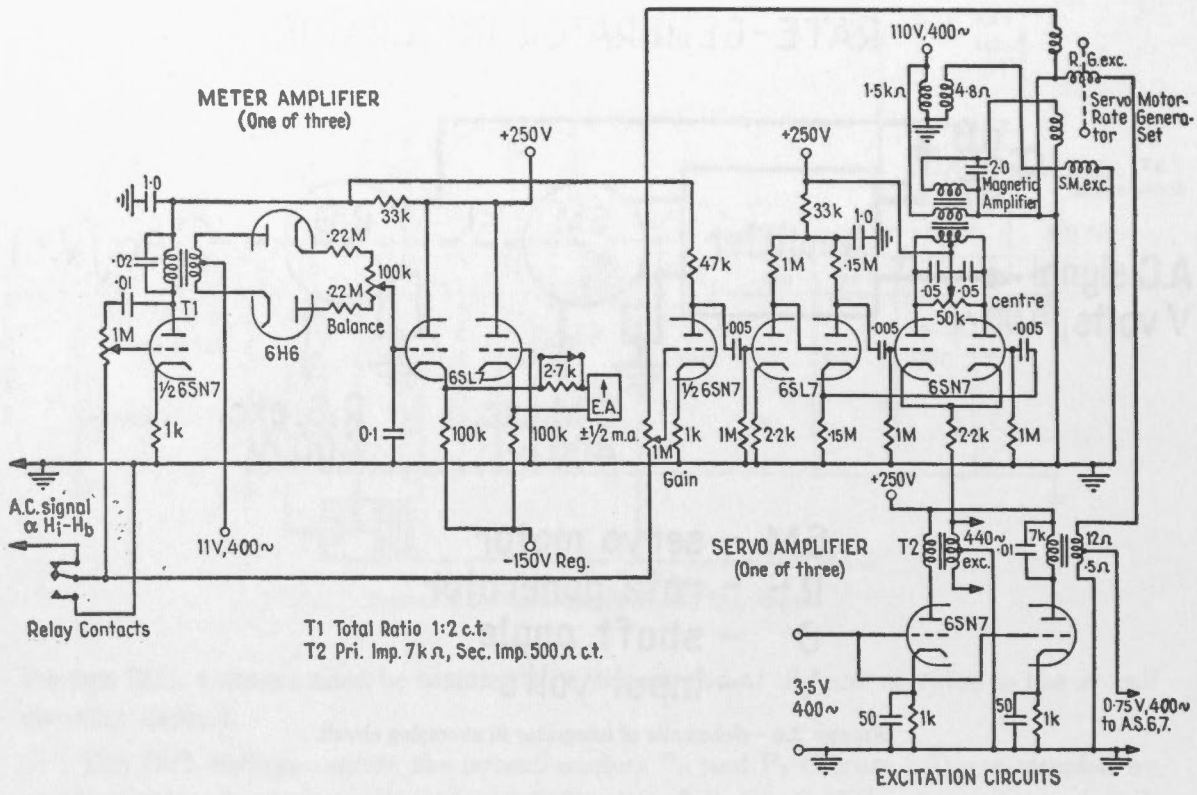

FIGURE 2.7.—Meter amplifier and averager servoamplifier.

While the indicators are being realigned with the integrators at the end of each 5-minute averaging cycle, the inputs of the meter amplifiers are grounded, allowing the amplifiers to be checked for zero-drift as well as producing time marks on the traces. When the traces are being analyzed, their sensitivities can be checked by comparing the size of the discontinuity in the trace with the change in indicator reading at the end of an averaging period. The timing of the averaging process is controlled by a clock with contacts which close for 10 seconds at the end of each 5-minute interval.

2.5 MAGNETOMETER ALIGNMENT AND ADJUSTMENT

The sensitive axes of the three field-measuring units must be mutually perpendicular and must be horizontal or vertical when the platform is level. To assist in making these adjustments, the assembly which supports the three units is mounted on a vertical axis similar to that of a theodolite. The vertical axis is attached to the stabilized platform by three levelling screws. Two level bubbles on the mounting allow this axis to be made accurately vertical in ground tests.

For alignment, the magnetometer head is removed from the stabilized platform and is levelled on a tripod away from buildings in a uniform magnetic field. Nuts on the three threaded brass rods supporting the bakelite plate carrying the vertical component measuring unit are adjusted until the Z indicator shows no change in reading as the head is rotated about the vertical axis, indicating that the axis of the Z unit is paralled to the vertical axis.

To make the axes of the horizontal component measuring units perpendicular to the vertical axis, the bakelite plate carrying them is adjusted on the vertical rods until the H indicator shows equal readings with the head oriented north and south, and equal readings with it oriented east and west. The scale values for the two horizontal coils can now be made equal by adjusting R_Y (Figure 2.3) until these four readings are equal. If the readings of the H indicator at headings NE, SE, SW, NW are compared, departure from perpendicularity of the two horizontal units is evident, and the orientation of one unit is adjusted relative to the other until these readings are equal.

In practice it is found that the simplest method of removing alignment and scale errors is to note the readings of the H indicator as the head is rotated, and plot them against heading. Levelling errors appear as a first harmonic component of the plot. Inequality of scale values appears as a second harmonic component with maxima at multiples of 90°. Lack of mutual perpendicularity of the horizontal units appears as a second harmonic component with maxima at odd multiples of 45°.

It should be noted that the method of adjustment outlined above eliminates any errors of the first or second harmonic type which may be present in the resolver. It has proved possible to make the adjustments to an accuracy of 1 in 1000, corresponding to angular errors of 4 minutes in the horizontal plane and 1 minute in the vertical plane.

After these adjustments have been completed, the magnetic field at the tripod is measured by means of a portable electronic magnetometer, of the type built by the Dominion Observatory for use in ground surveys (11). The horizontal and vertical component indicators are then calibrated by adjusting the direct currents in the two potentiometer circuits until the indicators show the proper values of the two components. The variable resistors in the voltage sampling networks are adjusted until the standardizing circuits balance against the standard cell; the settings of the variable resistors are noted and their control knobs are clamped.

Errors remaining in the magnetometer after all the alignment and calibration procedures are completed are largely absorbed in the coefficients of the magnetic field of the aircraft. The determination of these coefficients is described in Part 3 of this paper.

2.6 THE ACCURACY OF THE MAGNETOMETER

The accuracy of the magnetometer in measuring the field at the magnetometer head is now discussed, assuming that the vertical axis of the head is accurately vertical and that the true azimuth of the head is supplied to the declination indicator.

It will have been noticed that in the design of the magnetometer, null-seeking devices have been used wherever possible. This technique has the advantage—in addition to the usual factors of independence from variations in tube characteristics etc.—, that a rapid check of the nulls in the system can be made with simple built-in test equipment, without interrupting the operation of the instrument. Practically any malfunction of an element of the system, such as amplifier drift, instability or mechanical sticking of a servo, can be quickly detected and corrected by the operator.

It can therefore be assumed that the many closed-loop elements of the system operate with negligible error. The remaining sources of error are:

(a) The fact that the magnetic detectors do not always give zero signal output in zero field. The 'bias' of a given detector is not necessarily constant.

(b) The mechanical alignment of the measuring units can change because of creeping of the plastic non-magnetic parts supporting them.

(c) Changes in temperature affect the constants of the solenoids, standard cell and resistors.

(d) The resolver has inherent errors of the order of 1 part in 1000.

(e) The helical potentiometers used in the final measurement of the output have inherent errors of 1 part in 2000.

One source of zero-error in the magnetic detectors was discussed in section 2.2.2, where it was shown that errors due to harmonic distortion of the excitation current when there is an unbalance between the Mumetal cores can be eliminated. A second source is the possibility that the Mumetal cores might become permanently magnetized. Although the excitation field drives the cores well past saturation, this field decreases toward the end of the cores, and the possibility cannot be ruled out. There is evidence, however, from the use of similar magnetic detectors in portable magnetometers (11), where the magnitude of this effect can be determined in the process of aligning the instrument, that zero-errors of this sort are consistently less than 5 gammas.

It has been found that mechanical creeping occurs in the coil mountings after adjustment. By allowing a day to reach equilibrium before the final measurements are made, this effect is reduced to less than 10 gammas.

The temperature coefficient of the solenoids is of the order of 3 gammas per degree centigrade in the vertical component. Thermostating to a few degrees makes this effect negligible. The temperature coefficient of the standard cell amounts to 2.5 gammas per degree centigrade in the vertical component. In standardizing the measuring circuits corrections could be applied for the standard cell temperature, but this has not been considered justified in view of the larger uncertainties in the field of the aircraft. The temperature coefficients of the sensitive resistors are negligible.

The method of alignment of the magnetic detectors described in section 2.5 eliminates resolver error to an accuracy of 20 gammas.

The automatic potentiometers, which indicate the values of H and Z, were checked for linearity by applying a series of accurately known D.C. voltages to the circuits in place of the magnetometer signals. Measurements at 10 points showed maximum departures from linearity of ± 20 gammas; a more detailed investigation would probably show maximum errors of 30 or 40 gammas. Since the errors vary rather slowly with the position of the potentiometer slider, and the whole apparatus must be recalibrated in different regions for the effects of the magnetic field of the aircraft, it is assumed that the probable effect of potentiometer errors on survey results is of the order of 20 gammas.

It is concluded that the accuracy of the magnetometer in measuring the field at the magnetometer head with respect to the axes supplied by the direction reference system is 0.1° in declination (in southern Canada), and 20 gammas in the horizontal and vertical components.

PART 3

DISCUSSION OF SURVEY RESULTS

3.1 INTRODUCTION

The second model of the three-component airborne magnetometer which has been described in Parts 1 and 2 of this paper was completed in 1953. Through the co-operation of the R.C.A.F., it has been flown a total of approximately 400 hours during three periods of two to three weeks in 1953, 1954 and 1955. The type of aircraft used was the North Star, a four-engined airplane somewhat similar to the DC-4.

Since the aircraft was available for only short periods, it was not possible to compensate the instrument for the magnetic field of the aircraft. The aircraft field was measured by swinging the aircraft over areas where the field on the ground is accurately known. After the completion of a survey, corrections for the effect of the aircraft field are applied to the observations before they are plotted.

The techniques used in the estimation of the errors of observation and in the reduction and presentation of the results are described. The speed and ease of the reduction of the observations is a noteworthy result of the design of the instrument.

3.2 A DISCUSSION OF THE ERRORS OF THE THREE-COMPONENT AIRBORNE MAGNETOMETER

The error of an observation made in flight by an instrument of this kind may be considered as the sum of five independent errors of the following types:

(a) errors in measuring the magnetic field of the magnetometer with respect to the direction reference system.
(b) errors in the direction reference system.
(c) errors due to changes in the magnetic field of the aircraft.
(d) errors due to magnetic disturbances, and
(e) errors in geographical position.

3.2.1. *Errors in Measuring the Magnetic Field at the Magnetometer with Respect to the Direction Reference System*

Errors of this type were discussed in section 2.6. It was shown that the accuracy of the magnetometer is 20 gammas in any component of the magnetic field.

3.2.2. *Errors in the Direction Reference System*

The effect of errors in the azimuth system and in the horizontal platform on magnetic observations are now considered.

The determination of magnetic declination is illustrated in Figure 3.1, which shows the relationship between true north, magnetic north, the directional gyroscope and the aircraft heading. The instrument subtracts the magnetic heading of the aircraft β from the gyro heading of the aircraft ψ_g, and the difference $D_g = \psi_g - \beta$ is the recorded declination. This angle is independent of yawing motions of the aircraft. The electrical angle transmission system which performs the subtraction was described in section 2.3.3.

True declination is of course $D = \psi - \beta = D_g + (\psi - \psi_g)$. After the flight, the declination readings are corrected for gyro error by adding the angle $(\psi - \psi_g)$, which varies slowly because of the gyro drift.

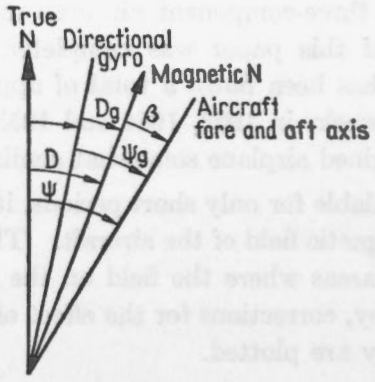

NOTATION:
D = True declination
D_g = Declination recorded on magnetometer indicator
ψ = True heading of aircraft
ψ_g = Gyro heading of aircraft
β = Magnetic heading of aircraft
Then $D = D_g + (\psi - \psi_g)$
and $D_g = \psi_g - \beta$

FIGURE 3.1.—Notation for angles in the horizontal plane.

In flight the angle $(\psi - \psi_g)$ is measured at 10-minute intervals by taking sets of three sights on the sun or stars with the synchronous periscopic sextant. The sextant operator holds the image of the sun on the cross-hairs by operating the altitude knob and the azimuth tangent screw. When the warning light comes on, indicating that the apparent vertical is close to the true vertical and the sextant bubble error is small, he reads the angle which appears in the field of view. This is the angle between the astronomical body and the directional gyro. The azimuth of the body is computed by interpolating in the H.O. No. 214 tables, and the angle $(\psi - \psi_g)$ calculated. This angle is the difference between the computed azimuth and the angle read in the modified sextant. The computation is usually done in flight, and a gyro plot is kept. A typical plot of the angle $(\psi - \psi_g)$ against time is shown in Figure 3.2. From the scatter of the points it would appear that the probable error of a single sight is about 0.3°, and the smooth curve is probably accurate to better than 0.2°.

The errors in D, H, and Z due to errors in the horizontal platform are now discussed. In Part 1 it was concluded that under normal survey conditions the stabilized platform is horizontal to an accuracy of 2 or 3 minutes of arc. If the platform error is p about the pitch axis and r about the roll axis, and p, r are small angles, the error in the measured magnetic heading of the aircraft β is

$$d\beta = \frac{r - p \tan \beta}{p + r \tan \beta + \dfrac{H}{Z \cos \beta}}, \text{ or}$$

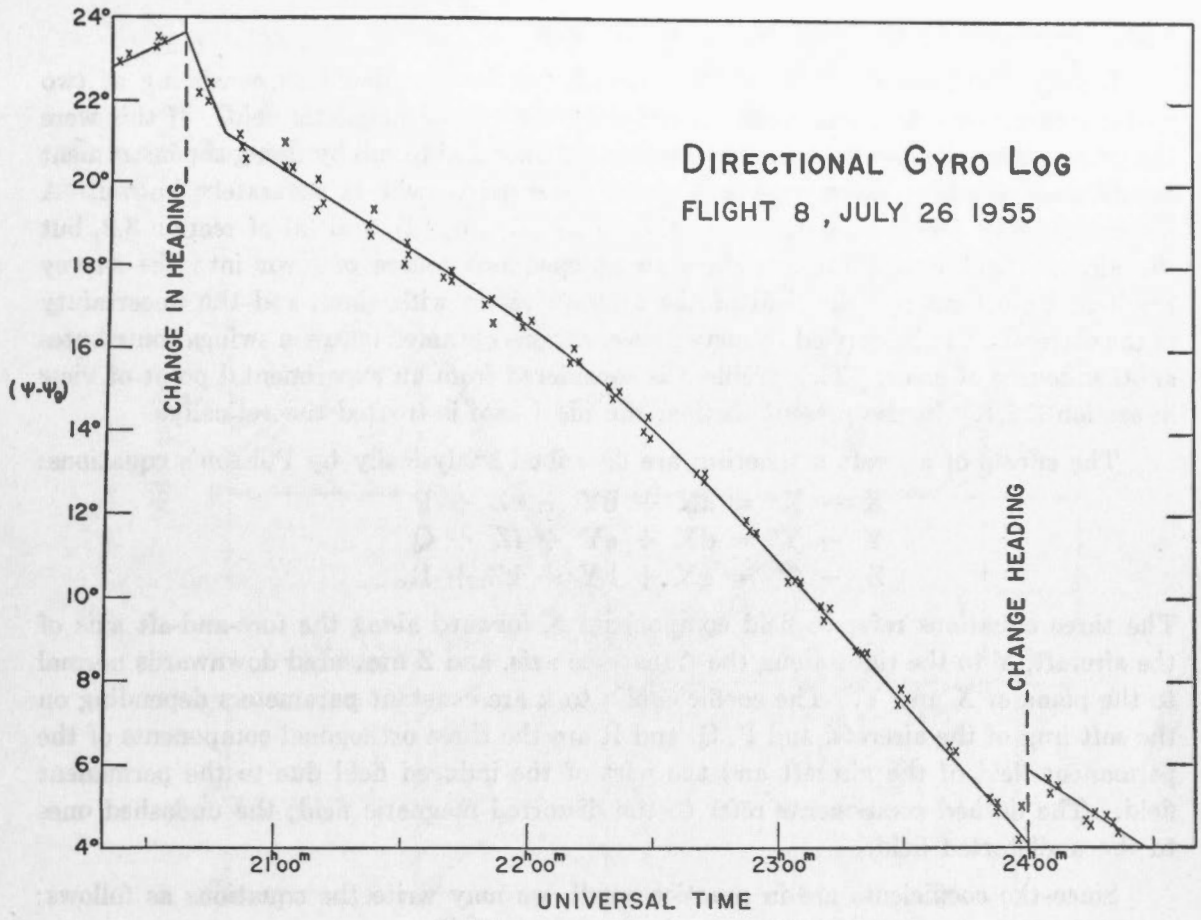

FIGURE 3.2.—Sample log of directional gyro.

$$d\beta_{(\beta=0)} = \frac{Zr}{H}, \text{ and}$$

$$d\beta_{(\beta=90°)} = -\frac{Zp}{H}.$$

Errors in the stabilized platform thus produce large angular errors in declination at high magnetic latitudes, and even in southern Canada a tilt of 3 minutes produces errors of 0.2°.

The error in the horizontal field intensity is

$$dH = Z\ (p \cos \beta + r \sin \beta), \text{ or}$$
$$dH_{(\beta=0)} = Zp, \text{ and}$$
$$dH_{(\beta=90°)} = Zr,$$

and in the vertical field intensity is

$$dZ = -H\ (p \cos \beta + r \sin \beta), \text{ or}$$
$$dZ_{(\beta=0)} = -Hp \text{ and}$$
$$dZ_{(\beta=90°)} = -Hr.$$

In Canada, where Z is about 60,000 gammas, the maximum error in H is about 17 gammas per minute of arc of tilt, and the error in Z is correspondingly smaller. A tilt of 3 minutes can produce an error in H of 50 gammas.

3.2.3. *Corrections for the Magnetism of the Aircraft*

Ideally, the magnetic field of the aircraft can be considered as consisting of two parts: a permanent field and a field induced by the earth's magnetic field. If this were the true picture, the two fields could be measured once and for all by flying the instrument on different headings over a region where the earth's field is accurately known. A measurement of this type is subject to the errors (a), (b), (d), and (e) of section 3.2, but the aircraft field would not introduce an independent source of error into the survey results. Unfortunately, the field of the aircraft varies with time, and the uncertainty in the corrections to be applied to survey observations obtained between swings contributes another source of error. This problem is considered from an experimental point of view in section 3.5.1. In the present section, the ideal case is treated theoretically.

The effects of aircraft magnetism are described analytically by Poisson's equations:

$$\begin{aligned} X - X' &= aX + bY + cZ + P \\ Y - Y' &= dX + eY + fZ + Q \\ Z - Z' &= gX + hY + kZ + R. \end{aligned}$$

The three equations refer to field components X forward along the fore-and-aft axis of the aircraft, Y to the right along the transverse axis, and Z measured downwards normal to the plane of X and Y. The coefficients a to k are constant parameters depending on the soft iron of the aircraft, and P, Q, and R are the three orthogonal components of the permanent field of the aircraft and the part of the induced field due to the permanent field. The dashed components refer to the distorted magnetic field; the undashed ones to the undistorted field.

Since the coefficients are in practice small, we may write the equations as follows:

$$\begin{aligned} X - X' &= aX' + bY' + cZ' + P \\ Y - Y' &= dX' + eY' + fZ' + Q \\ Z - Z' &= gX' + hY' + kZ' + R \end{aligned}$$

and refer the components to the orthogonal axes defined by the true vertical and the horizontal. This approximation is valid for all normal attitudes of the aircraft.

In Canada, the vertical component of the earth's field is constant to $\pm$ 8 per cent over the whole country, and it is difficult to separate the fields induced by the vertical component from the permanent fields of the aircraft. For the same reason, it is not necessary to separate them, as long as surveys are confined to Canada. For convenience we write $cZ' + P = P'$ etc., and the equations become:

$$\begin{aligned} X - X' &= aX' + bY' + P' \\ Y - Y' &= dX' + eY' + Q' \\ Z - Z' &= gX' + hY' + R'. \end{aligned}$$

The nine parameters are determined by swinging the aircraft over a region where the earth's field is known. The methods adopted are described in section 3.5.1.

The corrections to be applied to the observed values of D, H, and Z in terms of the nine parameters are:

$$\begin{aligned} \triangle H = H - H' = H'[a \cos^2\theta + e \sin^2\theta - (b + d) \sin\theta \cos\theta] \\ + P' \cos\theta - Q' \sin\theta \end{aligned}$$

$$\Delta D = D - D' = \frac{H' [d \cos^2 \theta - b \sin^2 \theta] + P' \sin \theta + Q' \cos \theta}{H' [1 - (b + d) \sin \theta \cos \theta] + P' \cos \theta - Q' \sin \theta}$$

$$\Delta Z = Z - Z' = H'[g \cos\theta - h \sin\theta] + R',$$

where θ is the apparent magnetic heading. Figure 3.3 shows the corrections ΔH, ΔD and ΔZ from the nine parameters adopted for the 1953 survey, computed for five different

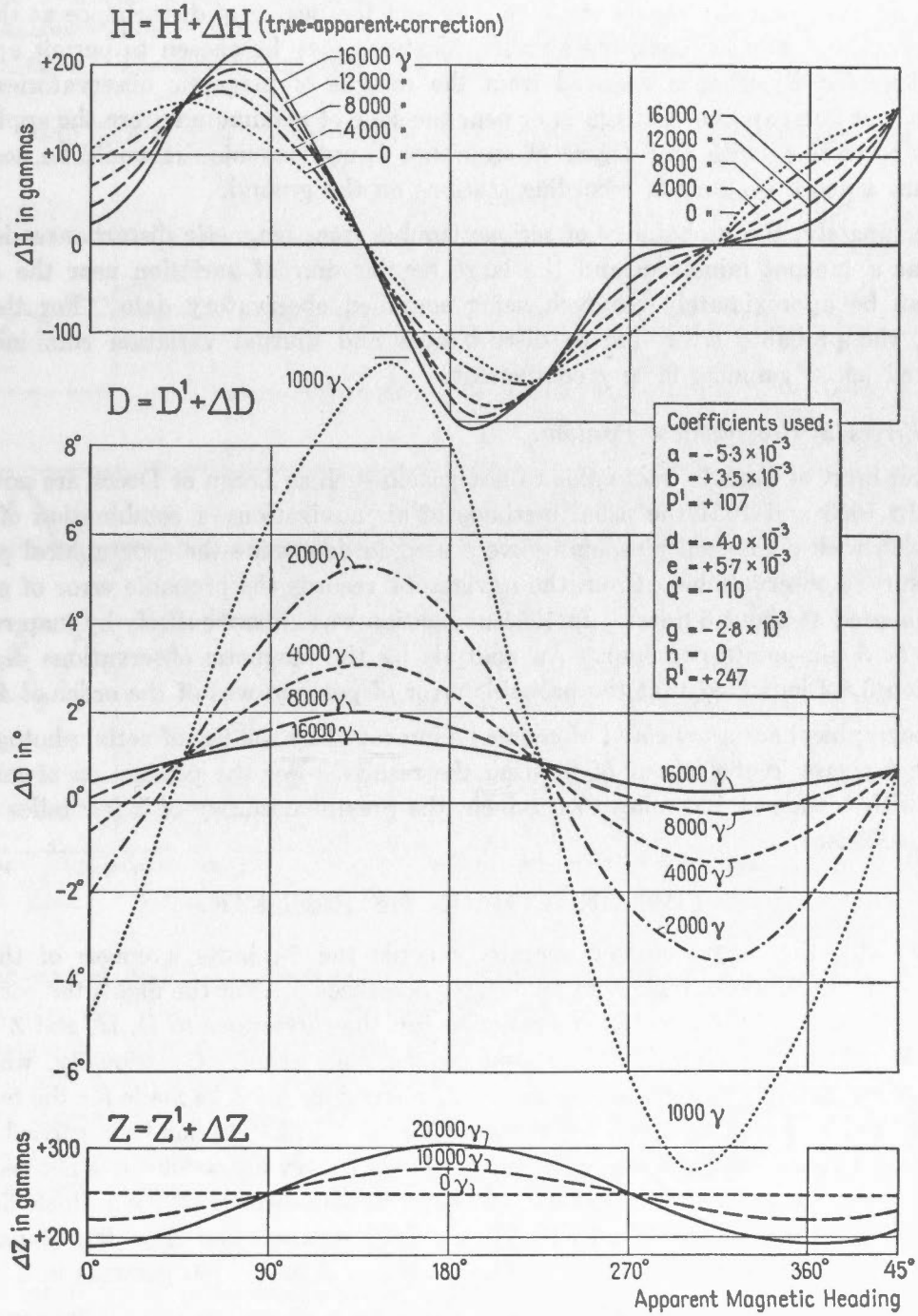

FIGURE 3.3.—Corrections adopted in 1953 for the magnetic field of the aircraft, plotted against apparent magnetic heading for different values of H'.

values of H′ and plotted against the uncorrected magnetic heading of the aircraft. In reducing the survey results, the corrections can be quickly read from these curves to an accuracy of 10 gammas.

3.2.4. *Errors due to Magnetic Disturbances*

The effect of magnetic disturbances on the airborne magnetic observations will depend on the particular region of the survey and the degree of disturbance at the time of observation. For swinging the aircraft, locations may be chosen to permit applying corrections for disturbance deduced from the records of magnetic observatories. For surveys over large areas of Canada in or near the zone of maximum aurora the application of such corrections with any degree of assurance is not possible—it would be necessary to set up a dense network of recording stations on the ground.

Fortunately, the probability of serious trouble from magnetic disturbances is fairly low near a sunspot minimum and the large regular diurnal variation near the auroral zone can be approximately removed using compiled observatory data. For the 1955 survey, the probable error due to disturbances and diurnal variation combined was estimated at 30 gammas in any component.

3.2.5. *Errors in Geographical Position.*

Over most of Canada, radio aids to navigation such as Loran or Decca are not available. In 1953 and 1954 the usual methods of air navigation—a combination of astro-navigation with occasional pin-points—were used to determine the geographical position of the survey observations. From the navigators' records the probable error of position was estimated at about 6 miles. In 1955 navigation was almost entirely by map reading, with 4 or 5 pin-points per hour. An analysis by the magnetic observations described in section 3.5.2 indicated that the probable error of position was of the order of 4 miles.

Geographical accuracy could of course be improved by the use of aerial photography, with an increase in the labour of plotting the results. For the production of magnetic charts with a scale of 100 miles to the inch, the present accuracy of a few miles is considered sufficient.

3.3 THE REDUCTION OF RESULTS

In flight, the magnetometer operator records the 5-minute averages of the field components and Universal Time on an observation sheet. After the flight, the correction to D for the drift of the directional gyroscope and the corrections to D, H, and Z for the magnetic field of the aircraft are entered on the same sheet. Occasionally, when the rate of the directional gyroscope is large, small corrections must be made for the resulting error in the horizontal platform. If the swinging of the aircraft has been carried out at the approximate altitude and magnetic latitude of the survey operations, it is not necessary to correct the observations for altitude. In any case the corrections for a dipole field are small; at an altitude of 8000 feet with H = 15,000 gammas and Z = 60,000 gammas, the correction to sea-level would be + 15 gammas in H and + 60 gammas in Z.

When the flight-lines are isolated, as in the surveys of 1953 and 1954, the results are presented as profiles. In the case of the 1955 survey, where a systematic pattern was

flown, the 5-minute averages were also plotted directly on charts, ready for contouring. One man in a day can correct and plot the results from an 8-hour flight comprising nearly 100 observations of the magnetic vector, each observation representing the average of the components over a 20-mile segment of the flight path.

Figures 3.4 and 3.5 show profiles from two of the 1953 flights, drawn by joining the 5-minute averages of the components. In Figure 3.5, the dotted lines represent the instantaneous values of the field as read from the continuous recordings of the Esterline-Angus meters. The smoothing effect of the automatic averaging is apparent.

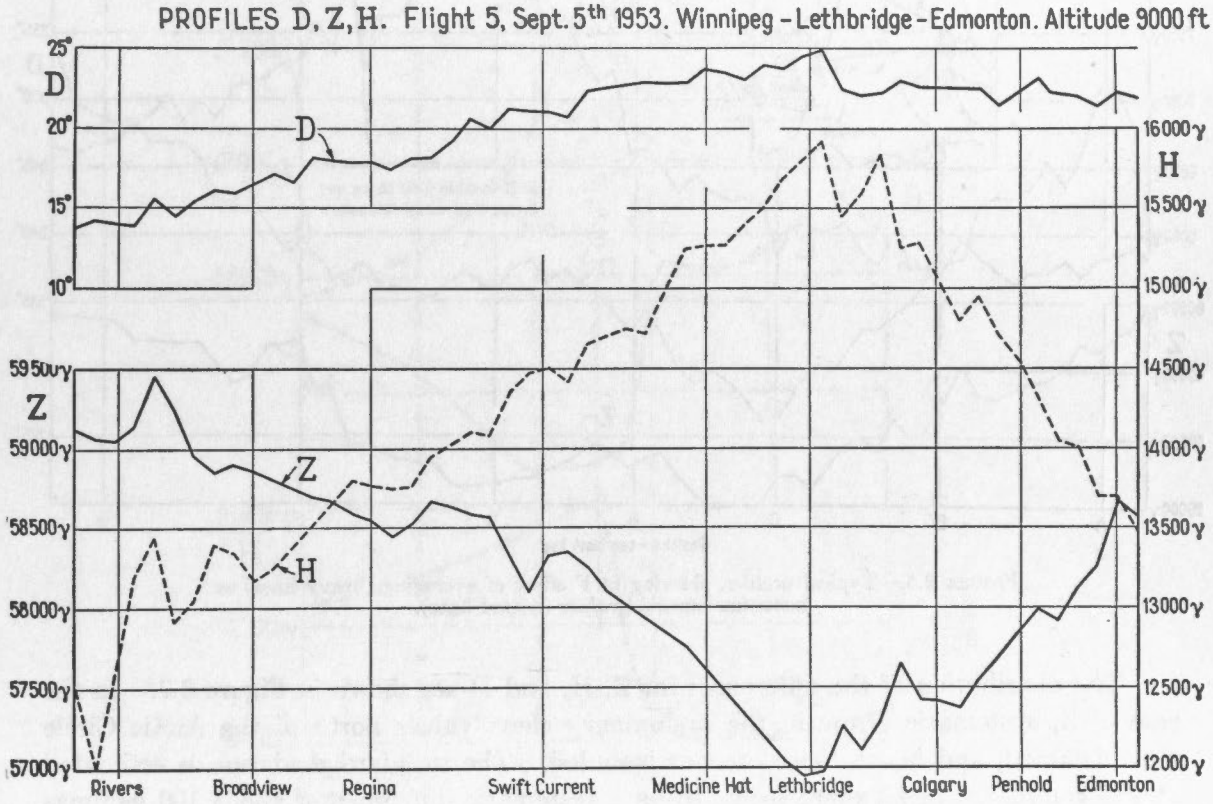

FIGURE 3.4.—Typical profiles, plotted by joining 5-minute averages.

The survey flights have been planned for the production of large scale magnetic charts rather than for the detailed study of local anomalies, but an example of a typical large anomaly in three components may be of interest (Figure 3.6). The flight path was due magnetic W across the coast line, which strikes about 50° E of N. The form of the anomaly suggests a strike in the general direction SW—NE, and the form of the Z trace suggests a fairly steeply dipping body. The agreement of the profiles shown with some theoretical examples is striking; for example, see Heiland (12).

3.4 COMPARISON OF THE 1953 RESULTS WITH EXISTING CHARTS

During the first season's operation of the instrument, a tour of Canada was made with the aim of testing the equipment in different magnetic latitudes. After the survey, the airborne results were compared with the charts for 1955.0 prepared by the Division

of Geomagnetism, Dominion Observatory. In H and Z, comparisons were made at 160 equally spaced points; in D only 50 points were compared, since the complete map for 1955 was not ready. Corrections were made for the altitude of the observations and for secular change. No attempt was made to select magnetically smooth areas.

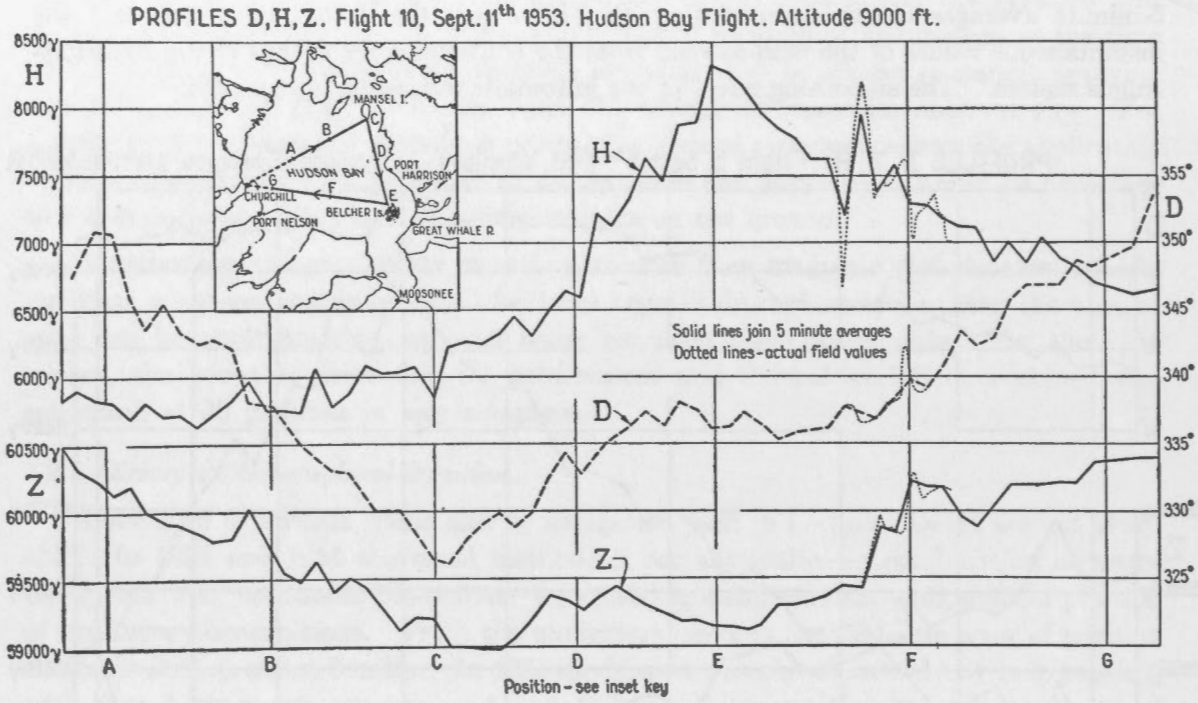

FIGURE 3.5.—Typical profiles, showing at F effect of averaging (heavy lines) on instantaneous field values (dotted lines).

The distribution of the differences for Z, H, and D are shown in Figure 3.7. In the case of Z, systematic errors in the preliminary chart values north of the Arctic Circle were detected, and hence these are not included. The standard deviation is estimated at 250 gammas. In H, there seems to be a systematic difference of about 100 gammas in all parts of Canada, with a standard deviation of 230 gammas north of latitude 60°, and 390 gammas south of latitude 60°. In the declination comparison the statistical evidence is less convincing, but the histogram is shown with its standard deviation of 1.3°.

A comparison of this sort indicates more about the degree of smoothing of the magnetic charts than it does about accuracy of the airborne observations. The standard deviations calculated above are interpreted as showing the average magnitude of local anomalies which are too small in horizontal extent to appear on large scale charts such as the magnetic map of Canada. There seem to be many anomalies in all components of the order of several hundred gammas with a width somewhere between 20 miles and a few hundred miles. A detailed analysis of the magnitude and extent of magnetic anomalies has been made from the observations of the 1955 airborne survey, and will be published elsewhere (13).

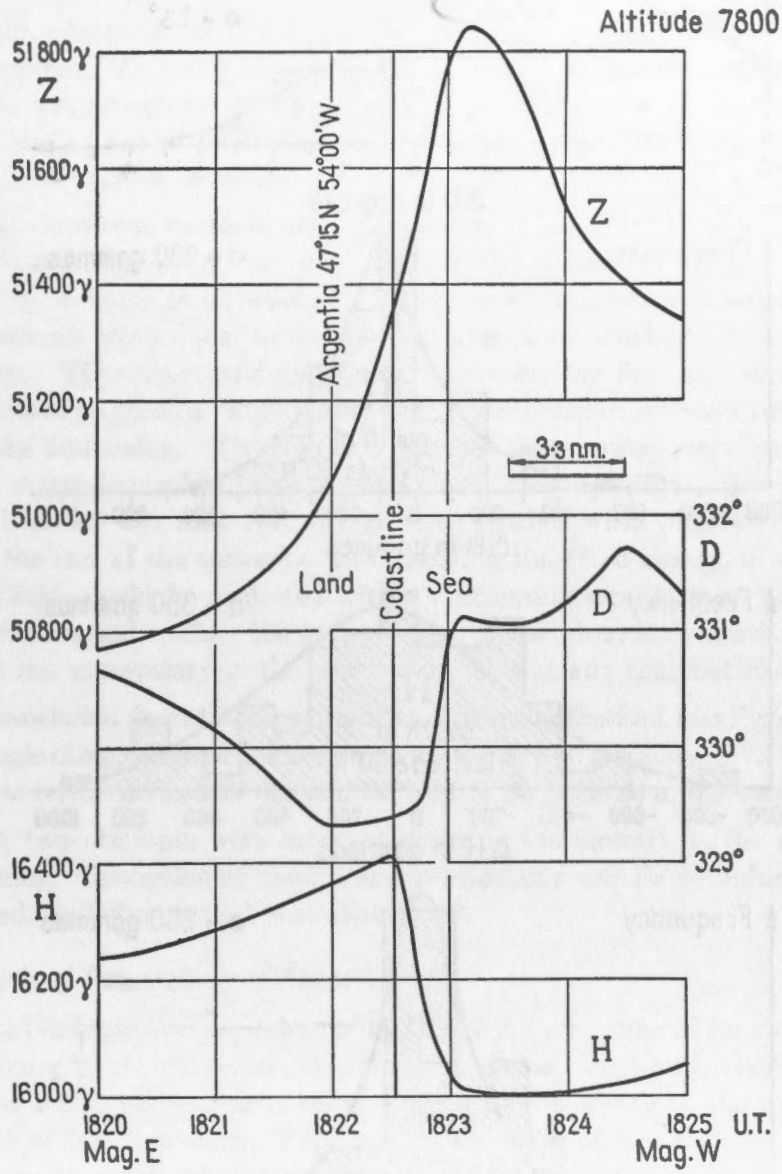

FIGURE 3.6.—Magnetic anomaly over Argentia, Newfoundland.

3.5 ANALYSIS OF AIRBORNE MAGNETIC SURVEY OF 1955

In 1955, a survey of the provinces of Manitoba, Saskatchewan and Alberta was made by the three-component airborne magnetometer. The survey was completed in three weeks, covering an area of 700,000 square miles with a total flying time of some 150 hours. Twelve lines were flown at an altitude of 9,000 feet along parallels of latitude one degree apart. Three north-south lines were also flown, giving 36 intersections of flight lines from which an indication of the over-all accuracy of the survey could be obtained. Navigation was by map-reading, with 4 or 5 pin-points per hour.

3.5.1. *Determination of the Magnetic Field of the Aircraft*

To determine the magnetic field of the aircraft four swings were made—two over Ste. Rosaire, Quebec, before and after the survey, and two over Meanook, Alberta, during

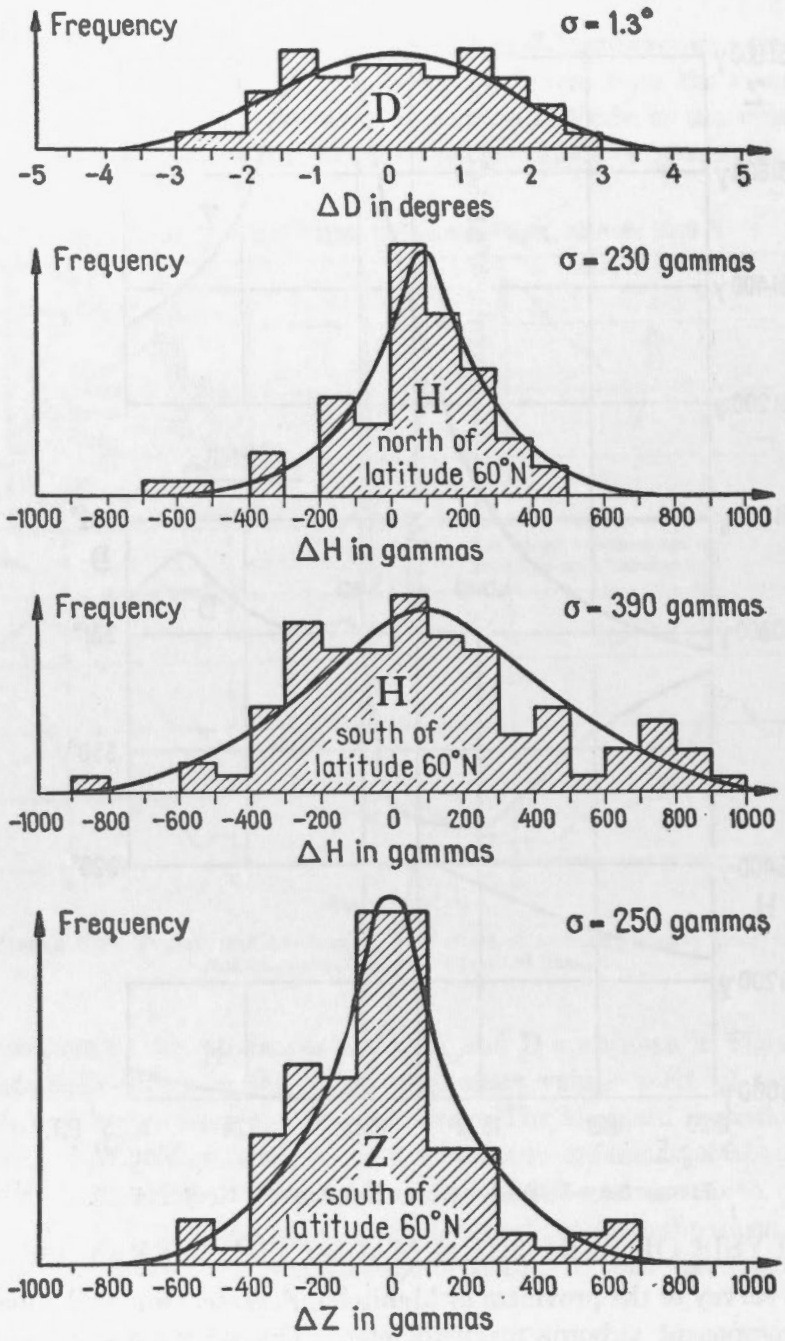

FIGURE 3.7.—Frequency distribution of discrepancies between observations of 1953 airborne survey and preliminary version of magnetic charts for 1955.0, based on ground observations.

the 1955 survey. The swings were made at an altitude of 9,000 feet. At both locations the magnetic field on the ground is known to a few gammas, and the gradients are less than 20 gammas per mile within 5 miles of the stations. A swing consists of eight 20-minute flights passing over the station on four different headings. This plan allows 10 minutes for the decay of transients developed in the stabilized platform during changes in heading of the aircraft. Readings of D, H, and Z are taken every half-minute with the

magnetometer operating on "Direct". The readings are plotted as profiles and the differences between the airborne observations and the magnetic field on the ground as deduced from magnetograms are computed. These differences are inserted in the equations of Section 3.2.3, and the 9 parameters are obtained in a least-squares solution with the aid of a small analog computer.

Table 3.1 shows the values of the 9 parameters obtained from the four swings of 1955. The probable errors given in the table indicate the accuracy with which the equations are satisfied by a single observation. It is apparent that between swings the magnetic field of the aircraft was subject to changes too large to be attributed to errors in the individual swings. The largest change occurred between the first and second swings; the aircraft may have acquired a "semi-permanent" magnetization during a two-week overhaul just before the first swing. The results of the last three swings were combined to give a single set of corrections which were applied to all survey results. (Results obtained on two flights between the first two swings were treated with suspicion—one flight was repeated at the end of the survey). In combining the three swings, it was noticed that the induced fields could be neglected without increasing significantly the probable error of a single observation. Thus the induced part of the aircraft field was negligibly small compared to the uncertainty in the permanent fields at any time between swings.

It was concluded from these results that, excepting the first two flights, the probable error of a single observation of the magnetic vector is ± 60 gammas ($\pm 0.3°$) in declination, $\pm$ 60 gammas in the horizontal component, and $\pm$ 30 gammas in the vertical component.

In 1953, two attempts were made at swinging the aircraft on the ground with the engines running. Inconclusive results and particularly unreliable induction coefficients were obtained, and the method was abandoned.

3.5.2. *Analysis of Intersections of Flight-lines*

After the 5-minute average values of D, H, and Z were corrected for aircraft magnetism and directional gyro error and rate, they were written on charts with a scale of 1:3,000,000 (47 miles per inch), each average being written at the centre of the corresponding 20-mile segment of the flight-line. For every intersection of two flight-lines, values of D, H, and Z were interpolated linearly from the adjacent averages, and the discrepancies were examined for systematic differences which would indicate errors in the corrections for aircraft magnetism, but no statistically significant differences were found. The most probable values of the discrepancies were 1.2° in D, 140 gammas in H, and 120 gammas in Z, or more than twice as large as would be expected from the probable errors of the swing observations. (The probable difference of 1.2° in D would correspond to something less than 200 gammas, since H varies between 6,000 and 14,000 gammas in the region surveyed). This result is not surprising, since 20-mile averages on orthogonal paths would not be expected to agree unless the gradients were constant over that distance. Instantaneous readings would be expected to show better agreement than the smoothed values. Accordingly, the times of the intersections were read from the chart to the nearest half-minute, and the instantaneous values of D, H, and Z for these times were extracted from the continuous records. Although at individual intersections the discrepancies from instantaneous values differed considerably from those computed from the

TABLE 3.1

	Fore-and-aft Component				Transverse Component				Vertical Component			
	a	b	P′ γ	probable error of one observation γ	d	e	Q′ γ	probable error of one observation γ	g	h	R′ γ	probable error of one observation γ
July 18.....	−.0067	−.0044	−654	±135	−.0024	+.0200	+416	±80	−.0037	−.0038	+415	±8
July 21.....	−.0056	−.0011	−184	± 8	+.0086	−.0091	+119	±37	−.0018	+.0007	+623	± 9
Aug. 6.....	−.0107	+.0057	− 80	± 70	+.0033	+.0045	+ 77	±28	−.0002	+.0029	+690	±10
Aug. 8.....	+.0017	+.0021	− 32	± 8	−.0003	+.0048	+ 39	±38	−.0023	+.0025	+584	± 6
Weighted Mean *.....	−.0024	+.0008	−106	± 63	+.0038	+.0006	+ 78	±58	−.0016	+.0021	+621	±33
Weighted Mean **.....	0	0	− 98	± 66	0	0	+ 75	±63	0	0	+632	±34

* Neglecting July 18.

** Neglecting induced fields and July 18.

5-minute averages, the probable values of the discrepancies were not significantly changed, as is shown in Table 3.2.

TABLE 3.2

	D°	Hγ	Zγ
Probable discrepancy at intersections			
by 5-minute averages	1.2	140	120
by instantaneous readings	1.4	140	140
Probable error of one instantaneous reading due to			
(a) change in aircraft field	0.3	70	30
(b) magnetic disturbances	0.24	22	21
(c) navigation errors of ± 4 miles	0.62	95	95
Total probable error due to (a), (b), (c)	0.73	120	100
Expected probable discrepancy at intersections	1.0	170	140

A check was made of the magnetograms of Meanook Observatory to see how much of the disagreement at the intersections could be attributed to magnetic disturbance. Although one disturbance of 200 gammas and two of 100 gammas occurred at times of intersection, the most probable disturbance (including diurnal variation) at the 72 times amounted to only 0.24° in D, 22 gammas in H, and 21 gammas in Z. No attempt was made to correct the observations for disturbances, since much of the survey lay in the zone of maximum aurora.

Next, an investigation was made of the local magnetic gradients at the points of intersection to see whether the discrepancies could be explained by reasonable errors in navigation. The maximum variations in each component which could be caused by errors of ± 1 minute in the times of intersection were read from the continuous records. The most probable values of the maximum variation in the magnetic field over 4 miles were 0.62° in D, 95 gammas in H, and 95 gammas in Z. Table 3.2 shows that the discrepancies observed at the intersections can be accounted for statistically if it is assumed that there are in fact navigational errors of the order of 4 miles. Navigational errors of this magnitude are not unreasonable when it is remembered that they include errors in plotting the flight lines and in reading the times of intersection from charts at a scale of 47 miles to the inch.

If the most important source of error is in navigation, the largest discrepancies would be expected to occur at intersections with large local gradients. The magnitudes of the discrepancies at individual intersections were plotted against the corresponding local gradients, as shown in Figure 3.8. Some correlation is apparent. A theoretically more satisfactory test can be based on the following argument. Let x be the correction to the time of intersection measured along one flight-line, and y be the correction measured

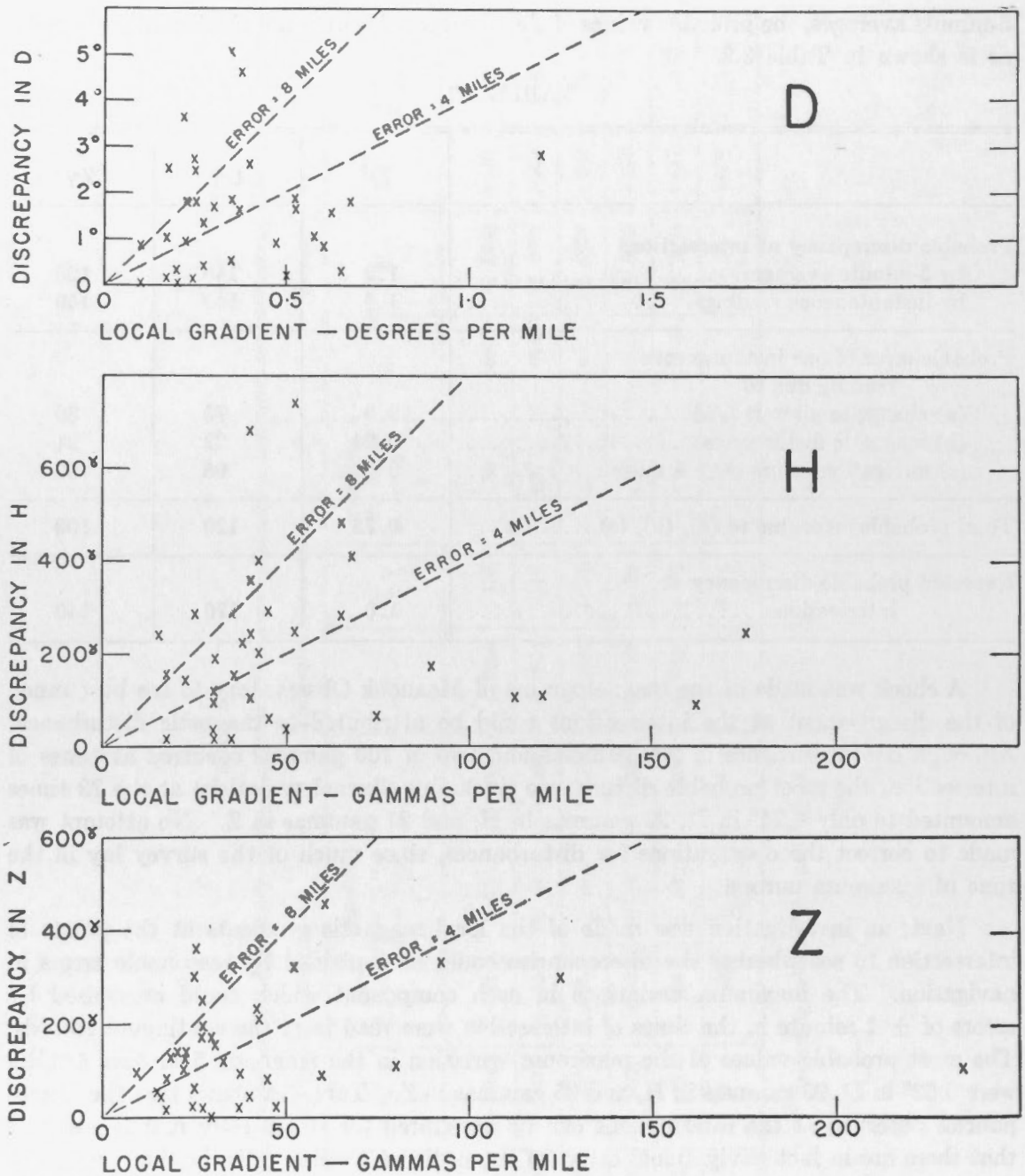

FIGURE 3.8.—Discrepancies at intersections of 1955 flight lines plotted against the local gradients.

along the other. There are generally an infinite number of pairs of corrections (x,y) for which the declination readings on the two flight-lines will agree exactly, and a line can be plotted on the x,y plane for which there is no disagreement in D. Similarly, a line can be plotted on the same diagram for H, and a third line for Z. If the discrepancies are entirely due to navigational errors, the three lines should intersect at a point, locating the flights relative to the magnetic field in a way somewhat similar to the three-star position-line method in navigation. This technique, which involves a good deal of work,

was tried for four intersections. The solution for one intersection on a well-defined anomaly indicated an error of 7 miles, but the other intersections each gave several solutions within a radius of 10 miles of the assumed point of intersection any of which would make the three components agree to within 20 gammas. The method is apparently of doubtful value because the anomaly field is usually so complicated that the probability is rather large of a purely accidental coincidence, within 20 gammas, of the three position lines.

It was concluded from this analysis of intersections of flight-lines, that the probable error of an instantaneous airborne observation of the magnetic field as plotted on the charts was $\pm 1.0°$ in D, ± 100 gammas in H, and ± 100 gammas in Z. The chief source of error was the uncertainty in geographical position of the order of 4 miles, including errors in plotting the flight-lines as well as actual errors in navigation.

3.6 RELIABILITY OF THE INSTRUMENT

During the first season's operation of the magnetometer in 1953, less than 10 per cent of the flying time was lost in servicing the equipment in the air. In 1954 and 1955 unserviceability was of the order of 1 or 2 per cent. This record is considered very satisfactory in view of the complicated nature of the instrument.

The main source of trouble in the equipment has been the gyroscopes. As was explained in Part 1, the stabilized platform is designed to give the required accuracy with gyroscopes of quite modest performance by modern standards. Trimmed drift-rates of several degrees per hour would be satisfactory. It was soon found that the performance of the gyroscopes in the air bore little relation to the figures published by the manufacturers of the units. One difficulty was that the performance of the gyroscopes deteriorated rapidly owing to the formation of bubbles in the fluid by air leaking through the gyro case. Overhaul of the units by the manufacturer corrected this trouble only temporarily. Another effect, apparently not related to air bubbles, is that some units have a rate very sensitive to small accelerations, of the order of 0.02 g, when they are operated in certain positions. Non-linear relations of this type between rate and acceleration were not expected, and it was several years before laboratory tests were devised to detect them.

In survey flying, the imperfections of the roll and pitch gyroscopes do not cause as much trouble as might be anticipated. Air bubbles eventually migrate to the top of the gyro case. If the relation between rate and acceleration is fairly linear over the region of the normal aircraft accelerations, part of its effect is cancelled by adjusting empirically in the laboratory the constants of the erection system for the proper transient response. When changes in aircraft heading are made, however, as in the swinging procedure, large transient errors can be produced. On a few occasions, the platform has developed errors as large as 1° during turns of 180°. The slow decay of these errors makes the interpretation of the swings extremely difficult. In the case of the directional gyroscope, air bubbles have a more serious effect because of its horizontal attitude. Sudden changes in rate of 50° per hour have occurred in some units, making necessary frequent astronomical observations and adding to the labour of correcting the magnetic observations. The type HIG-5 gyroscopes will soon be replaced by carefully tested HIG-4 units, which it is hoped will prove more reliable.

3.7 CONCLUSIONS

Experimental results, obtained by flying on different headings over a region where the gradients of the magnetic field are small and accurate corrections for magnetic disturbances are available, show that the probable error of a single observation, after correction for the magnetic field of the aircraft, is 40 gammas in the azimuth and intensity of the horizontal magnetic vector and 10 gammas in the vertical component. This indicates that the probable error of the stabilized platform is of the order of 3 minutes of arc under conditions of frequent manoeuvering. The magnetic field of the aircraft changes over periods of a few weeks, producing an uncertainty in the corrections for the aircraft field which increases the probable error of survey observations to 60 gammas in the horizontal vector and 30 gammas in the vertical component. Errors in navigation and plotting the flight-lines and the effect of magnetic disturbances result in a further increase in the probable error of an observation, as plotted on the charts, to 100 gammas in any component.

Since the most important source of error is in navigation, the first step toward increasing the accuracy would be to reduce the navigation error by the use of aerial photography, for example. This would increase considerably the labour of plotting the observations, and where charts at a scale of 50 or 100 miles to the inch are concerned, the results would be quite indistinguishable from charts based on navigation of the present accuracy of a few miles. It is concluded that with the present techniques, the over-all accuracy of the airborne measurements is sufficient for the present purpose—the production of large-scale magnetic charts.

ACKNOWLEDGMENTS

The authors wish to thank Dr. C. S. Beals, Dominion Astronomer, and R. G. Madill, Chief of the Division of Geomagnetism, Dominion Observatory, Ottawa, for their advice and encouragement, and the staff of the Observatory machine shop for their advice in mechanical design, and skill in the construction of the instrument.

The history of this project is reviewed in the introduction to this paper. The initial direction of Professors E. C. Bullard and J. T. Wilson at the University of Toronto and the support and advice of the Navigation Research Panel of Defence Research Board, and its forerunner, are gratefully acknowledged. In particular, we are indebted to W/C D. A. MacLulich, R.C.A.F., who played an important part in the early development.

Experimental results were obtained with the kind cooperation of the Central Experimental and Proving Establishment, R.C.A.F., which provided a North Star aircraft and personnel for flights in 1953, 1954 and 1955.

REFERENCES

1. S. Chapman: *Proc. Phys. Soc.* London 33, 650, 1941.
2. H. Spencer-Jones and P. J. Melotte: *Monthly Notices Roy. Astron. Soc., Geophys. Suppl.*, 6, 7, 1953.
3. E. O. Schonstedt and H. R. Irons: *Trans. Am. Geophys. Union*, 34, 3, 1953.
4. C. A. Jarman: *S. and T. memo. TPA3*, Technical Inf. Bureau, Ministry of Supply, Nov. 1949.

5. S. Z. Mack: *D.R.B.S. 4—1200—53—1.* Arctic.
6. P. H. Serson: Unpub. Ph.D. Thesis, University of Toronto, 1951.
7. S. Z. Mack: Unpub. Ph.D. Thesis, University of Toronto, 1951.
8. H. Lauer, R. Lesnick and L. E. Matson: "Servomechanism Fundamentals", McGraw-Hill, New York, 1947.
9. C. D. Perkins and R. E. Hage: "Airplane Performance, Stability and Control", John Wiley and Sons, New York, 1949.
10. V. V. Vacquier, and Gulf Research and Development Co., U.S. Patent No. 2406870, 1946.
11. P. H. Serson and W. L. W. Hannaford: *Can. J. Technol.* 34, 232, 1956.
12. C. A. Heiland: "Geophysical Exploration", Prentice-Hall Inc., New York, 1946.
13. P. H. Serson and W. L. W. Hannaford: *J. Geophys. Res.*, 62, 1, 1957.